Universidade de Lisboa

Faculdade de Farmácia

Role of the *N*-glycolylation of mycobacterial peptidoglycan in host immune recognition and antibiotic resistance

Cátia Raquel Lopes Silveiro

Dissertation report supervised by Professor Maria João Catalão (PhD)

Biopharmaceutical Sciences
Microbiology

2020

Universidade de Lisboa

Faculdade de Farmácia

Role of the *N*-glycolylation of mycobacterial peptidoglycan in host immune recognition and antibiotic resistance

Cátia Raquel Lopes Silveiro

Dissertation report supervised by Professor Maria João Catalão (PhD)

This project was funded by FCT (Fundação para a Ciência e Tecnologia) - PTDC/BIA -MIC/31233/2017 & IF/00414/2015 – and by ESCMID (European Society of Clinical Microbiology and Infectious Diseases) - ESCMID Research Grant 2018 - to Maria João Catalão.

Biopharmaceutical Sciences
Microbiology

2020

Abstract

In the past years, tuberculosis (TB) has become a global health emergency, namely due to the emergence of multi-drug and extensively-drug resistant strains of its etiologic agent, *Mycobacterium tuberculosis* (*Mtb*). This problem is accentuated by the relative ineffectiveness of the BCG vaccine and of currently known antimycobacterial agents and, by the lack of alternative TB therapeutics. The pathogenesis of *Mtb* is poorly understood due to the highly complex structure of the cell wall (CW). The peptidoglycan (PG) layer of the mycobacterial CW is specifically relevant since it features unique modifications, of which the *N*-glycolylation of PG muramic acid, catalyzed by the activity of the N-acetyl muramic acid hydroxylase (NamH), is of special interest. Previous studies have demonstrated that the *N*-glycolylation of PG increases β-lactams/lysozyme resistance as well as the immunogenicity of the mycobacterial CW. Despite not being essential, the *namH* gene is highly conserved in *Mtb* clinical isolates, implying a vital function for the *N*-glycolylation of PG in antibiotic resistance or/and in TB pathogenesis. Therefore, the main goal of this thesis was to modulate *namH* expression in order to understand the significance of the *N*-glycolylation of mycobacterial PG in antibiotic resistance and in host immune recognition.

To do that, several *namH* knockdown (*namH*$^{-}$) mutants were constructed in both *M. smegmatis* and *M. tuberculosis* H37Ra, using a new effective transcription regulation tool, CRISPR interference (CRISPRi). This technique employs a dCas9-sgRNA complex to repress any target gene by sterically hindering its transcription, thus, enabling the inquiry of the functional significance of *namH*. The *M. smegmatis namH*$^{-}$ mutants were phenotypically characterized by performing growth curves and spotting dilutions. These experiments demonstrated that *namH* knockout/repression does not produce severe growth defects, thus, confirming the non-essentiality of *namH*. Moreover, a residual level of $dCas9_{Sth1}$ toxicity was uncovered by performing growth curves. Although it was not possible to confirm the repression of *namH* in all knockdown mutants, the repression of *namH* in the induced knockdown mutant *M. smegmatis* C2 in the presence of anhydrotetracycline (ATc) was assessed by quantitative real-time PCR (qRT-PCR) and confirmed. Furthermore, CRISPRi was found to cause a significant level of downstream polarity. Nevertheless, it was not possible to probe how the strength of the employed PAM, the targeted DNA strand and the target site affect the efficiency of CRISPRi.

In addition, the role of the *N*-glycolylation of PG in antibiotic susceptibility was determined by performing minimum inhibitory concentration (MIC) and minimum bactericidal concentration (MBC) assays for all *M. smegmatis namH* knockdown mutants, with and without inducer (ATc).

The MIC assays showed that meropenem is more efficient at inhibiting the growth of mycobacteria, when compared to amoxicillin or cefotaxime. Besides, the *N*-glycolylation of PG was found to have a role in β-lactams resistance, as both *M. smegmatis* ΔnamH and the induced knockdown mutants exhibited increased susceptibility to most β-lactams. Likewise, a strong link between the *N*-glycolylation of PG and the mechanism of action of cefotaxime was uncovered, as the *namH* knockdown mutants displayed a particularly significant decrease in MIC values for cefotaxime or cefotaxime-clavulanate in the presence of inducer. Furthermore, differences in the hydrolytic efficiency of the main β-lactamase of *M. smegmatis* (BlaS) to various β-lactams were verified as the addition of clavulanate to β-lactams considerably decreased the MIC of amoxicillin, as opposed to cefotaxime and meropenem.

The MBC assays showed that all β-lactams were bactericidal against most of the tested *M. smegmatis* samples, indicating that the *N*-glycolylation of PG does not severely affect the killing activity of β-lactams.

Subsequently, the disk diffusion assays enabled the assessment of the meropenem zones of inhibition for all *M. smegmatis* knockdown mutants, with and without inducer. These experiments suggested that NamH plays a role in meropenem resistance as both *M. smegmatis* ΔnamH and the induced *namH* knockdown mutants displayed an exacerbated meropenem hypersusceptibility phenotype.

Overall, these antibiotic susceptibility tests demonstrated that the *namH* knockout/knockdown mutants display increased susceptibility to most β-lactams. This "β-lactams hypersusceptibility phenotype" may be explained by the inhibition of: **i)** the hydrolytic activity of NamH as a β-lactamase; **ii)** the activity of NamH as a monooxygenase, which modifies PG sugars; **iii)** both activities, enabling a synergy between the inhibition of β-lactamase activity and the inhibition of the *N*-glycolylation of PG. Indeed, the reduced hydroxylase activity of NamH can lead to: **i)** decreased PG integrity due to a lower availability of *N*-glycolyl groups to establish hydrogen bonds; **ii)** altered PG polymerization due to a lower availability of *N*-glycolylated PG precursors.

The contribution of the *N*-glycolylation of PG in host immune recognition and pathogenesis was assessed by performing infections of RAW 264.7 macrophages with a selected *namH*$^{-}$ mutant. Macrophages were found to be more effective at killing the induced knockdown mutant C2 ATc than any other bacteria at t=24h, suggesting that the presence of *N*-glycolylated PG promotes intracellular survival, possibly by increasing the fitness of mycobacteria inside macrophages.

In conclusion, the work presented in this thesis helped enlighten the role of the *N*-glycolylation of PG in antibiotic susceptibility by posing new hypothesis as to how NamH enables β-lactams resistance and raised important questions about the role of the *N*-glycolylation of PG in host-pathogen interactions, which may lead to a better understanding of TB pathogenesis in the future.

Keywords: Tuberculosis; Mycobacterial cell wall; Peptidoglycan modifications; Antibiotic resistance; Host-pathogen interactions.

Resumo

Nos últimos anos, a tuberculose (TB) tornou-se uma emergência de saúde global, principalmente devido ao surgimento de estirpes multirresistentes e extensivamente resistentes do seu agente etiológico, *Mycobacterium tuberculosis* (*Mtb*). Este problema é acentuado pela relativa ineficácia da vacina BCG e dos agentes antimicobacterianos atualmente conhecidos e, pela falta de alternativas terapêuticas para a TB. Com quase dois milhões de mortes por TB anualmente, é urgente encontrar uma vacina eficaz contra a doença, desenvolver ferramentas de diagnóstico rápido e criar melhores esquemas de tratamento. Assim, é fundamental um melhor esclarecimento do mecanismo da patogénese da TB, que é atualmente mal compreendido, devido à estrutura altamente complexa da parede celular micobacteriana. A camada de peptidoglicano (PG) da parede celular micobacteriana é particularmente relevante, uma vez que apresenta modificações únicas, das quais a *N*-glicolilação do ácido murâmico, catalisada pela atividade da hidroxilase do ácido *N*-acetil murâmico (NamH), é de especial interesse. Estudos anteriores demonstraram que a *N*-glicolilação do PG promove a resistência a antibióticos β-lactâmicos e à lisozima. Da mesma forma, outros estudos demonstraram que a *N*-glicolilação do PG parece estimular a imunogenicidade da parede celular micobacteriana. Apesar de não ser um gene essencial, o *namH* é altamente conservado em estirpes clínicas de *Mtb*, o que indica que a *N*-glicolilação do PG possui uma função importante na resistência a antibióticos e/ou na patogénese da TB. Assim, o objetivo principal desta tese foi modular a expressão do *namH* de modo a compreender a importância da *N*-glicolilação do PG micobacteriano na resistência aos antibióticos e no reconhecimento das micobactérias por parte do hospedeiro.

Para isso, vários mutantes *knockdown* do *namH* (*namH*$^{-}$) foram construídos em *M. smegmatis* e *M. tuberculosis* H37Ra, usando uma nova e eficaz ferramenta molecular de regulação da transcrição, o CRISPR de interferência (CRISPRi). Esta técnica baseia-se na expressão induzida, com anidrotetraciclina (ATc), de um complexo dCas9-sgRNA para impedir a transcrição da sequência alvo, o que permite a investigação da função do gene de interesse, neste caso do *namH*. Os mutantes *knockdown* do *namH* construídos em *M. smegmatis* foram caracterizados através da realização de várias experiências: curvas de crescimento e plaqueamento de diluições seriadas de cada cultura numa área circular delimitada designada por spot. Estas experiências mostraram que quer a deleção quer a repressão do gene *namH* não origina defeitos graves no crescimento de *M. smegmatis*, confirmando-se assim que este gene não é essencial. Além disso, foi possível observar um nível residual de toxicidade da dCas9$_{Sth1}$ durante as curvas de crescimento, ao verificar-se que o controlo *M. smegmatis*:PLJR962 cresce ligeiramente mais devagar na presença de indutor. Embora não tenha sido possível confirmar a repressão do *namH* em todos os mutantes *knockdown*, a repressão deste gene no mutante *knockdown* induzido *M. smegmatis* C2 ATc foi avaliada por PCR quantitativo em tempo real (qRT-PCR) e confirmada. Além disso, constatou-se que o CRISPRi provoca polaridade, ou seja, uma diminuição significativa da transcrição do gene a jusante. No entanto, não foi possível investigar de que modo a força da PAM escolhida, a cadeia de DNA alvo e o local alvo afetam a eficiência do CRISPRi.

De seguida, o papel da *N*-glicolilação do PG na suscetibilidade a vários antibióticos foi investigado através da realização de ensaios para determinar a concentração mínima inibitória (CMI) e a concentração mínima bactericida (CMB) de diversos β-lactâmicos (amoxicilina, cefotaxima, meropenem), na presença e ausência do inibidor de β-lactamase clavulanato, e de alguns agentes antimicobacterianos (etambutol e isoniazida) para todos os mutantes

knockdown em *M. smegmatis*, na presença e ausência de indutor. Os resultados obtidos mostraram que o meropenem é mais eficiente ao inibir o crescimento das micobactérias do que a amoxicilina ou a cefotaxima. Este efeito parece ser causado pela resistência inerente do meropenem às β-lactamases micobacterianas e, também, devido a uma inibição simultânea de L,D-transpeptidases e, algumas D,D-transpeptidases e D,D-carboxipeptidases. Além disso, constatou-se que a *N*-glicolilação do PG tem um papel significativo na resistência aos β-lactâmicos, uma vez que tanto o mutante de deleção do *namH* (ΔnamH) quanto os mutantes *knockdown* induzidos exibiram um fenótipo de suscetibilidade à maioria dos β-lactâmicos. Da mesma forma, foi observada uma correlação relevante entre a *N*-glicolilação do PG e o mecanismo de ação da cefotaxima pois os mutantes *namH*$^{-}$ exibiram uma diminuição particularmente significativa da CMI da cefotaxima ou da cefotaxima-clavulanato na presença de indutor. Verificou-se ainda que a principal β-lactamase de *M. smegmatis* (BlaS) hidrolisa os antibióticos β-lactâmicos com diferente eficiência, pois a adição de clavulanato aos β-lactâmicos diminuiu consideravelmente a CMI da amoxicilina, o que não aconteceu no caso da cefotaxima e do meropenem. Os ensaios de CMB mostraram que todos os β-lactâmicos possuem atividade bactericida para a maioria das amostras de *M. smegmatis* testadas, o que indica que a *N*-glicolilação do PG não afeta consideravelmente a capacidade dos β-lactâmicos matarem as micobactérias. No entanto, verificou-se que a indução do sistema de CRISPRi pareceu aumentar a atividade bactericida dos β-lactâmicos em alguns casos, em que os mutantes *knockdown* do *namH* eram mais facilmente mortos na presença de indutor.

Os ensaios de difusão em disco permitiram a determinação das zonas de inibição do meropenem para todos os mutantes *knockdown* construídos em *M. smegmatis*, com e sem indutor. Tal como tinha sido demonstrado anteriormente, os resultados destes testes sugeriram que a proteína NamH desempenha um papel na resistência ao meropenem, pois tanto o mutante de deleção do *namH* (ΔnamH) quanto os mutantes de *knockdown* do *namH* induzidos exibiram um fenótipo exacerbado de hipersuscetibilidade ao meropenem.

Estas experiências demonstraram que os mutantes de deleção/repressão do *namH* são mais suscetíveis à maioria dos β-lactâmicos. Este "fenótipo de hipersuscetibilidade aos β-lactâmicos" pode, então, ser explicado pela inibição: **i)** da atividade hidrolítica de β-lactamase da NamH; **ii)** da atividade de monooxigenase/hidroxilase da NamH, que modifica os açúcares do PG micobacteriano; **iii)** ambas as atividades, permitindo uma sinergia entre a inibição da atividade de β-lactamase e a inibição da *N*-glicolilação do PG. De facto, a redução da atividade de hidroxilase da NamH tem como consequências: **i)** a diminuição da integridade do PG devido a uma menor disponibilidade de grupos *N*-glicolil para estabelecer ligações de hidrogénio; **ii)** a alteração da polimerização do PG devido a uma menor disponibilidade de precursores do PG que estejam *N*-glicolilados. Assim, a deleção/repressão do *namH* pode ser utilizada em sinergia com o tratamento com β-lactâmicos para diminuir a integridade do PG micobacteriano.

A contribuição da *N*-glicolilação do PG para o reconhecimento pelo sistema imunitário do hospedeiro foi avaliada através da realização de infeções de macrófagos de ratinho RAW 264.7 com um mutante *namH*$^{-}$ selecionado, *M. smegmatis* C2. Verificou-se que os macrófagos são mais eficazes a erradicar o mutante de *knockdown* induzido C2 ATc do que qualquer outra bactéria no t=24h, o que sugere que a presença do PG *N*-glicolilado promove a sobrevivência intracelular, possivelmente ao aumentar o *fitness* das micobactérias dentro dos macrófagos. Esta observação parece indicar que a *N*-glicolilação do PG provoca um menor

reconhecimento das micobactérias por parte dos macrófagos, o que não é unânime visto que grande parte dos estudos anteriores verificou que a *N*-glicolilação do PG potencia o reconhecimento imunológico e a subsequente resposta imune.

Em conclusão, o trabalho apresentado nesta tese ajudou a esclarecer o papel da *N*-glicolilação do PG na suscetibilidade aos antibióticos, ao levantar novas hipóteses sobre a forma como a proteína NamH promove a resistência aos β-lactâmicos. Do mesmo modo, esta tese também levantou questões importantes sobre o papel da *N*-glicolilação do PG nas interações patogénio-hospedeiro, nomeadamente ao nível do reconhecimento imune. Os resultados apresentados e as conclusões alcançadas poderão ser relevantes para uma melhor compreensão da patogénese da TB e para o desenvolvimento de terapêuticas alternativas para o tratamento da TB, no futuro.

Palavras-chave: Tuberculose; Parede celular micobacteriana; Modificações do peptidoglicano; Resistência a antibióticos; Interações patogénio-hospedeiro.

Acknowledgments

This dissertation is the outcome of many hours of hard work and dedication of a phenomenal group of people, who have taught me and inspired me to want to be a scientific researcher. Therefore, I would like to demonstrate my appreciation for all of you.

First, I would like to thank my supervisor, Dr. Maria João Catalão for her immense support, patience, guidance, and motivation. I have known Maria João for some time now and she has been a true mentor to me. Thank you so much for believing in me and fueling my interest in microbiology! If it were not for you, I would not have learnt how much I enjoy science. I have learned a lot with your experience and your wisdom. I am glad to have chosen you as a supervisor because I enjoy the challenging and demanding experience of belonging to the ever-growing Mycobacterial Pathogenesis group. I would also like to thank you for considering me as a prospective PhD student. I am hopeful to learn more from you and from this amazing group of people. Thank you for helping me deliver this dissertation.

Second, I would like to thank Professor Cecília for the endless patience, availability, and for supporting me and all my colleagues in the master course of Biopharmaceutical Sciences. Moreover, I would like to emphasize how amazing the curricular program of this course is. The units of “Scientific Writing and Communication” and “Experimental Design in Research and Innovation”, during which I was supervised by Maria João Catalão, were helpful to the writing of this dissertation.

Third, I would like to show my appreciation to Nuno Carmo. I appreciate all the lessons you have taught me, either in science or in life. Thank you for helping me solve the hardest of problems. I am grateful to have had the chance listen to your reflections and questions on science and, on how the world works. I believe that listening to your “reasonings” has made me a better scientist. You have been incredibly helpful in the execution of this thesis. Thank you for helping me deliver an interesting dissertation.

Posteriorly, I would like to thank Francisco Miguel for everything he taught me (quite a lot!!) and for his endless support. Thank you for teaching me almost everything I know about the handling of mycobacteria in the lab. You have been of incredible assistance and encouragement to me. Thank you so much for mentoring me, being so patient, for always being there to help me and, for all the philosophic conversations we have shared throughout the years. You have been a great teacher and an awesome friend! Thank you for listening to my dramatic thoughts. Moreover, thank you for encouraging my scientific path and my interest in microbiology. You have had a very important role in my scientific career, I hope I can keep learning from you for a long time.

After, I would like to thank my lab partner, Mariana Marques, who was always super dedicated, super focused and super helpful! We started this journey as two master students trying to do our best and, ended up working as a “dream team”. Thank you so much for all your help, I know that I could not have done as much if it were not for you. Thank you for being a great listener, for all your support and encouragement, for our endless conversations about science, music, the Arrowverse series, whatever. I will always remember how curious it was that the radio played Adele when we were performing the MIC assays. We overcame a lot of obstacles together and I believe that our thesis are quite good because we had each other to rely on! I have learnt a lot from you, and I am glad we went through this process together. I deeply

appreciate you and I believe that you will be a great scientist one day. Thank you for being a GIANT part of this dissertation.

Next, I would like to thank David for his endless support and assistance. Thank you for helping me whenever I did not know what to do and for all the lab techniques and protocols you taught me. It was an incredible experience to work with you and I hope we get to work together again in the future. Thank you for your immense contribution to this dissertation.

Subsequently, how could I not thank Luis, Andreia and Angela? Angela, thank you for the company in the long hours of lab work. Andreia and Luis, thank you for letting me use your vortex! It was of great importance to this dissertation. In addition, I really appreciated all our conversations about techniques and how you helped me understand some science concepts I could not gather.

After, I want to thank my lab colleagues Bianca, Fred and Tomás. Bianca, I did not have the chance to know you well, but I saw a hardworking person in you, and I admire that. Fred, I am grateful for all our conversations, mainly those about politics. Thank you for helping whenever it was needed. Tomás, you were the most similar person to me when it came to cleaning and organizing things at the laboratory. Thank you for shinning the light on some chemistry concepts which I could not understand very well and, for all the joyful moments.

In sum, I would very much like to thank Prof. Elsa Anes for receiving me so well at her lab and all the colleagues at the Host-Pathogen Interactions group. You have all been incredible to me and you all have contributed to the success of this dissertation. Thank you very much!

I would also like to thank Dona São and Lucy for their assistance with the lab materials, I could never have done so much without your help!

In addition, I would like to thank Martin Pavelka, Stanley Qi, Atul Singh and Sarah Fortune for their availability to answer my scientific questions. I would also like to thank Prof. Madalena Ludovice for her incessant support. Thank you all for your help.

Finally, I must thank the most important people in my life, my friends and family. My friends have had an important role in this dissertation, for all the support, motivation, and companionship they showed to me. A sincere thank you to Francisca, Zé, Patrícia, Helena, and Rafael. Thank you for always being by my side, for always listening to me, and for helping me with my dilemmas and my moments of anxiety.

I want to thank my family for being so supportive and understanding during this period of my life. You have always supported me and my dreams and, that means a lot to me. I am incredibly thankful for all of you, you are those who make me who I am, and you will always be my greatest “fans”. Thank you mom, dad, Davide, grandma, grandpa, aunt, uncle and, the “little devils” Pedrinho and Tiaguinho. You are my rock and you all have contributed immensely to the success of this dissertation.

I am super proud to present this dissertation, which I have shared with all these special people. It has been a great year despite all the encountered obstacles. This dissertation was the outcome of months of research and hours of teamwork. I could say it took my blood, sweat and tears. I cannot thank you all enough.

Index

Index of Figures

Index of Tables

Abbreviation list

6-APA – 6-aminopenicillanic acid

7-ACA – 7-aminocephalosporanic acid

AG - Arabinogalactan

AMK - Amikacin

AMPs – Antimicrobial peptides

AMX – Amoxicillin

AMX+CLAV – Amoxicillin + Clavulanate

AO – Annealed oligos

AraTs - Arabinofuranosyltransferases

AsnB – Asparagine synthetase B

ATc - Anhydrotetracycline

BCG - Bacillus Calmette-Guérin

Bp – base-pair

BSL – Biosafety level

CAP – Capreomycin

Cas – CRISPR-associated

CCC – Chemically competent cells

cDNA – Complementary DNA

CFUs – Colony Forming Units

CIs – Confidence intervals

CLAV – Clavulanate

CM – Cytoplasmic membrane

CR – Complement receptors

crRNA – CRISPR RNA

CRISPR – Clustered Regularly Interspaced Short Palindromic Repeats

CRISPRi – CRISPR interference

CTX – Cefotaxime

CTX+CLAV – Cefotaxime-clavulanate

CW – Cell wall

dCas9 – Endonuclease-deficient Cas9

DEPC - Diethyl Pyrocarbonate

DHP-I – Dehidropeptidase-I

DMEM - Dulbecco's Modified Eagle's medium

DNA – Deoxyribonucleic acid

DOTS – Directly observed treatment strategy

DPA – Decprenylphosphoryl-β-D-arabinofuranose

ECC – Electrocompetent cells

EMB – Ethambutol

ETH - Ethionamide

EUCAST – European Committee on Antimicrobial Susceptibility Testing

FAS – Fatty acid synthetase

FBS – Fetal bovine serum

GalN - Galactosamine

GCs – Growth curves

GL - Glycolipids

GlcNAc – *N*-acetylglucosamine

GlfTs - Galactofuranosyltransferases

Glu - Glucose

HGT – Horizontal gene transfer

HIV – Human immunodeficiency virus

HMM – High molecular mass

IFN-γ – Interferon-γ

IGRAs – Interferon gamma release assays

IL – Interleukin

IMD - Immune deficiency

INH – Isoniazid

InhA – Enoyl-acyl carrier protein reductase

IR-TB – Isoniazid-resistant Tuberculosis

KAN – Kanamycin

KAN^R – Kanamycin resistant

LAM - Lipoarabinomannan

LB – Luria-Bertani

Ldts – L,D-transpeptidases

LEV – Levofloxacin

LK – Luria-Bertani media supplemented with kanamycin

LM - Lipomannan

LMM – Low molecular mass

LU – Linker unit

LTBI – Latent tuberculosis infection

MA – Mycolic acids

mAGP complex – Mycolyl-arabinogalactan-peptidoglycan complex

MAPK – Mitogen-activated protein kinase

MBC – Minimum bactericidal concentration

MBL – Metallo-β-lactamase

m-DAP – meso-Diaminopimelic acid

MDP – Muramyl dipeptide

MDR-TB – Multidrug-resistant tuberculosis

MEM – Meropenem

MEM+CLAV / Mc – Meropenem + Clavulanate

MIC – Minimum inhibitory concentration

MOI – Multiplicity of infection

MR – Mannose receptors

mRNA – messenger RNA

MRSA – Methicillin-resistant *Staphylococcus aureus*

Mtb – *Mycobacterium tuberculosis*

MTBC – *Mycobacterium tuberculosis* complex

MTBCA – *Mycobacterium tuberculosis* complex's common ancestor

MurNAc – *N*-acetyl muramic acid

MurNGlyc – *N*-glycolyl muramic acid

MurT/GatD - Lipid II isoglutaminyl synthase

MyD88 – Myeloid differentiation primary response protein 88

NAD – Nicotinamide adenine dinucleotide

NamH – *N*-acetyl muramic acid hydroxylase

namH^{-} - *namH* knockdown mutants

NaPyr – Sodium Pyruvate

NF-κB – Nuclear Factor kappa-light-chain-enhancer of activated B cells

NLRs – Nod-like receptors

NMHR – NOD2 mediated host responses

NOD – Nucleotide oligomerization domain

NTM – Non-tuberculous mycobacteria

OADC – Oleic acid dextrose catalase

OD_{600} - Optical density at 600 nanometers

OFX – Ofloxacin

OL – Outermost layer

ON - Overnight

ORF – Open reading frame

PAM – Protospacer adjacent motif

PAMPs – Pathogen Associated Molecular Patterns

PBPs – Penicillin binding proteins

PBS – Phosphate buffer saline

PCR – Polymerase chain reaction

PG – Peptidoglycan

PGBD – Peptidoglycan binding domain

PGRPs – Peptidoglycan recognition proteins

PK-PD – Pharmacokinetics-Pharmacodynamics

PIMs – Phosphatidyl-*myo*-inositol mannosides

PRRs – Pattern recognition receptors

R – Side chain

RD – Regions of difference

RGE – Relative gene expression

RIF - Rifampicin

RT – Reverse transcription

qRT-PCR – Quantitative real-time polymerase chain reaction

rRNA – ribosomal ribonucleic acid

RR-TB – Rifampicin-resistant Tuberculosis

SEM – Standard error of the mean

sgRNA – Single-guide RNA

SR – Scavenge receptors

STB – Smooth tubercle bacilli

TB – Tuberculosis

TbD1 - *Mycobacterium tuberculosis* specific deletion 1

TC – Tissue culture

TDM – Trehalose dimycolate

TDR-TB – Totally drug-resistant Tuberculosis

TLRs – Toll-like receptors

TMM – Trehalose monomycolate

TNF-α - Tumor Necrosis Factor α

tracrRNA – Trans-acting RNA

TSS – Transcription Start Site

Tyl – Tyloxapol

U – Enzymatic units

UDP-GlcNAc – Uridine diphosphate-*N*-acetylglucosamine

UTR – Untranslated region

UV - Ultraviolet

WHO – World Health Organization

WT – Wild-type

XDR-TB – Extensively drug-resistant Tuberculosis

Introduction

1. Tuberculosis

1.1. Epidemiology

Human tuberculosis (TB), mainly caused by the remarkably successful obligate pathogen *Mycobacterium tuberculosis* (*Mtb*), is the deadliest infectious disease in the world[1-3]. In 2018, there were around 10 million new cases of TB and, about 1.5 million people succumbed to the disease[1]. Most cases took place at South-East Asia (44%), Africa (24%) and the Western Pacific (18%), with a high burden in overpopulated low-income countries such as India and China (**Figure 1**)[1-3]. Additionally, Portugal is the western European country with the highest incidence rate, accounting for 23 infection cases per 100 000 inhabitants and 2 deaths per 100 000 residents[4]. Besides, TB is the top cause of death in HIV-positive people[1-4].

The aim of the World Health Organization (WHO) "End TB strategy" is to end the TB epidemics by 2035[1-3]. Therefore, the WHO has defined the subsequent priorities to decrease TB incidence and mortality worldwide: **i)** to find a new effective vaccine for TB; **ii)** to develop rapid and attainable diagnostic tools; **iii)** to create enhanced and shorter treatment regimens[1-3].

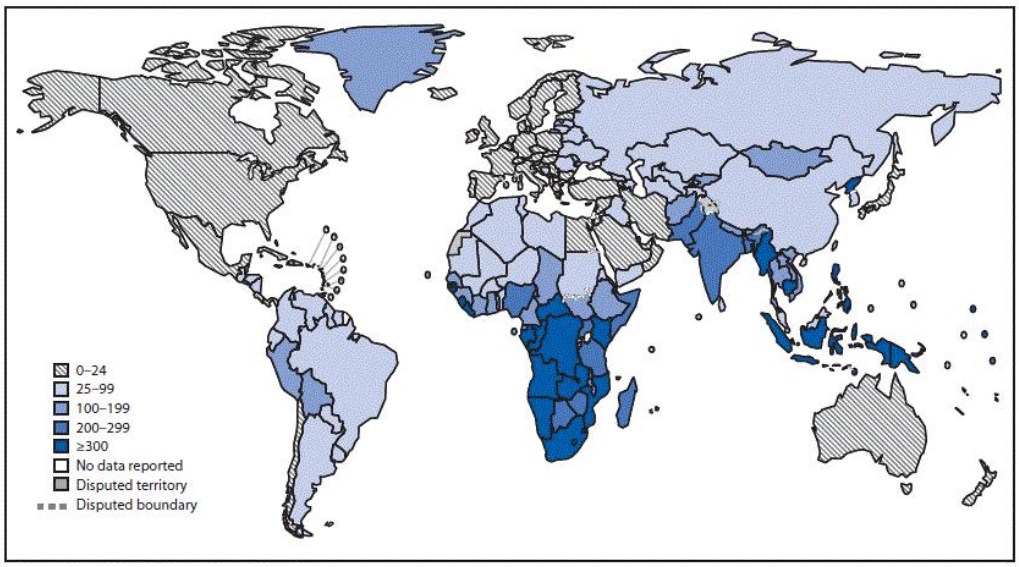

Fig. 1 - Tuberculosis incidence rates in 2017 (per 100,000 population). Adapted from MacNeil, A. *et al*. *MMWR. Morb. Mortal. Wkly. Rep.* **68,** 263–266 (2019).

Since *Mtb* is a severely contagious aero transmissible disease, it comes as no surprise that one-quarter of the world's population is latently infected, comprising the largest known ecological reservoir of *Mtb*, likely to evolve into future cases of active acute disease[1-3,5-7]. When tubercle bacilli containing droplets reach the respiratory tract of healthy individuals, the host mounts an effective adaptive immune response, enabling *Mtb* to infect its host for decades without causing active disease[6-9]. Latent TB is, therefore, a persistent infection characterized by the formation of a tubercle or granuloma, where the replication of *Mtb* and the host immune response are at balance[7-9]. However, a small fraction (10%) of the latently infected population can develop active TB, fueled by old age or sickness[6-9]. In this case, opportunistic mycobacteria can quickly replicate and become pathological to the host, disseminating through the lungs (pulmonary TB) and other organs (extrapulmonary TB)[7,9]. The consequent lesions

and symptoms are severe, and include bone lesions, lung cavitation, spitting blood, fever, fatigue and weight loss[6]. At this stage, TB-infected people usually transmit the disease to new hosts when they cough, speak or sneeze[6,7,9].

What makes *Mycobacterium tuberculosis* the most successful pathogen on Earth?

1.2. An ancient disease – the evolution of *Mycobacterium tuberculosis* throughout history

TB is an ancient disease as demonstrated by the existing archeological evidence[8,10]. The oldest molecular sample of *Mtb* is dated 17 500 years old and was taken from a bison bone in Wyoming, USA[11]. Other *Mtb* samples have also been found in 9000 years old Israeli human skeletons[12], in 4000 years old Egyptian mummies[13,14] and in 2000 years old Iron Age skeletons[15]. Hippocrates, the classical Greek writer, described TB as the disease "which proved fatal to many persons"[10].

It was during the Renaissance, when Europe was totally scourged by TB, that the first steps were taken to clarify its pathogenesis[10]. René Laennec, known for inventing the stethoscope, was the first to affirm that TB was not only pulmonary and to describe the main symptoms of the disease[10,16]. In 1865, Jean-Antoine Villemin inoculated a rabbit with a tuberculous sample only to find out that the rabbit suffered from a widespread TB infection a few months later[10]. It was only in 1882 that Robert Koch announced the isolation of the etiologic agent of TB, for which he was awarded the Nobel Prize in 1905[10,17]. At that time, a vaccine to fight TB was extremely desired and, investigations using *Mycobacterium bovis* were conducted albeit with poor results since *M. bovis* was observed to be as virulent as *M. tuberculosis*. In 1908, Albert Calmette and Camille Guérin observed that mycobacteria seemed to grow less virulent on glycerin potato medium and then, aimed to produce an attenuated strain to be used as an anti-TB vaccine[10,18]. The Bacillus Calmette-Guérin (BCG) vaccine was first used in 1921 and, since then 4 billion individuals have been vaccinated, leading to a severe decline in TB-associated mortality[10,19,20]. Ever since, significant advancements were made with the discovery of bactericidal antibiotics against TB such as streptomycin (1944), isoniazid (1952) and rifampicin (1957)[10,19].

1.2.1. The genus *Mycobacterium*

The genus *Mycobacterium* comprises more than 170 species of gram-positive, acid-fast, non-motile, rod-shaped aerobic bacteria within the phylum of Actinobacteria[5,6,21]. *Mycobacterium* are characterized by a GC-rich genomic DNA and, most are environmental organisms, also known as non-tuberculous mycobacteria (e.g.: *Mycobacterium smegmatis*)[5,21].

As illustrated in **Figure 2**, Rue-Albrecht *et al.* have been able to demonstrate the mycobacterial phylogenetic relationships using comparative functional genomics[22]. While some mycobacterial species are slow-growers and representative human pathogens (the *Mycobacterium tuberculosis* complex, *Mycobacterium leprae* and *Mycobacterium ulcerans*), non-tuberculous mycobacteria (NTM) can be either slow or fast growers and are opportunistic pathogens, only infecting immunocompromised individuals[5,6].

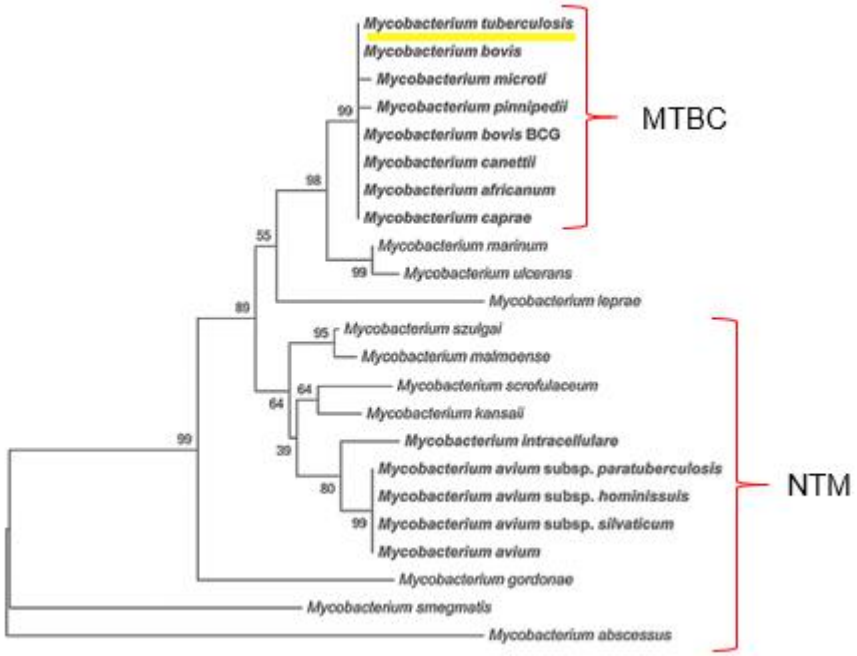

Fig. 2 – A phylogenetic tree of mycobacteria based on partial 16S rRNA sequences. Adapted from Rue-Albrecht, K. *et al. Front. Immunol*. **5,** 1–14 (2014).

1.2.2. The *Mycobacterium tuberculosis* complex

The *Mycobacterium tuberculosis* complex (MTBC) comprises several slow-growing species and sub-species that can cause tuberculosis in humans or in animals[5,8,23]. The MTBC members share more than 99.95% of nucleotide sequence identity and an identical 16S rRNA sequence[5,8,22]. This genome similarity coupled with little evidence for recombination and horizontal gene transfer (HGT) indicates that these species have evolved from a common ancestor[5,8,22,23]. However, the members of the MTBC have developed distinct host ranges[5,8,22]. According to their host range, these species can be placed into three groups: the human-adapted MTBC, the animal-adapted MTBC and *Mycobacterium canettii*[5,8,19].

1.2.2.1. The human-adapted MTBC

Both *M. tuberculosis* and *M. africanum* are known to cause TB in human hosts and thus, comprise the human-adapted MTBC[5,8,24]. These human-adapted forms can be further classified as seven diverse phylogenetic lineages[5,8,24], some of which are globally widespread such as L2 (*Mtb* strains from East Asia, including the Beijing strains) and L4 (*Mtb* strains widespread through Europe, America and Africa, including the Harleem, X and LAM families) while others have adapted to a certain population and possess a characteristic geographical distribution: L1 (*Mtb* strains present in East Africa, The Philippines and the Rim of the Indian Ocean), L3 (*Mtb* strains found in East Africa and Central Asia), L5 (*M. africanum* West African clade 1), L6 (*M. africanum* West African clade 2) and L7 (strictly Ethiopian *Mtb* lineage). The geographical distribution of these lineages reflects both human migrations as well as adaptations to certain populations throughout history: some lineages can infect and persist in different populations while others have specialized in a preferred host population[5,8,24]. Previous

studies have revealed that disease transmission is higher between individuals of the same population[5,8,25] and that, in this case, TB symptoms are less severe[26].

According to Comas *et al.*, the common ancestor of all MTBC members (MTBCA) originated in Africa approximately 73 000 years ago[23,24]. The MTBCA is thought to have been represented by environmental opportunistic bacteria with a broad host range, including humans[27,28]. Through time, the MTBC members became professional pathogens since they: **i)** lost the ability to perform HGT and to replicate outside a host; **ii)** became more virulent; **iii)** overcame the immune system of the host to guarantee disease transmission[5,8,28]. At this point, most of the MTBC members were able to specialize in different hosts[5,8].

The phylogenetic history of the MTBC reveals genome downsizing through the deletion of nonessential sequences and the inability to repair genomic deletions due to nonexistent HGT as the principal mechanism of evolution of these species[5,22,23,27]. Comparison genomic analysis between MTBC lineages has revealed that while some lineages lack a DNA sequence named TbD1 (TbD1$^-$), other "more conserved" lineages possess this sequence (TbD1$^+$)[23,24,27]. Therefore, MTBC lineages can be classified as modern (TbD1$^-$) or ancient lineages (TbD1$^+$)[23,24,27]. The analysis of the phylogenetic tree depicted in **Figure 3** demonstrates that animal strains (e.g.: *M. bovis*) and the common ancestor of *M. africanum* strains have diverged early (~70 000 years ago) from the MTBCA[24,27]. The members of the MTBC can be distinguished by the presence or absence of RD *loci*[23,27]. While *M. africanum* lineage 5 has lost the RD9 region, lineage 6 is more closely related with animal strains since it has lost the RD7, RD8, RD9 and RD10 sequences[27,29]. Meanwhile, the common ancestor of all *Mtb* lineages emerged[5,8,24]. In contrast to *M. africanum*, most regions of difference (namely RD1, RD2, RD4, RD7, RD8, RD9, RD10, RD12, RD13 and RD14) are highly conserved in *Mtb* strains[27]. In fact, RD1 is thought to be essential for the virulence of *Mtb*[30]. Around 67 000 years ago, the branching of the ancient lineage 1 (TbD1$^+$) occurred concurrently with the first human migrations and, was swiftly followed by the divergence of ancient lineage 7[8,24]. After, a new branching event originated the common ancestor of all modern lineages (TbD1$^-$)[24,27]. Consequently, the genomes of modern lineages are smaller when compared with the MTBCA genome. The first modern lineage (L2) appeared 35 000 years ago[24]. This branching event was quickly followed by the emergence of lineages 4 and 3[8,24].

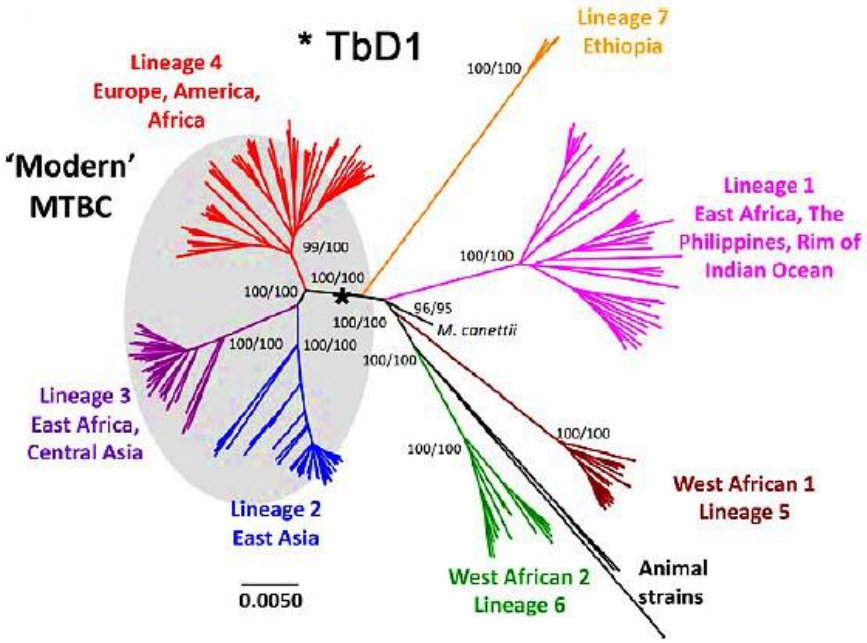

Fig. 3 - Genome-wide phylogeny of the MTBC. The lineages present in the grey area are the 'modern' lineages, while the other lineages are 'ancestral'. The asterisk indicates the occurrence of a TbD1 deletion. Adapted from Comas, I. *et al. Nat. Genet.* **45,** 1176–1182 (2013).

Lately, globalization has led to a rise in the number of patients infected by nonendemic strains, consequently suffering a more severe form of TB disease[19]. Indeed, modern lineages such as L2 and L4 have caused most of all worldwide TB infections[5,8,29,31]. Hence, globalization has facilitated the emergence and spread of drug-resistant strains of *Mtb*, making the eradication of TB a challenging goal[19]. Some L2 and L4 strains such as Beijing and Harleem have been accountable for the main outbursts of drug-sensitive and drug-resistant TB[8,31,32]. Ford *et al*. have demonstrated that L2 *Mtb* strains develop *in vitro* resistance to isoniazid and ethambutol three times faster than L4 *Mtb* strains[33]. Moreover, these "modern" strains are thought to be more transmissible, virulent and pathogenic when compared with ancient lineages (e.g.: *M. africanum* L5 and L6), indicating their evolutionary success[24,31,32]. Previous studies showed that L2 progresses five times faster to active TB than *M. africanum* L6[34]. This increase in virulence is often seen as a strategy to optimize transmission rates in the presence of increasing population densities, which accompanied human migrations throughout history, starting in the Neolithic period until today[24,29]. In contrast, latency or persistence of *Mtb* inside host macrophages might have evolved as a strategy for *Mtb* to survive in small populations[5,8,32]. Furthermore, Comas *et al*.[35] have revealed that the MTBC and *Homo sapiens* have co-evolved for a long time: **i)** essential mycobacterial genes were conserved during the species evolution[35]; **ii)** genes encoding the epitopes of mycobacterial antigens were hyper-conserved throughout time[35]. These findings have suggested that the pathogen benefits from being recognized by the host immune system, namely by causing strong detrimental inflammatory responses and by increasing the likelihood of *Mtb* transmission[8,32,35].

1.2.2.2. The animal-adapted MTBC

The animal-adapted MTBC includes *Mycobacterium bovis* (cattle), *Mycobacterium pinnipedii* (seal and sea lions), *Mycobacterium caprae* (goats), *Mycobacterium microti* (voles), *Mycobacterium orygis* (antelopes) and others[5,8]. These species seem to have a broad host range since they can cause infection in several animals and in humans, although with a lower transmissibility[5,8]. Until the last decade, it was believed that humans acquired TB from cattle during the Neolithic period, when animal domestication started[8,9,23,27]. However, the animal-adapted forms are nowadays thought to be more modern than the human-adapted MTBC because: **i)** they have smaller genomes than human-adapted lineages[5,8] and; **ii)** animal-adapted species have lost the RD7, RD8, RD9 and RD10 regions of difference[23,27].

1.2.2.3. *Mycobacterium canettii*

M. canettii belongs to a group of environmental opportunistic bacteria termed smooth tubercle bacilli (STB), originated from the Horn of Africa[5,27,28,36]. These bacteria rarely cause TB disease[5,8,36]. *M. canettii* is mostly successful at infecting expatriate individuals, children and the immunocompromised[5,8,36]. STB have larger genomes than most MTBC species[5], undergo horizontal gene transfer[5,8,28], have conserved regions of difference[22,27] and, have a lower virulence than *Mtb* H37Rv[8,28]. Thus, *M. canettii* is thought to have diverged from the common ancestor of all mycobacteria (oftentimes called *Mycobacterium prototuberculosis*) before the emergence of non-smooth MTBC lineages[27-29].

1.3. The problematic of antibiotic resistance

Despite the clinical progress attained in the 20th century, with the creation of a live attenuated vaccine (BCG) and the discovery of antimycobacterial agents, the excessive misuse of antibiotics has led to the emergence of multidrug-resistant (MDR; resistant to both rifampicin and isoniazid), extensively drug-resistant (XDR; resistant to rifampicin, isoniazid at least one fluoroquinolone and a second-line injectable agent) and totally drug-resistant (TDR; resistant to isoniazid, rifampicin, streptomycin, ethambutol, pyrazinamide, ethionamide, para-aminosalicylic acid, cycloserine, ofloxacin, amikacin, ciprofloxacin, capreomycin, kanamycin) strains of *Mtb*[4]. While multi-drug resistance is frequently common in TB-treated patients who undergo relapse (**Figure 4**), this "acquired resistance" is not the only form of MDR-TB[6].

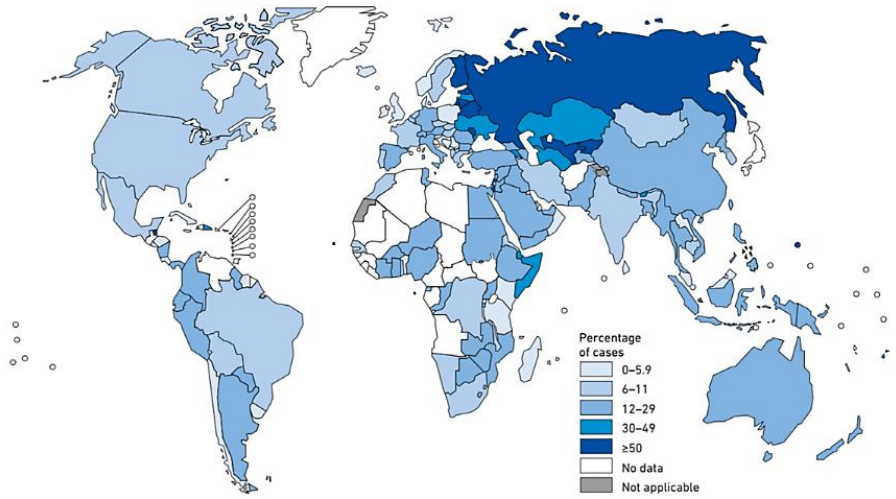

Fig. 4 – **Percentage of MDR-TB in previously treated cases in 2018.** Adapted from WHO.

In fact, "primary resistance" occurs when healthy people become infected after they contact with MDR-TB-infected people[6]. As pictured, MDR-TB is particularly widespread in India, China and Russia[3]. In 2018, the number of new cases of MDR-TB (**Figure 5**) was estimated to be around 187 000, of which 6.2% were XDR-TB[1]. Currently, only 56% of MDR-TB infections and 23% of XDR-TB infections are successfully treated[1]. Hence, drug-resistance remains a major health concern, accentuated by the intrinsic resistance of *Mtb* to β-lactams and by the lack of effective alternative therapeutics[1,3,4,5]. Thus, new strategies are urgently needed to replace the current therapeutic regimens, to reduce treatment duration and, to fight MDR-TB infections[4].

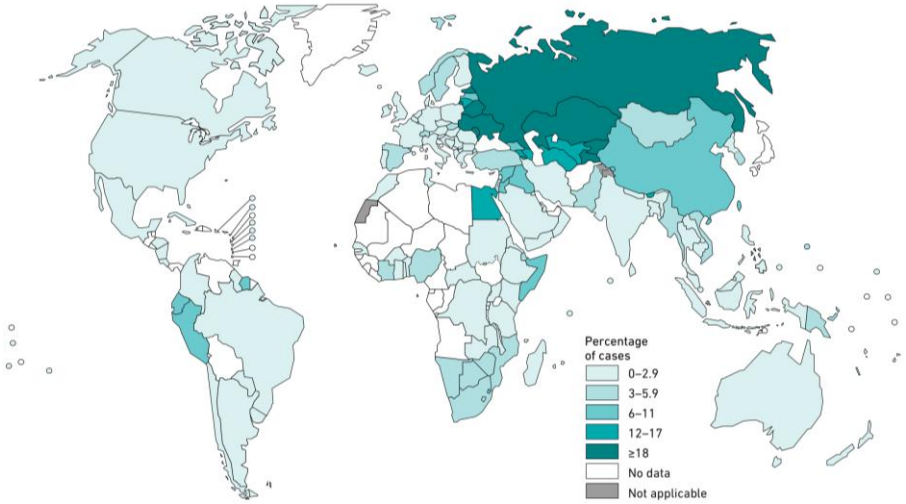

Fig. 5 – **Percentage of new cases of MDR-TB in 2018.** Adapted from WHO.

1.4. Current treatment of TB and new directives to treat drug-resistant TB

The current treatment of drug-susceptible TB consists of a highly efficient and cost-effective 6-month combination regimen of four first-line drugs (isoniazid, rifampicin, ethambutol, and pyrazinamide) under a directly observed treatment strategy (DOTS)[3,37]. This type of strategy is recommended by the WHO in order to avoid poor patient adherence, which typically leads to treatment failure, relapse and, the emergence of drug-resistance[3,37]. Not unlike active disease, latent TB also requires treatment to decrease the only known ecological reservoir of *Mtb*. The drug regimens employed to treat latent TB include isoniazid once daily for 6 or 9 months, isoniazid plus rifampicin once daily for 3–4 months, rifampicin once daily for 3–4 months, and isoniazid plus rifapentine once a week for 3 months[3].

Despite the effort put into treating TB, resistance to first-line drugs is a recognized public health problem[1,3]. Over the last decades, the incidence of rifampicin-resistant tuberculosis (RR-TB), isoniazid-resistant tuberculosis (IR-TB) and MDR-TB (resistance to both rifampicin and isoniazid) has severely increased, threatening the targets of the "End TB Strategy" set by the WHO[3,37]. In patients with confirmed rifampicin-susceptible and isoniazid-resistant tuberculosis, a 6-month treatment with rifampicin, ethambutol, pyrazinamide and levofloxacin is recommended[37]. Since first-line drugs cannot be used to fight MDR-strains of *Mtb*, drug regimens to fight MDR-TB tend to be longer (approximately 18–20 months)[37]. These drug regimens ought to include at least four anti-TB agents likely to be effective in the first 6 months (preferentially fluoroquinolones, bedaquiline, linezolid, clofazimine and cycloserine) and three agents thereafter[37]. The use of injectable agents is no longer recommended in long treatment regimens as fully oral regimens are now endorsed by the WHO[37]. However, shorter MDR-TB regimens, with the duration of 9-12 months, may be offered to eligible patients[3,37]. These short drug regimens consist of seven drugs (kanamycin, moxifloxacin, protionamide, clofazimine, pyrazinamide, plus high-dose ethambutol and high-dose isoniazid) and, usually increase the likelihood of treatment completion[3,37].

In the future, the WHO is expected to recommend all-oral MDR/RR-TB drug regimens, with less than 12-months duration[38]. The preferred regimens will include a combination of pretomanid, bedaquiline and linezolid or the use of bedaquiline concurrently with delamanid for more than 6 months[38]. However, incorrect or incomplete treatment of MDR-TB can cause relapse, leading to the emergence of XDR-TB and TDR-TB[1,3]. These particularly dangerous strains of *Mtb* threaten the eradication of this ancient disease. Thus, further research should be done to improve treatment options and assure the treatability of TB.

2. Model organisms

The direct study of *Mtb* is essential to gain insight into its pathogenesis[39]. However, the virulent strain *Mtb* H37Rv is considered a laborious study object: **i)** *Mtb* is only manageable in a biosafety level 3 laboratory, requiring substantial training prior to handling; **ii)** *Mtb* has a 24-hours generation time, taking one month to yield colonies and making each experiment extremely time consuming[39,40]. Hence, simpler and less dangerous mycobacterial models are frequently used to study *Mtb*'s pathogenesis and virulence: *Mycobacterium smegmatis* and the highly attenuated strain *Mtb* H37Ra.

2.1. *M. smegmatis*

Unlike *Mtb*, *M. smegmatis* is a fast-growing saprophytic bacterium that rarely causes disease[39,40]. Accordingly, the homology between their genomes, earned *M. smegmatis* a place as a mycobacterial study model. This mycobacterial species has a short doubling time (3 hours), is easy to manipulate and, generates colonies in two days[39,40]. Until the late 20th century, an effective DNA transfer system for *Mtb* did not exist[40]. It was the effort of Jacobs, Snapper and Kieser that made possible the development of *Escherichia coli*–mycobacterial shuttle plasmids, which presented the simplest approach to identify the drug targets or virulence factors of *Mtb*[40,41]. These shuttle plasmids were based on the L1 temperate phage, and its ability to site-specifically integrate a kanamycin resistance *cassette* into the genome of *M. smegmatis*[40,41]. The use of a random insertion library to interrogate the DNA sequence that caused replication of the plasmid pAL5000[42], isolated from *Mycobacterium fortuitum*, was also crucial[40,41]. The next step was to electroporate *M. smegmatis* with recombinant DNAs from the *E. coli* plasmid pAL5000 chimeric library[40,41]. The resulting transformants were isolated and, electroporated into both *E. coli* and *M. bovis* BCG, thus validating the first plasmid transformation system for mycobacteria[40,41]. One of the original transformants (namely, mc^{2}154) was propagated in the absence of kanamycin[40,43]. A resulting clone, mc^{2}155, was found to yield 10^4 to 10^6 transformants when compared to the parental strain[40,43]. Thus, *M. smegmatis* mc^{2}155 is a particularly convenient model of study due to its ease of genetic manipulation, mainly because of its high transformation efficiency.

2.2. *M. tuberculosis* H37Ra

In 1905, Edward Baldwin isolated the virulent strain *Mtb* H37 from a 19-year-old male with active pulmonary tuberculosis[44]. *Mtb* H37 is the parental strain of two common tuberculosis study models, the virulent strain H37Rv and its avirulent counterpart H37Ra[44,45]. Both H37Rv and H37Ra were obtained by repeated *in vitro* passages of the H37 clinical isolate through laboratory media[44,45]. While H37Ra produced smooth colony morphology and did not generate disease in guinea pigs, its virulent counterpart H37Rv produced a rough colony morphology and retained the virulence of the parental strain H37[44,45]. The avirulent strain H37Ra differs severely from its virulent counterpart, being characterized by: **i)** smooth and raised colony morphology[44,45]; **ii)** loss of cord formation[44,46]; **iii)** reduced survival under anaerobic conditions[44,47] and inside the macrophages[44]; **iv)** decreased ability to disrupt phagosomes[44,48]; and **v)** unreported virulence in guinea pigs[44,45] and mice[44,49].

The genetic basis of the virulence attenuation of H37Ra has been interrogated through genetic comparisons between H37Ra, H37Rv and the closely related clinical strain CDC 1551 (**Figure**

6)[44]. While these studies revealed a highly conserved gene content and order between H37Rv and H37Ra, they also identified 76 single nucleotide polymorphisms in 32 genes, amongst which mutations in genes involved in transcription, metabolic functions (e.g.: mutation in *mazG*), cell wall biosynthesis (e.g.: mutation in *phoP*), *in vivo* growth (e.g.: decreased expression of *sigC*) and virulence (namely variations in the PE/PPE/PE-PGRS family)[44].

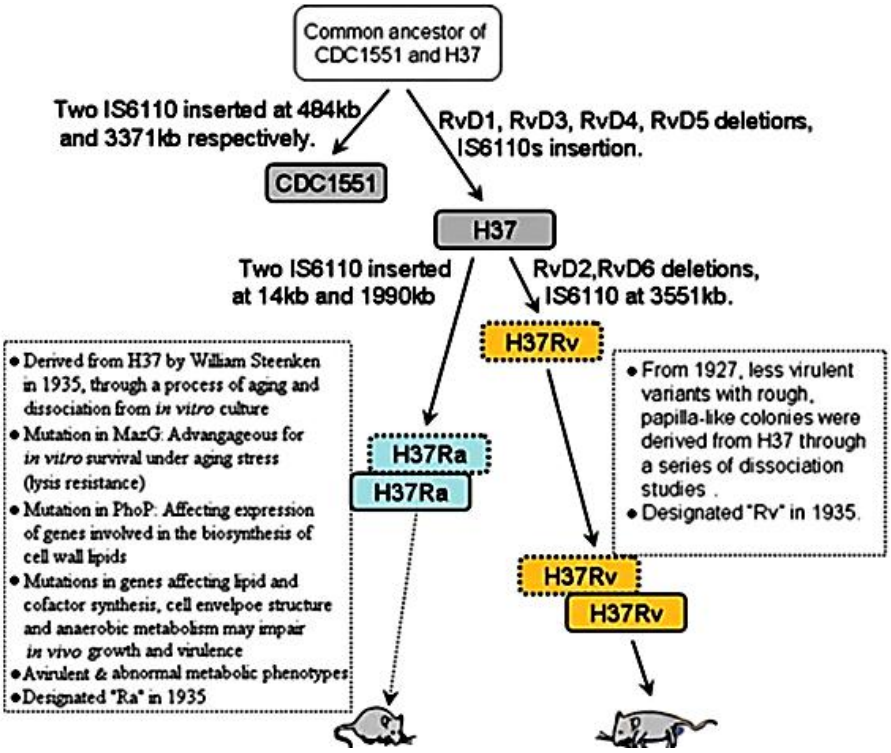

Fig. 6 - **Phylogenetic Relationship of H37Ra, H37Rv, H37, and the closely related clinical isolate CDC1551.** The various appearances of H37Ra and H37Rv represent frequent *in vitro* passages. Adapted from Zheng, H. *et al. PLoS One* **3,** e2375 (2008).

Because *Mtb* H37Ra is avirulent, it can be manipulated in a BSL-2 environment and has lower costs, being less laborious while maintaining the core characteristics of *Mtb* H37Rv[44,50]. Therefore, it is a widely used study model to study the pathogenesis, antibiotic resistance and cell wall modifications of *Mtb*[44]. Additionally, H37Ra strain is comparable to H37Rv in regards the prediction of antibiotic susceptibility of clinical isolates[50].

What makes *Mtb* a very successful human pathogen?

3. The mycobacterial cell wall

The great success of *Mtb* as a pathogen relies on its peculiar cell envelope (**Figure 7**), which includes three entities: **i)** a conventional cytoplasmic membrane (CM); **ii)** a notable, complex cell wall (CW); and **iii)** an outermost layer (OL)[51-55]. The CW, commonly mentioned as the mycolyl-arabino-galactan-peptidoglycan (mAGP) complex, consists of three main structural layers: **i)** a very cross-linked and modified network of peptidoglycan (PG); **ii)** a highly branched arabinogalactan (AG) polysaccharide; and **iii)** characteristic long-chain mycolic acids (MA)[51-

[55]. The mAGP complex is essential for cell viability, virulence, and innate immune response modulation during mycobacterial infections[51-55]. Moreover, the mAGP complex contributes to the intrinsic drug resistance of *Mtb* to various anti-TB agents[51,54,55]. Indeed, inhibition of the mAGP complex assembly has been proven useful for TB therapeutics; drugs such as ethambutol, D-cycloserine, ethionamide and isoniazid effectively target the CW biosynthesis[54-56]. The emergent resistance to these drugs is caused by the accumulation of chromosomal mutations in genes encoding proteins involved in CW biosynthesis, because of the selective pressure associated with undue antibiotic use[54-56].

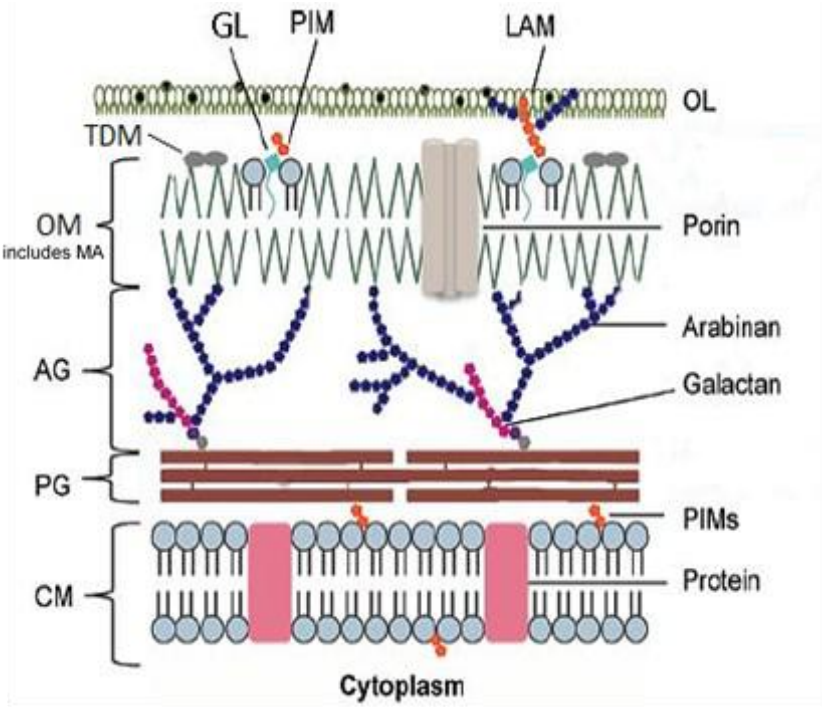

Fig. 7 – Schematic representation of the mycobacterial cell envelope, which includes a cytoplasmic membrane (CM), the mAGP complex and, an outermost layer (OL). The mAGP complex is composed of peptidoglycan (PG), arabinogalactan (AG) and mycolic acids (MA). The inner part of the outer membrane (OM), is linked to the OL by glycolipids (GL), including trehalose dimycolate (TDM) and phosphatidyl-*myo*-inositol mannosides (PIMs), such as lipoarabinomannan (LAM). GLs are virulence factors, playing a role in host-pathogen interactions. The OL or capsule is found on the outside of the CW. In *Mtb*, the OL is constituted by a layer of proteins, glucans, and a few lipids. In *M. smegmatis*, the OL is mostly composed of proteins. Adapted from Catalão, M. J. *et al*. *Front. Microbiol*. **10,** 1–11 (2019).

3.1. Mycolic acids

The MA are high molecular weight long-chain α-alkyl-β-hydroxy fatty acids that contain up to 90 carbons (up to 25C on the α-branch and 60C on the meromycolic acid chain)[51-53]. The MA are characterized by the presence of alkyl chain double bonds and, by rigidly organizing themselves side by side, perpendicularly to the surface of the cell[51-53]. While the MA are attached to the AG, the MA also represent the inner, insoluble part of the asymmetric lipid bilayer whereas the outer leaflet is characterized by a higher permeability and is composed by a mixture of extractable glycolipids (GL), which have an important role in the context of host-pathogen interactions[51-53]. These GLs trehalose dimycolate (TDM), trehalose monomycolate

(TMM) and phosphatidyl-*myo*-inositol mannosides (PIMs)[51-53]. Therefore, the asymmetric lipid bilayer acts as a differential permeability barrier to both nutrients and substances (e.g.: antibiotics) and is essential for cell viability and virulence[51-53]. The MA can be classified as α-mycolates (*cis*), methoxy-mycolates (*cis*/*trans*) or keto-mycolates (*cis*/*trans*)[51-53].

3.1.1. Mycolic acids biosynthesis

The biosynthesis of MA (**Figure 8; Table 1**) starts in the cytoplasm, with the action of two distinct fatty acid synthetases (FAS): FAS-I and FAS-II[52,53]. First, the FAS-I system synthetizes short-chain esters (C_{16-24}), that can form a saturated α-branch (C_{24}) or be extended by FAS-II in order to generate the meromycolate chain (C_{56})[52,53]. The FAS-II system involves the stepwise action of five enzymes (FabH, MabA, HadAB/BC, InhA, KasA/B), which increase the acyl chain by two carbons each cycle until the saturated long-chain meromycolate (C_{42-62}) is produced[52,53,57]. Afterwards, the meromycolate chain suffers several modifications (*cis-trans*-cyclopropanation and addition of keto and methoxy groups), which affect CW permeability and modulate the host immune response[52,53]. The activation of the modified meromycolates is catalyzed by FadD32 and, the resulting meromycolyl-AMP is converted to a mycolic β-ketoester by the action of Pks13[52,53]. After, a reduction step catalyzed by CmrA generates a mature mycolate[58], which is then transported to the PG-AG complex by MmpL3, in the form of TMM[52,53]. Later, the attachment of MA to AG is catalyzed by the antigen 85 mycolyltransferase complex, also responsible for the generation of TDM/cord factor, a virulence factor of *Mtb*[52,53].

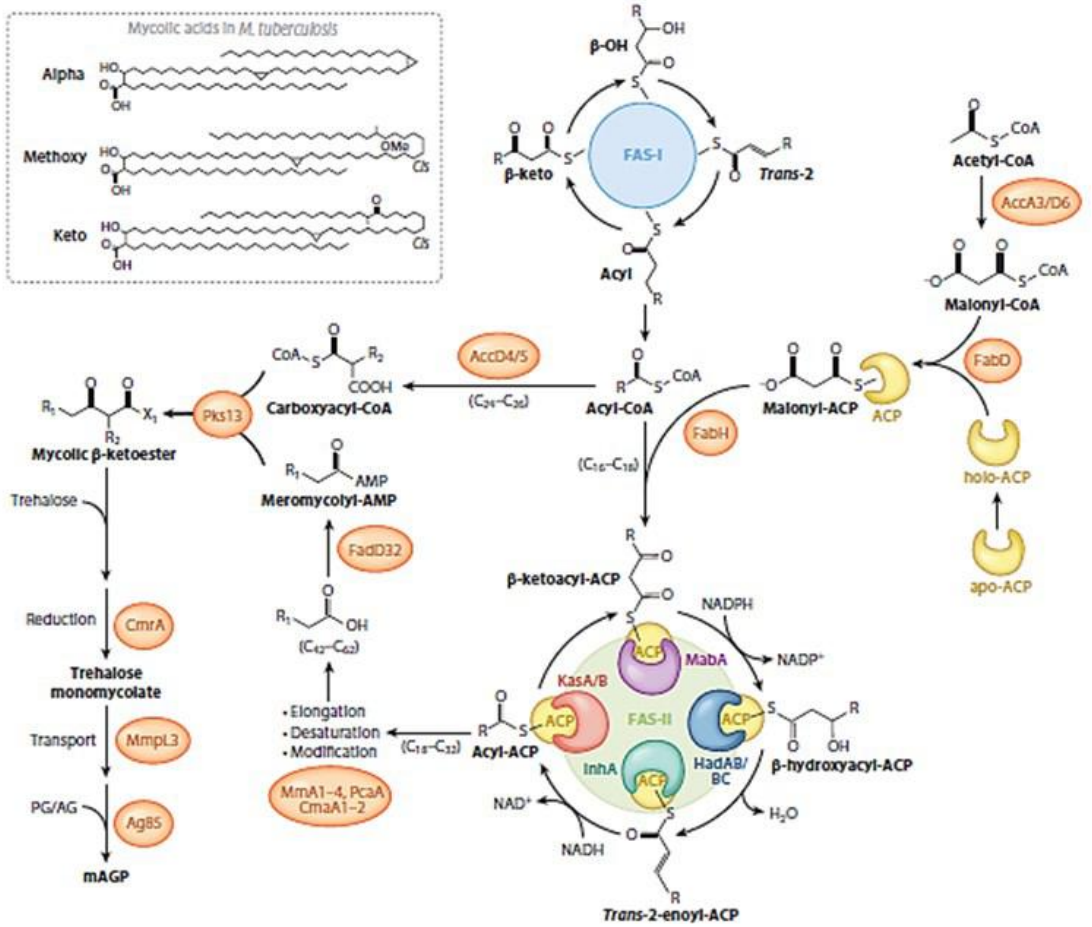

Fig. 8 – Mycolic acid biosynthesis in *Mycobacterium tuberculosis*. Adapted from Jankute, M. *et al*. *Annu. Rev. Microbiol.* **69**, 405–423 (2015).

Anti-TB agents usually target the synthesis of MA, since antibiotic resistance is often attributed to their impermeability[51-53,59]. One example of a promising drug target is the *inhA* gene, that encodes the enoyl-acyl carrier protein reductase (InhA), an essential enzyme in the FAS-II extension cycle[54]. Both the 1st-line antibiotic isoniazid (INH) and its analogue ethionamide (ETH) are pro-drugs that are activated via cleavage by KatG and EthA, respectively[54,60]. This activation reaction generates an isonicotinic acyl radical, which will form a complex with nicotinamide adenine dinucleotide (NAD)[54,60]. This INH-NAD adduct will bind to InhA, inhibit its enzymatic activity and, eventually lead to cell death[54,60]. Resistance to isoniazid is often accompanied by ethionamide resistance and, arises mainly due to mutations in *inhA* or *katG*[54,60] or, due to the overexpression of *inhA*[54,60].

Table 1 – Relevant information about proteins involved in MA biosynthesis.

Mycolic acid biosynthesis							
Protein			Gene identifier			Essentiality	Inhibitors
			Mtb H37Rv	*Mtb* H37Ra	*M. smegmatis*		
FasI			Rv2524c	MRA_2551	MSMEG_4757	Essential	5-chloropyrazinamide
FasII	FabH		Rv0533c	MRA_0540	-	Non-essential	2-carboxy-1-(6-chloropiperonyl)-5-(2,6-dichlorobenzyloxy)indole; 4,5-dichloro-1,2-dithiole-3-one; Thiolactomycin analogues
	MabA		Rv1483	MRA_1493	MSMEG_3150	Essential	Pteleoeagic acid
	HadAB/BC	HadA	Rv0635	-	MSMEG_1340	Essential	Thiacetazone; Isoxyl; NAS-21 analogues 4/5
		HadB	Rv0636	MRA_0647	MSMEG_1341	Essential	Thiacetazone; Isoxyl; NAS-21 analogues 4/5; Butein, isoliquirtigenin, 2.2',4' - trihydroxychalcone and fisetin
		HadC	Rv0637	-	MSMEG_1342	Non-essential	Thiacetazone; Isoxyl; NAS-21 analogues 4/5
	InhA		Rv1484	MRA_1494	MSMEG_3151	Essential	Isoniazid; Ethionamide; Triclosan; GSK693; Arylamides; Pyrrolidine carboxamides
	Kas A/B	KasA	Rv2245	MRA_2265	MSMEG_4327	Essential	Cerulenin; Platensimycin; Thiolactomycin; GSK3011724A
		KasB	Rv2246	MRA_2266	MSMEG_4328	Essential	Cerulenin; Platensimycin; Thiolactomycin
		FadD32	Rv3801c	MRA_3841	MSMEG_6393	Essential	Diarylcoumarin
		Pks13	Rv3800c	MRA_3840	MSMEG_6392	Essential	Benzofuran; Thiophenes
		CmrA	Rv2509	MRA_2535	MSMEG_4722	Essential	
		MmpL3	Rv0206c	MRA_0214	MSMEG_0250	Essential	SQ109; THPP; BM212; Adamantyl urea; C215
Ag85		FbpA	Rv3804c	MRA_3844	MSMEG_2078, MSMEG_6398	Non-essential	i3-AG85
		FbpB	Rv1886c	MRA_1897	MSMEG_2078, MSMEG_6398	Non-essential	
		FbpC	Rv0129c	MRA_0136	MSMEG_3580	Non-essential	
		FbpD	Rv3803c	MRA_3843	MSMEG_6396	Non-essential	

3.2. Arabinogalactan

The AG is a hydrophilic polysaccharide mostly composed of arabinose and galactose in the furanose ring form, as it represents 35% of the total mass of the CW[51-54,61]. Its structure can be divided into three individual components: the linker unit (LU), galactan and arabinan[51-54,61]. The LU connects about 11% of muramyl pentapeptide residues of PG to the galactan chain of AG[51-54,61]. The galactan component consists of 30 β-D-galactofuranosyl residues arranged with alternating β-(1→5) and β-(1→6) glycosidic linkages[51-54,61]. Three highly branched arabinan chains, each composed of approximately 30 residues of D-arabinofuranosyl, are linked to some galactan residues through C5[51-54,61]. Some of the arabinan nonreducing ends are bound to the MA in a species dependent proportion[51-54,61].

3.2.1. Arabinogalactan biosynthesis

The biosynthesis of AG (**Figure 9; Table 2**) starts in the cytoplasm with the generation of the linker unit, catalyzed by WecA and WbbL[52-54,61,62]. Afterwards, the bifunctional galactofuranosyltransferases GlfT1 and GlfT2 catalyze the synthesis of the galactan chain: GlfT1 adds two galactofuranosyl residues to L-rhamnose; GlfT2 catalyzes the stepwise addition of 30 β-D-galactofuranosyl residues in alternating β-(1→5) and β-(1→6) glycosidic linkages[52-54,61,63,64].

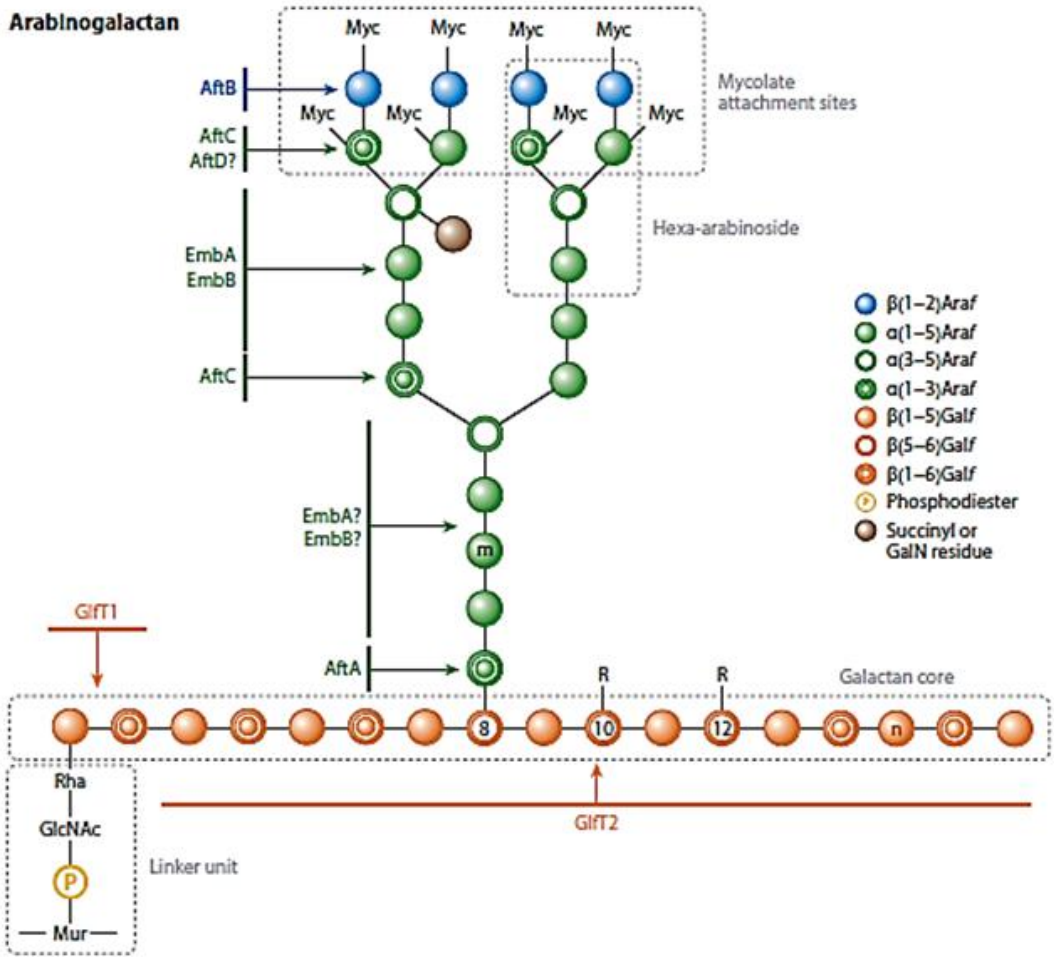

Fig. 9 – **Arabinogalactan biosynthesis in *Mycobacterium tuberculosis*.** Adapted from Jankute, M. *et al*. *Annu. Rev. Microbiol.* **69**, 405–423 (2015).

The subsequent synthesis of the arabinan chain occurs outside the plasma membrane[52-54,61]. The addition of arabinofuranosyl residues to the galactan chain is catalyzed by several arabinofuranosyltransferases that use decprenylphosphoryl-β-D-arabinofuranose (DPA) as a substrate[52-54,61]. First, AftA adds arabinofuranosyl residues to the 8th, 10th and 12th residues of the galactan chain[52-54,61,65]. After, EmbA and EmbB catalyze the α(1→5) polymerization of the arabinan chain, prompting the generation of the terminal hexa-arabinoside motif[52-54,61]. Then, AftC catalyzes the α(1→3) branching of AG and of lipoarabinomannan (LAM)[52-54,61,66]. Another α(1→3) branching enzyme, AftD, is involved in the assembly of AG[52-54,61,67]. Subsequently, AftB catalyzes the addition of β(1→2) arabinofuranosyl residues to the hexa-arabinofuranoside motif at the AG termini[52-54,61,68]. The arabinan residues from *Mtb* can be further modified through the addition of succinyl and galactosamine (GalN) residues, which have unknown functional significance[52-54,61]. The hexa-arabinofuranoside termini can then be fully or partially mycolated[52-54,61]. Finally, the attachment of AG to PG is catalyzed by Lcp1[53,69].

The biosynthesis of AG involves the action of several promising drug targets. For example, the 1st-line anti-TB agent ethambutol inhibits the arabinosyltransferases EmbA and EmbB, therefore compromising CW integrity[53,54]. Resistance to ethambutol occurs due to mutations in the *embABC* locus, which increase the transcription levels of *embA* and *embB*[70]. Some of the enzymes involved in the AG biosynthesis participate in the biosynthesis of the glycolipids phosphatidyl-*myo*-inositol mannosides (PIMs), and its multiglycosylated products lipomannan (LM) and lipoarabinomannan (LAM)[53,54]. These lipoglycans are important drug targets with roles in CW integrity, cell division and modulation of host-pathogen interactions[53,54]. Indeed, ethambutol can hinder the biosynthesis of LAM since it inhibits the action of EmbC[53,54,70].

Table 2 – Relevant information about proteins involved in AG biosynthesis.

Arabinogalactan biosynthesis						
Protein		**Gene identifier**			**Essentiality**	**Inhibitors**
		***Mtb* H37Rv**	***Mtb* H37Ra**	***M. smegmatis***		
	WecA	Rv1302	MRA_1310	MSMEG_4947	Essential	Caprazamycin derivatives
WbbL	**WbbL1**	Rv3265c	MRA_3306	MSMEG_1826	Essential	
	WbbL2	Rv1525	MRA_1537	-	Non-essential	
GlfTs	**GlfT1**	Rv3782	MRA_3822	MSMEG_6367	Essential	UDP-Gal*f* derivatives
	GlfT2	Rv3808c	MRA_3848	MSMEG_6403	Essential	
Arabino furanosyl transferases (AraTs)	**AftA**	Rv3792	MRA_3832	MSMEG_6386	Essential	DPA analogues
	EmbA	Rv3794	MRA_3834	MSMEG_6388	Essential	Ethambutol and analogues
	EmbB	Rv3795	MRA_3835	MSMEG_6389	Essential	
	EmbC	Rv3793	MRA_3833	MSMEG_6387	Essential	
	AftC	Rv2673	MRA_2701	MSMEG_2785	Essential	DPA analogues
	AftD	Rv0236c	MRA_0244	MSMEG_0359	Essential	
	AftB	Rv3805c	MRA_3845	MSMEG_6400	Essential	
	Lcp1	Rv3267	MRA_3308	MSMEG_1824	Essential	

3.3. Peptidoglycan

PG is a rigid structure that disposes a mesh-like layer outside the plasma membrane, maintains cellular shape and sustains the osmotic equilibrium of the cell[51-55,61]. The PG is, therefore, essential for the survival of *Mycobacterium*[51-55,61]. The mycobacterial PG is of type A1γ, consisting of long glycan strands significantly cross-linked by interlinked peptide branches of the sequence L-Ala-γ-D-Glu-*meso*-DAP-D-Ala-D-Ala[51-55,61].

As opposed to most bacteria, mycobacterial PG consists of alternating residues of *N*-acetylglucosamine (GlcNAc) and a mixture of muramic acid residues, containing both *N*-glycolyl and *N*-acetyl modifications, linked in a β-(1→4) configuration[51-55,61,71,72]. The *N*-glycolylation of these residues is an evolutionary advantage characteristic of *Mycobacterium* and closely related genera (*Tsukamurella*, *Gordonia*, *Nocardia*, *Rhodococcus* and *Micromonospora*)[72]. This modification, catalyzed by the *N*-acetyl muramic acid hydroxylase (NamH), occurs when the *N*-acetyl function of the muramic acid residues is converted to the *N*-glycolyl function, generating *N*-glycolyl muramic acid (MurNGlyc)[72] (**Figure 10**). The hydroxylase responsible for the *N*-glycolylation of PG is encoded by the nonessential gene *namH*, a promising drug target[72]. The generation of a *namH* knockout mutant in *M. smegmatis* has resulted in hypersusceptibility to both β-lactams and lysozyme, implying that the presence of *N*-glycolylated muropeptides increases CW integrity through the generation of additional hydrogen bonds[71,72,73]. In another perspective, Raymond *et al.* have speculated that the *N*-glycolylation of PG muramic residues may affect the recognition of PG precursors by flippases or/and by glycosyltransferases and transpeptidases, therefore, resulting in altered PG polymerization and antibiotic sensitivity[72]. In addition, the *N*-glycolylation of PG is also thought to potentiate the immunogenicity of the mycobacterial CW[73,74].

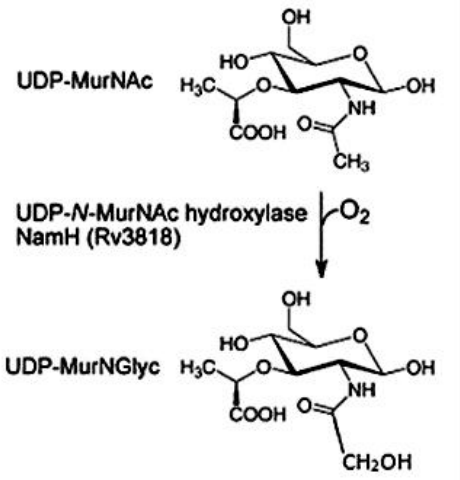

Fig. 10 – **The *N*-glycolylation of PG muramic residues**. The methyl group of the *N*-acetyl moiety (UDP-MurNAc) in carbon 2 of the muramic acid residues is hydroxylated by the action of NamH, generating *N*-glycolyl muramic acid (UDP-MurNGlyc). Adapted from Crick, D. C., *et al*. *Compr. Nat. Prod. II Chem. Biol.* **6,** 381–406 (2010).

The mycobacterial PG is highly cross-linked, contributing to the increased resistance and complexity of the CW[52-55,61]. The cross-linking of PG is catalyzed by D,D-transpeptidases and, mostly, by non-classical L,D-transpeptidases, resulting in 4→3 (D-Ala-*m*DAP) and 3→3 (*m*DAP-*m*DAP) linkages, respectively[51-55,61,75,76]. The degree and type of cross-linking modulates the host immune response and is also correlated with CW stability and β-lactams resistance[77].

Other unique features of the mycobacterial PG are the amidation of D-iso-glutamate, the amidation of *m*-DAP carboxylic acids and, the occurrence of complex side chains (by addition of glycine or serine residues)[53,55,61].

The amidation of the free carboxyl group of the D-iso-glutamate residue present at the second position of both lipid I/II is catalyzed by the MurT/GatD amidotransferase complex, which has been recently identified in *Staphylococcus aureus* and *Streptococcus pneumoniae*[78,79]. This reaction involves the concerted action of GatD, which hydrolyzes L-glutamine to produce glutamate and ammonia and, Mur-T, a Mur ligase-like protein, which utilizes ammonia to catalyze the amidation of D-iso-glutamate into D-iso-glutamine, in a ATP and Mg^{2+}-dependent

manner[78-80]. The *murT*/*gatD* operon is a promising drug target since it is essential for the viability of several bacteria, including *Mtb*[81]. Studies with MurT/GatD conditional mutants have revealed that the inhibition of D-iso-Glu amidation in *S. aureus* causes reduced growth rates as well as β-lactam and lysozyme susceptibility[78,82]. Moreover, Mir *et al.* have demonstrated that amidated muropeptides are the preferred substrates for the Ser/Thr kinase PknB in *Mtb*, not only suggesting a link between amidation and transpeptidation but also indicating that the amidation of D-iso-Glu may regulate PknB-dependent cell division/growth and PG turnover[83]. This observation is in accordance with other studies[78,79], which have hypothesized that D-iso-Glu amidated PG is the favored substrate for transpeptidases in *S. aureus.* In fact, Pidgeon *et al.* have recently demonstrated that D-iso-Glu amidation is essential for PG cross-linking in *M. smegmatis* and *Mtb* and, thus, may regulate the activity of L,D-transpeptidases in mycobacteria[84]. Additionally, the amidation of D-iso-Glu results in a less polar PG layer and, facilitates the translocation of lipid II across the CM[78,79]. Overall, the amidation of D-iso-Glu is thought to be involved in: **i)** PG cross-linking[78-80,82-84]; **ii)** cell division/growth[78,79,82,83]; **iii)** PG turnover[83]; **iv)** resistance to β-lactams[78,79,82]; **v)** resistance to lysozyme[78,82]; **vi)** resistance to hydrolysis by endopeptidases[21,83]; and **vii)** immune evasion[78].

In a similar fashion, the amidation of *m*-DAP, catalyzed by the glutamine amidotransferase AsnB, occurs with the transfer of ammonia from glutamine to a *m*-DAP acceptor on PG precursor lipid II[85-87]. The enzyme responsible for the amidation of *m*-DAP was first identified in *Lactobacillus plantarum*, where it is encoded by *asnB1*[86]. Ever since, homologues of *asnB1* have been identified as essential for the viability of several bacteria and annotated as promising drug targets: *ltsA* in *Corynebacterium glutamicum*[87] and *Rhodococcus erythropolis*[88]; *asnB* in *Bacillus subtilis*[89], *M. smegmatis*[90] and *Mtb*[81,91]. Previous studies in *L. plantarum* and *C. glutamicum* have revealed that the absence of AsnB causes impaired cell growth and cell shape as well as hypersusceptibility to β-lactams and lysozyme[86,87]. Surprisingly, experiments with a *asnB* transposon insertion mutant in *M. smegmatis* have indicated increased susceptibility to rifampicin, erythromycin and novobiocin and, unchanged susceptibility to isoniazid, ethambutol and β-lactams[90]. Moreover, Dajkovic *et al.* have reported that AsnB depletion leads to increased susceptibility to antibiotics and lysozyme as well as uncontrolled PG degradation due to autolysins deregulation in *B. subtilis*[89]. Most importantly, Ngadjeua *et al.* have revealed that the amidation of *m*-DAP is essential for cell growth and for the activity of L,D-transpeptidases in *Mtb*[91]. In sum, the amidation of *m*-DAP is hypothesized to: **i)** be important for cell growth[86,87]; **ii)** affect the susceptibility to certain antibiotics and lysozyme[86-90]; **iii)** regulate the activity of autolysins[89]; **iv)** be essential for L,D-transpeptidation in *Mtb*[91] and; **v)** modulate the host innate immune response by enabling immune evasion[92].

3.1.1. Peptidoglycan biosynthesis

Most antibacterial drugs target the biosynthesis of PG. However, concealment of PG within the mAGP complex provides protection against hydrophilic drugs, enabling *Mtb* to survive inside host macrophages and to resist antibiotic pressure[53-56]. The biosynthesis of mycobacterial PG (**Figure 11; Table 3**) starts in the cytoplasm with the generation of uridine diphosphate-*N*-acetylglucosamine (UDP-GlcNAc), catalyzed by GlmS, GlmM and GlmU[52-55,61,93]. Then, the MurA-F ligase pathway catalyzes the formation of the muramyl-pentapeptide, constituted by both UDP-*N*-acetylmuramic acid (UDP-MurNAc) and UDP-*N*-glycolylmuramic acid (UDP-MurNGlyc)[52-55,61,93]. The conversion of UDP-GlcNAc into UDP-MurNAc is catalyzed by the

concerted action of MurA and MurB[52-55,61,93]. Subsequently, the UDP-*N*-acetylmuramic acid hydroxylase NamH catalyzes the hydroxylation of UDP-MurNAc to UDP-MurNGlyc, producing *N*-glycolylated and *N*-acetylated derivatives in a 7:3 proportion[52-55,61,71,72,93]. The subsequent addition of L-Ala (MurC), D-Glu (MurD), *meso*-DAP (MurE) and D-Ala-D-Ala (MurF) generate the pentapeptide, also known as Park's nucleotide[52-55,61,93,94]. The assembled pentapeptide is then anchored to the plasma membrane by MraY/MurX, generating lipid I[52-55,61,93,94]. The final intracellular step of PG synthesis, the formation of lipid II, is catalyzed by the glycosyltransferase MurG[52-55,61,93,94]. Both lipid I and II are then amidated at D-Glu by the amidotransferase complex MurT/GatD[78-80]. Likewise, lipid II is amidated at *m*-DAP by the amidotransferase AsnB[85,93]. After the translocation of amidated lipid II across the plasma membrane, carried out by an unidentified flippase, the PG is polymerized by the action of transglycosylases, penicillin-biding proteins (PBPs) and L,D-transpeptidases (Ldts)[52-55,61,93].

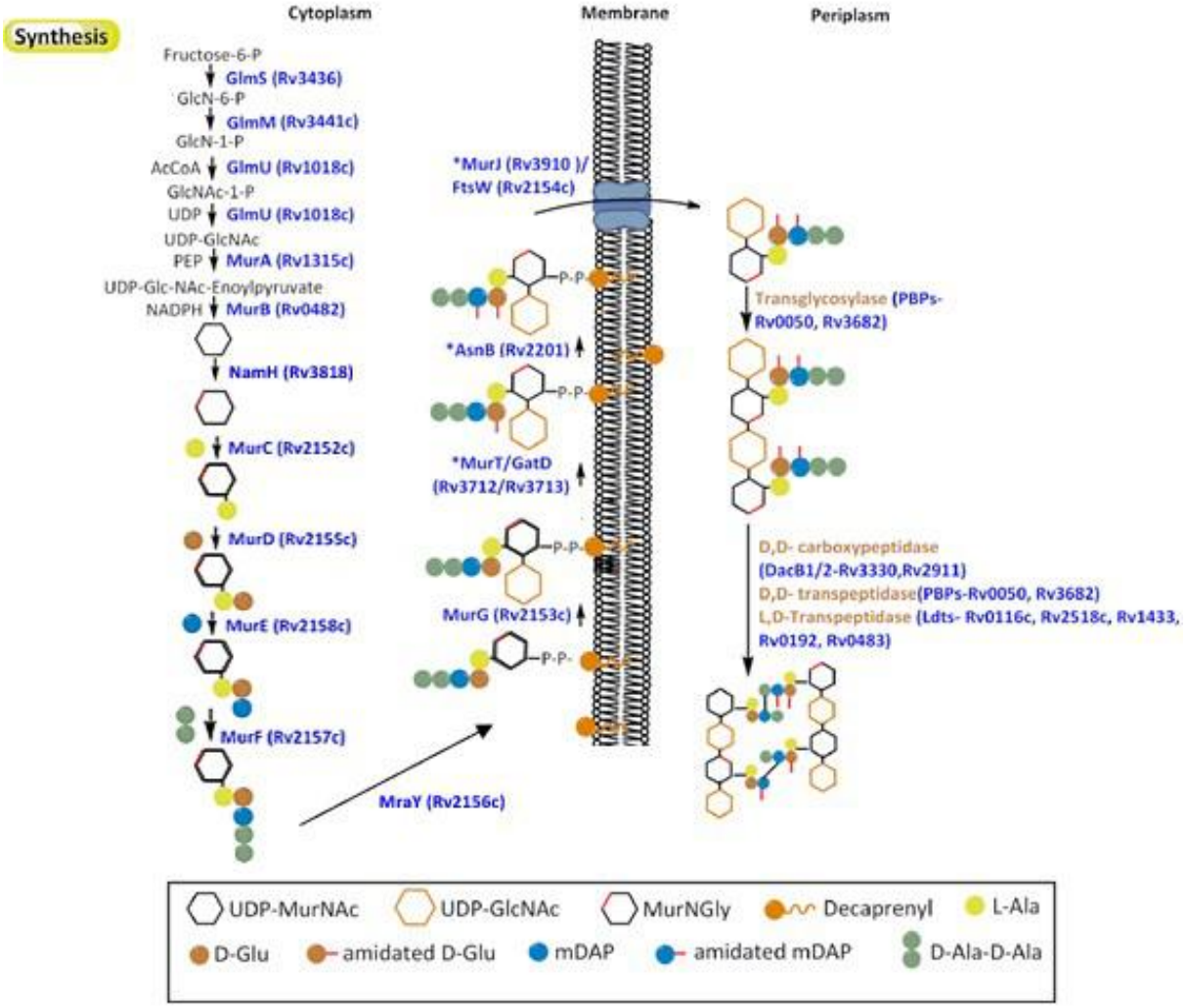

Fig. 11 – The biosynthesis of mycobacterial peptidoglycan. The PG precursors are produced in the cytoplasm, PG assembly occurs in the inner leaflet of the plasma membrane and polymerization occurs at the periplasm. Adapted from Maitra, A. *et al*. *FEMS Microbiol. Rev.* **43,** 548–575 (2019).

Table 3 – Relevant information about proteins involved in PG biosynthesis.

Peptidoglycan biosynthesis						
Protein		Gene identifier			Essentiality	Inhibitors
		Mtb H37Rv	*Mtb* H37Ra	*M. smegmatis*		
Glm	GlmS	Rv3436c	MRA_3477	-	Essential	
	GlmM	Rv3441c	MRA_3482	MSMEG_1559	Essential	
	GlmU	Rv1018c	MRA_1026	MSMEG_5426	Essential	Substrate of GlcN-1-P
MurA/MurB	MurA	Rv1315	MRA_1323	MSMEG_4932	Essential	
	MurB	Rv0482	MRA_0489	MSMEG_0928	Essential	Dioxopyrazolidines; Benzylidene thiazolidinedione derivatives
	NamH	Rv3818	MRA_3858	MSMEG_6410	Non-essential	
Mur Ligases	MurC	Rv2152c	MRA_2167	MSMEG_4226	Essential	
	MurD	Rv2155c	MRA_2170	MSMEG_4229	Essential	
	MurE	Rv2158c	MRA_2173	MSMEG_4232	Essential	
	MurF	Rv2157c	MRA_2172	MSMEG_4231	Essential	
	MraY/MurX	Rv2156c	MRA_2171	MSMEG_4230	Essential	Muraymycin; Liposidomycin; Caprazamycin; Capuramycin
	MurG	Rv2153c	MRA_2168	MSMEG_4227	Essential	Uridine-linked transition state analogues; Ramoplanin
Amidotransferases	MurT	Rv3712	MRA_3749	MSMEG_6276	Essential	
	GatD	Rv3713	MRA_3750	MSMEG_6277	Essential	
	AsnB	Rv2201	MRA_2217	MSMEG_4269	Essential	
Class A PBPs	PonA1/PBP1	Rv0050	MRA_0053	MSMEG_6900	Non-essential	β-lactams
	PonA2/PBP1A	Rv3682	MRA_3717	MSMEG_6201	Non-essential	
	PonA3	-	-	MSMEG_4384	Non-essential	
Class B PBPs	PbpA	Rv0016c	MRA_0018	MSMEG_0031	Non-essential	
	PbpB	Rv2163c	MRA_2178	MSMEG_4233	Essential	
	Pbp-lipo	Rv2864c	MRA_2889	MSMEG_2584; MSMEG_6319	Non-essential	
Class C PBPs or D,D-carboxypeptidases	DacB/PBP4	Rv3627c	MRA_3663	MSMEG_6113	Essential	
	DacB1	Rv3330	MRA_3372	MSMEG_1661	Non-essential	
	DacB2	Rv2911	MRA_2936	MSMEG_2433	Non-essential	
	DacB_AmpH1	Rv0907	-	MSMEG_5637	Non-essential	
	DacB_AmpH2	Rv1367c	MRA_1377	MSMEG_3040	Non-essential	
Ldts	LdtMt1/LdtA	Rv0116c	MRA_0123	MSMEG_3528	Non-essential	Carbapenems + Clavulanate
	LdtMt2/LdtB/LppS	Rv2518c	MRA_2545	MSMEG_4745	Non-essential	
	LdtMt3/LdtG	Rv1433	MRA_1442	MSMEG_0674	Non-essential	
	LdtMt4/LdtE	Rv0192	MRA_0200	MSMEG_0233	Non-essential	
	LdtMt5/LdtC/LprQ	Rv0483	MRA_0490	MSMEG_0929	Non-essential	
	LdtF	-	-	MSMEG_1322	Non-essential	

PBPs are a large family of evolutionarily related peptidases, usually classified according to their molecular weight as either high molecular mass (HMM) or low molecular mass (LMM)[95,96]. HMM PBPs or D,D-transpeptidases are further divided into class A and class B[95,96]. The class A PBPs are bi-functional enzymes with transpeptidase (catalyze 4→3 cross-linking between D-Ala and *m*-DAP stem peptides of glycan strands) and glycosyltransferase (polymerization of the glycan strand) activities[95,96]. In *Mtb*, class A PBPs include PonA1/PBP1 and PonA2/PBP1A[95,96]. In *M. smegmatis*, a duplication of *ponA2* is annotated as *ponA3*[96]. Whereas PonA1 maintains cell shape and integrity, PonA2 plays a part in the adaptation of *Mtb* to dormancy[96]. The class B PBPs are monofunctional enzymes with transpeptidase activity[95,96]. In *Mtb*, class B PBPs include PbpA, PbpB and PBP-lipo[95,96]. PbpA has a relevant role in the regulation of cell division and cell shape[94,97]. In contrast, PbpB is involved in cell integrity

functions and adaptation to oxidative stress, being essential for the viability of *Mtb*[94,98]. The LMM PBPs constitute class C PBPs or D,D-carboxypeptidases[95,96]. In *Mtb*, class C PBPs include DacB/PBP4, DacB1, DacB2, DacB_AmpH1 and DacB_AmpH2[95,96]. In *M. smegmatis*, there is a duplication of *dacB2*[96]. Most of the mycobacterial PG cross-linking is characterized by 3→3 linkages between *m*-DAP residues, catalyzed by non-classical Ldts, which are resistant to most β-lactams except for carbapenems[76,95,96,99]. L,D-transpeptidation requires the action of D,D-carboxypeptidases, which cleave the terminal D-Ala-D-Ala residue of the peptide stem and, consequently, inhibit the activity of D,D-transpeptidases (4→3 cross-linking)[96]. Accordingly, D,D-carboxypeptidases produce tetrapeptide PG precursors, the substrate of Ldts, and are thought to regulate the degree and type of PG cross-linking[94,96,100]. The dormant phase of *Mtb* is mostly characterized by 3→3 cross-links[52,54,76,96,101]. Five Ldts have been identified in *Mtb*: Ldt_{Mt1}, Ldt_{Mt2}, Ldt_{Mt3}, Ldt_{Mt4} and Ldt_{Mt5}[96,101,102]. The presence of these enzymes can markedly modify β-lactams susceptibility[99,101,103-107]. Gupta *et al*. have demonstrated that a ldt_{Mt2} deletion mutant is less virulent and has increased susceptibility to β-lactams[103]. Moreover, Schoonmaker *et al.* have showed that a *Mtb* ldt_{Mt1}/ldt_{Mt2} deletion mutant has altered cellular morphology, reduced growth, and virulence *in vitro* and *in vivo* and, increased susceptibility to amoxicillin-clavulanate and to vancomycin[104]. Furthermore, Ldt_{Mt2} is essential for the viability of *Mtb* when PonA1 and PonA2 are absent[75]. The regulation of PG cross-linking in accordance with environmental changes and bacterial growth phase is vital during persistence since it promotes CW integrity, resistance to β-lactams and to hydrolytic enzymes[76,93,103].

Which antibiotics are usually used to inhibit cell wall biosynthesis and can be repurposed to treat TB?

4. β-lactams

After the discovery of penicillin in 1928 by Alexander Fleming[108], several other β-lactams have been discovered or synthetized[109-111]. Despite being the most widely used class of antibiotics, β-lactams are not included in TB drug regimens mainly due to the intrinsic resistance of *Mtb* to these antibacterials[55,56,112,113]. Nevertheless, the emergence of MDR and XDR strains of *Mtb* coupled with the lack of alternative therapeutic approaches has propelled the interest of repurposing β-lactams following innovative approaches to tackle life-threatening TB[55,114,115].

4.1. The diversity of β-lactams and its mechanism of action

The core structure of β-lactams comprises a highly reactive four-membered cyclic amide β-lactam ring and five possible side chains (R), which define the β-lactam subgroup[109,116]. The four major β-lactam subgroups (**Figure 12**) include penicillin derivatives (penams), cephalosporins (cephems), carbapenems and monobactams[109,111,116].

The core ring of β-lactams gives these compounds a three-dimensional disposition that resembles the D-Ala-D-Ala dipeptide (**Figure 12**), the natural substrate for the transpeptidase activity of PBPs during CW assembly[95,96,109-111,113]. Therefore, β-lactams can effectively bind the active site serine of PBPs and, consequently generate an acyl-enzyme complex that inhibits PG cross-linking[95,96,109-111,113]. The inhibition of CW assembly can provoke cell death whether an essential PBP is targeted[95,96,109-111,113].

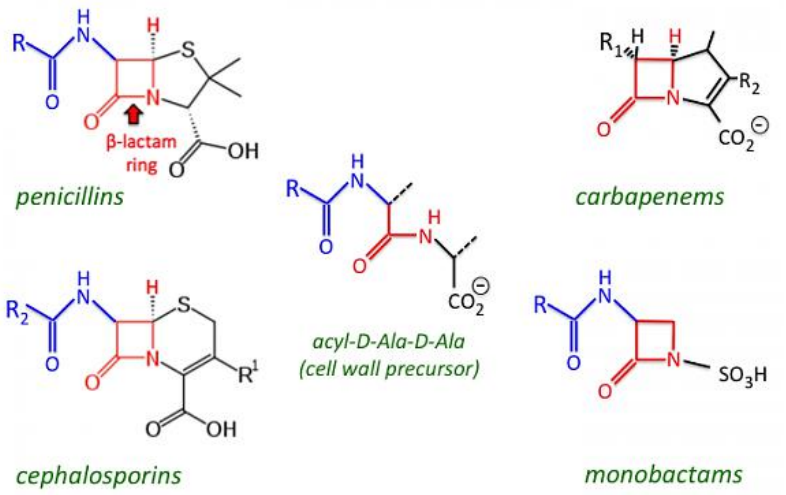

Fig. 12 – The core structure of β-lactams: includes a characteristic β-lactam ring (highlighted in red) and various side chains (R). The β-lactam ring mimics the natural substrate of PBPs, the D-Ala-D-Ala dipeptide. Adapted from Pallasch, T. J. *Dent. Clin. North Am.* **47**, 623–639 (2003).

4.1.1. Penicillins

Penicillin was discovered when Fleming observed a culture of *S. aureus* contaminated with the mold *Penicillium notatum*, around which there was no bacterial growth[108]. The compound around the mold was then isolated and named "penicillin"[108]. Later, it was found that penicillin could kill a wide range of bacteria[109,110]. Further research led to the development of multiple penicillin derivatives, classified as natural penicillins, β-lactamase resistant penicillins, aminopenicillins, carboxypenicillins and ureidopenicillins[109-111,117].

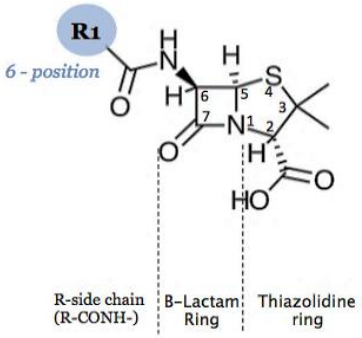

The structure of penicillins (**Figure 13**) entails a 6-aminopenicillanic acid (6-APA), which comprises the β-lactam ring fused with a five-membered thiazolidine ring[109-111,116].

Fig. 13 – The structure of penicillins: includes a R side chain and a squared β-lactam ring fused to a thiazolidine ring.

Amoxicillin (**Figure 14**) is a broad-spectrum, semisynthetic aminopenicillin, which has bactericidal activity against most gram-positive and some gram-negative bacteria (e.g.: *Haemophilus influenzae, E. coli, Salmonella, and Shigella*)[117]. This antibiotic was created by adding an extra amino group to penicillin G, which consequently increased its hydrophilicity and enhanced its absorption after oral administration[110,116,117]. Nevertheless, amoxicillin is a β-lactamase sensitive antibiotic, and hence is often given in combination with a β-lactamase inhibitor such as clavulanate[111,116,117]. This combination has been shown to be bactericidal for *Mtb in vitro*[118-120].

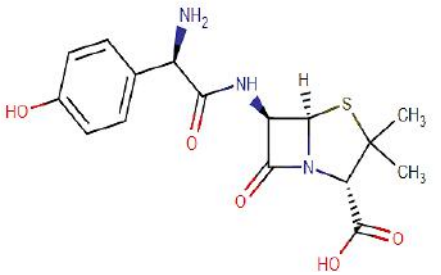

Fig. 14 – The structure of amoxicillin, a broad-spectrum antibiotic. Taken from Drug Bank.

4.1.2. Cephalosporins

Cephalosporins were discovered in 1945 by Giuseppe Brotzu[110,116]. He isolated the fungus *Cephalosporium acremonium* from a sewage in Sardinia and, demonstrated that this fungus was able to hinder the growth of some gram-negative bacteria such as *Salmonella typhi, Yersinia pestis* and *Vibrio cholerae*[110,116].

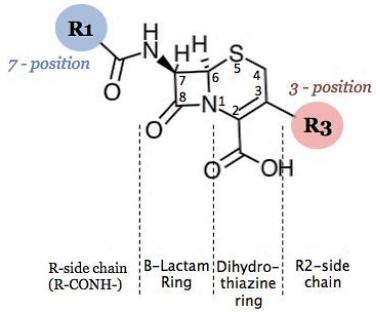

The structure of cephalosporins (**Figure 15**) entails a nucleus of 7-aminocephalosporanic acid (7-ACA), which comprises a β-lactam ring attached to a six-membered dihydrothiazine ring containing a sulfur and a nitrogen atom[109-111,116].

Fig. 15 – The structure of cephalosporins: includes two R-side chains and a β-lactam ring fused to a dihydrotiazine ring.

Cephalosporins differ in several aspects (β-lactamase sensitivity, absorption, metabolism, side effects) and, can be divided in five groups according to their antimicrobial spectrum[110,111,116]. First generation cephalosporins are highly bactericidal against gram-positive bacteria except enterobacteria and methicillin-resistant *S. aureus* (MRSA) and are active against some gram-negative bacteria[110,116]. Second generation cephalosporins are more potent against gram-negative bacteria[110,116]. Third generation cephalosporins have decreased potency against gram-positive bacteria but enhanced bactericidal activity against gram-negative cocci[110,116]. Fourth generation cephalosporins have enhanced bactericidal activity against *Pseudomonas aeruginosa*, *Enterobacter* and *Citrobacter*[110,116]. Fifth generation cephalosporins were designed to specifically target MRSA and, are active against both gram-positive and gram-negative bacteria[110,116]. Third, fourth and fifth generation cephalosporins can cross the blood brain barrier and reach the central nervous system[110,116].

Cefotaxime (**Figure 16**) is a broad spectrum third generation cephalosporin, with bactericidal activity against gram-positive and gram-negative bacteria[111,116]. Nevertheless, cefotaxime is susceptible to extended-spectrum β-lactamases encoding bacteria, where *Mtb* is included[111].

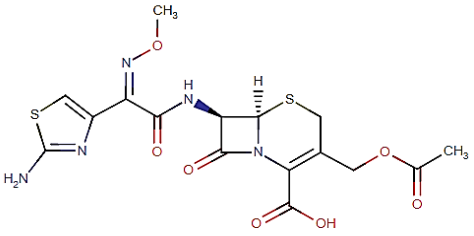

Fig. 16 – The structure of cefotaxime, a third-generation cephalosporin. Taken from Drug Bank.

4.1.3. Carbapenems

Carbapenems are synthetic analogs of thienamycin, a potent broad-spectrum antibiotic produced by *Streptomyces cattleya* that was discovered by Merck in the 1970s[121]. The structure of carbapenems (**Figure 17**) entails a β-lactam ring attached to a five-membered ring in which a carbon atom is present at the 1-position[111,116,121].

Carbapenems include imipenem, meropenem, ertapenem, doripenem, panipenem, biapenem and tebipenem[111]. These antibiotics are highly bactericidal against a very broad spectrum of bacteria, including gram-negative and gram-positive organisms[111,116]. Unlike other β-lactams,

carbapenems bind and inhibit the action of mycobacterial Ldts, the most active transpeptidases during PG cross-linking[55,76,77,99,101,106,107]. Besides targeting Ldts, carbapenems also target some PBPs of *Mtb*[55,77,106,107,122]. Carbapenems are especially resistant to hydrolysis catalyzed by β-lactamases, being poor substrates and even inhibitors of these enzymes[55,123]. Since carbapenems-resistance is rare, these antibiotics are commonly used for the treatment of MDR infections[111,116].

Fig. 17 – The structure of carbapenems: include a R-side chain and a β-lactam ring fused to a five-membered ring. Adapted from Pallasch, T. J. *Dent. Clin. North Am.* **47**, 623–639 (2003).

Meropenem (**Figure 18**) is a broad-spectrum carbapenem with a highly bactericidal activity against gram-negative bacteria, as opposed to gram-positive where its effect is mostly bacteriostatic[111,116].

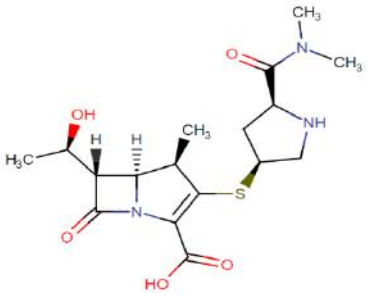

Fig. 18 – The structure of meropenem, a broad-spectrum carbapenem. Taken from Drug Bank.

4.2. Mechanisms of resistance to β-lactams

The major mechanism of exchange of resistance genes between bacteria is HGT[5,8]. However, *Mtb* does not undergo HGT[5,8] and, most antibiotic resistance phenotypes are caused by chromosomal mutations in genes encoding enzymes involved in CW biosynthesis[56,124]. Nevertheless, this is not common for β-lactams as they are not included in TB therapeutic schemes.

Mtb is intrinsically resistant to β-lactams (**Figure 19**) due to: **i)** CW impermeability; **ii)** drug inactivation; **iii)** multidrug efflux pumps; **iv)** enzymatic drug target modification; **v)** the predominance of non-classical Ldts[56,77,116,124].

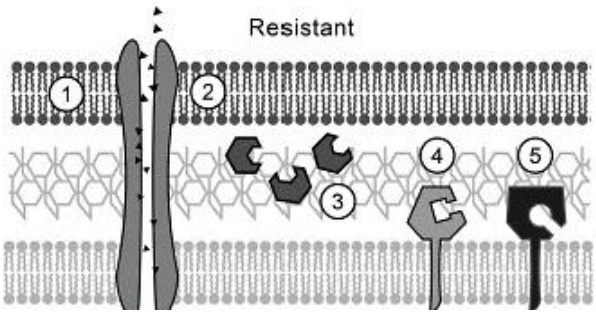

Fig. 19 - β-lactam resistance mechanisms: i) increased CW impermeability; ii) overexpression of efflux pumps; iii) overexpression of β-lactamases; iv) target site modification of PBPs; v) predominance of Ldts. Adapted from Wivagg, C. N. *et al*. *J. Antibiot. (Tokyo).* **67**, 645–654 (2014).

4.2.1. CW impermeability

The lipid-rich nature of the mycobacterial CW, due to the presence of a highly impermeable layer of MA, renders it extremely hydrophobic[21,51-53]. This hydrophobicity counteracts the diffusion of hydrophilic compounds (e.g.: antibiotics)[21,56,77,124]. Hence, β-lactams usually enter the cell through porins, which have its expression downregulated when mycobacteria are subjected to antibiotic stress[21,56,77,116,124].

4.2.2. Drug inactivation

After entering the cell, β-lactams can be degraded by β-lactamases, which hydrolyze the β-lactam ring[56,77,112,124]. *Mtb* possesses a highly active extended-spectrum β–lactamase: *Mtb* H37Ra encodes BlaA[125] whereas *Mtb* H37Rv encodes BlaC[112,126,127]. Similarly, *M. smegmatis* possesses a highly-active β–lactamase (BlaS) and a lowly-active β–lactamase (BlaE)[126,127]. However, these enzymes are irreversibly inhibited by the β-lactamase inhibitor clavulanate[128].

4.2.3. Multidrug efflux pumps

Mtb encodes several multidrug efflux pumps, which export various compounds out of the cell[56,77,124]. Most antibiotics used to treat TB (e.g.: streptomycin, rifampicin, isoniazid, ethambutol) can be extruded by these efflux systems[56,77,124]. Additionally, *Mtb* can regulate the levels of expression of these pumps by sensing environmental variations: the expression of efflux pumps increases when *Mtb* is exposed to antibiotics[56,77,124,129]. Furthermore, efflux pumps are regarded as essential for the intracellular growth of *Mtb* inside macrophages[56,77,124,130].

4.2.4. Enzymatic drug target modification

Mtb encodes several PBPs (**Table 3**), the targets of β-lactams[95,96]. PBPs can easily be modified by point mutations, escaping β-lactam binding[77]. These modifications can: **i)** alter the deacylation rate and, consequently, shorten the interaction between PBPs and β-lactams; **ii)** lead to the expression of low affinity PBPs, which promote PG transpeptidation by preferably binding PG over β-lactams[77]. For example, a loss of function mutation in PonA2 has been shown to confer resistance to cephalosporins[131].

4.2.5. The predominance of non-classical Ldts

As previously mentioned, *Mtb* encodes five Ldts (Ldt_{Mt1} to Ldt_{Mt5}; **Table 3**), which are insensitive to most β-lactams except for carbapenems[76,96,99,101,102]. Since mycobacterial PG transpeptidation occurs primarily (80%) through the enzymatic action of Ldts[55,76], β-lactams do not effectively inhibit CW assembly. Moreover, L,D-transpeptidation can be used as an alternative PG cross-linking mechanism by *Mtb* whether any PBP is inhibited by β-lactams[77,99].

4.3. Repurposing carbapenems in conjunction with β-lactamase inhibitors for the treatment of MDR/XDR TB

Recently, encouraging studies have shown that a combination of carbapenems with the β-lactamase inhibitor clavulanate can be effective against MDR-TB and XDR-TB[55,114,115]. Huggonet *et al.* were the first to show the usefulness of a carbapenem-clavulanate combination to treat MDR-TB *in vitro* by demonstrating that meropenem-clavulanate (Mc) exhibited equal minimum inhibitory concentrations (MICs) in both sensitive and MDR clinical isolates of *Mtb*, while combinations between clavulanate and other β-lactams were only bactericidal against drug sensitive isolates[132]. Carbapenems are more effective than other β-lactams because: **i)** carbapenems are poor substrates for BlaC[123]; **ii)** carbapenems severely inhibit the hydrolytic activity of BlaC[123]; **iii)** carbapenems target both PBPs and Ldts, producing a synergy between the inhibition of both types of transpeptidases[55,77,122,132]. Furthermore, Kumar *et al*. have revealed that a Mc combination resulted in quick cell lysis of *Mtb* H37Rv[133]. Moreover, Horita *et al.* have also demonstrated that *Mtb* clinical isolates are hypersusceptible when exposed to a carbapenem-clavulanate combination[134]. This observation has been further corroborated by other researchers[119,135,136]. Additionally, a combination of amoxicillin with Mc was shown to be synergistic due to the targeting of various transpeptidases[137]. Furthermore, England *et al*. have demonstrated the relevance of imipenem-clavulanate and Mc combinations *in vivo*, by observing a lower bacterial count in macrophages after treatment[138]. These combinations were also effective in a mice model of TB, leading to a higher host survival[139]. A combination of meropenem or faropenem with amoxicillin/clavulanate was shown to improve survival and decrease the bacterial count in an acute model of DHP-1 knockout mice[105]. All in all, *in vivo* studies point out that carbapenems treatment is only effective during the active growth phase of *Mtb*[114,115]. Some clinical trials have also demonstrated the efficacy of introducing various carbapenems (meropenem, imipenem and ertapenem) in the therapeutic schemes of MDR/XDR TB patients[140-146]. Overall, these observations have given hope of repurposing carbapenems to treat MDR/XDR TB.

How do host-pathogen interactions influence the success of *Mtb* as a human pathogen?

5. Host-pathogen interactions throughout TB infection

5.1. Innate immunity

5.1.1. First line defense

5.1.1.1. Lysozyme

Mycobacteria are naturally resistant to lysozyme, produced by the innate immune system[72]. This muramidase is capable of cleaving β-(1→4) bonds between *N*-acetylglucosamine (GlcNAc) and *N*-acetylmuramic acid (MurNAc)[72]. This inherent resistance to lysozyme might hinder the induction of the host's immune response by limiting the release of PG residues. However, a *namH* deletion mutant is hypersusceptible to lysozyme[72], underlying a role of the *N*-glycolylation of PG in CW integrity and pathogenesis.

5.1.1.2. Peptidoglycan recognition proteins

The first line of defense of the host innate immune system includes peptidoglycan recognition proteins (PGRPs), found in mammals and insects[147-151]. These molecules contain a conserved PG-binding domain (PGBD), homologous to bacteriophage and bacterial type 2 amidases[147,148]. This PGBD specifically binds tri- and, more frequently, tetra- and penta-muramyl peptides[147,148]. Mammals have four secreted PGRPs (PGLYRP1, PGLYRP2, PGLYRP3, PGLYRP4), of which PGLYRP1, PGLYRP3 and PGLYRP4 are bactericidal while PGLYRP2 is a *N*-acetylmuramoyl-L-alanine amidase[147,148]. The receptors PGLYRP1, PGLYRP3 and PGLYRP4 act by inducing several stress responses in bacteria, leading to membrane depolarization, increased production of reactive species, inhibition of biosynthetic pathways and, eventually, cell death[147,148]. On the other hand, PGLYRP2 is responsible for cleaving the bond between MurNAc and L-Ala, consequently leading to CW damage and cell lysis[147,148]. The model organism *Drosophila melanogaster* expresses 13 genes encoding PGRPs[147,148]. These PGRPs can discriminate between distinct PG stem peptide branches[147-151]. Both extracellular receptors PGRP-SA and PGRP-SD bind to Lys-type PG, characteristic of most gram-positive bacteria, and activate the Toll pathway[147-151]. Besides, PGRP-SA has recently been shown to recognize both Lys and DAP-type PG from gram-negative bacteria[151]. In contrast, the transmembrane PGRP-LC and intracellular PGRP-LE bind the DAP-type PG, occurring in gram-negative and some gram-positive bacteria, and activate the immune deficiency (IMD) pathway[147-151]. Both the Toll and IMD pathways induce NF-κB-dependent production of antimicrobial peptides (AMPs)[147-151]. Besides, PGRP-LE is protective against intracellular bacteria by facilitating autophagy[147,148]. Furthermore, PGRP-SB has bactericidal activity against DAP-type PG bacteria while PGRP-SC facilitates degradation of these bacteria in phagolysosomes[147,148]. Since the accessibility to PG plays a key role in bacterial sensing[147-151], mycobacteria might have evolved a highly resistant PG layer, concealed by the highly hydrophobic mAGP complex to avoid recognition by PGRPs.

5.1.2. Second line defense

5.1.2.1. The innate immune response

TB infection starts with the inhalation of virulent *Mtb*-containing aerosols into the lungs of the host, where mycobacteria are readily recognized and phagocytized by alveolar macrophages[9,152-154]. At this point, most bacteria are obliterated whereas some employ several immune evasion mechanisms to replicate inside macrophages and, eventually, cause macrophage rupture[152-154]. This will result in the production of pro-inflammatory cytokines (e.g.: TNF-α) and chemokines (e.g.: CCL2, CXCL10), leading to the recruitment of peripheral monocytes, which will later differentiate into macrophages and engulf *Mtb*[9,152-154]. At this stage, the granuloma starts to be assembled by subsequential interspersed aggregation of macrophages, dendritic cells and neutrophils into a containment structure, which is later surrounded by a lymphocyte net, containing CD4+ and CD8+ T-cells as well as B cells and natural killer cells[9,152-154]. Later, the activation of CD4+ T-cells and maturation into Th1 cells following the recognition of antigen-presenting macrophages through MHC II results in the release of IFN-γ and consequent macrophage activation (M1 polarization)[9,152-154]. After, macrophages have enhanced antigen presentation ability and act to eradicate intracellular bacteria using a plethora of mechanisms[152-154]: **i)** generation of antimicrobial reactive oxygen and nitrogen species; **ii)** phagosome-lysosome fusion; **iii)** phagosome maturation; **iv)** activation of autophagy. The onset of the adaptive immune response and the maturation of the

granuloma into a calcified lesion can then inhibit mycobacterial growth, resulting in latent TB infection (LTBI), caused by dormant bacilli[152-154]. Less than 10% of LTBI cases will progress to active TB infection in situation of host immunosuppression due to old age, disease or malnutrition[9,152-154]. This immunosuppressive state leads to granuloma caseation and rupture, enabling the transmission of infectious *Mtb*-containing aerosols to healthy individuals[9,152-154]. Even though the host's innate immunity seems to be protective, the selected immune response to the inhalation of *Mtb* depends on several factors such as initial microbial count, host's genetics and environmental influence[153]. Since a Th1 response is protective against TB infection, it is preferred over a Th2 response[153].

5.1.2.2. Immune recognition of mycobacteria by macrophages

After infection, macrophages recognize the pathogen associated molecular patterns (PAMPs) of *Mtb* through specific immune receptors, termed pattern recognition receptors (PRRs) (**Figure 20**)[152,153]. These PRRs include opsonizing receptors (e.g.: complement receptors CR1, CR3 and CR4), scavenger receptors, C-type lectin receptors (e.g.: mannose receptors) and innate immune receptors (e.g.: TLRs, NLRs)[152,153]. The polysaccharide components of the mycobacterial CW (e.g.: PIMs) can be recognized by opsonizing, scavenger and mannose receptors and lead to phagocytosis[152,153]. The PRRs that are mainly involved in the immune recognition of mycobacteria are Toll-like receptors (TLRs) and Nod-like receptors (NLRs)[152,153].

TLRs are expressed on the cell surface or on the membrane of endocytic vesicles of phagocytic cells (macrophages and dendritic cells)[152,153]. The TLRs that recognize specific mycobacterial structures are TLR2, TLR4 and TLR9[152,153]. The TLR2 receptor recognizes the LpqH lipoprotein, LM, LAM and PIMs[152,153]. The dimer TLR1-TLR2 recognizes diacylated lipoproteins while TLR6-TLR2 binds triacylated lipoproteins[152,153]. Moreover, TLR4 binds tri- and tetra-acylated LM, heat shock protein 65, and the 50S ribosomal protein[152,153]. In contrast, TLR9 recognizes mycobacterial DNA[152,153]. These receptors require a downstream adaptor protein, the myeloid differentiation primary response protein 88 (MyD88), critical for the signal transduction of the TLR signaling pathway[152,153]. MyD88 interacts with several proteins to produce a signaling cascade that culminates with the activation of the transcription factor NF-κB, which in turn stimulates the production of pro-inflammatory cytokines (e.g.: TNF-α, IL-1β, IL-6, IL-12, IL-18)[152,153]. The adaptive immune response is activated: the differentiation of CD4+ T-cells into Th1 cells triggers the production of IFN-γ and subsequent activation of macrophages, which act to eradicate intracellular bacteria[152,153].

The cytosolic NLRs cooperate with TLRs to mediate the innate immune response to mycobacterial PG[73,152,153]. NOD1 recognizes molecules containing D-Glu-*m*-DAP but the recognition of PG–derived muramyl dipeptide (MDP) is mostly accomplished by NOD2[73,74,155,156]. The recognition of MDP activates NOD2 mediated host responses (NMHR)[73,74]: **i)** polyubiquitination of the RIP2 kinase, which induces the activation of the transcription factor NF-κB and the mitogen-activated protein kinase (MAPK) pathways[73,74,155,156]; and **ii)** resultant stimulation of the production of pro-inflammatory cytokines (e.g.: TNF-α, IL-6, IL-1β) to initiate the adaptive immune response[73,74,155,156]. Previous studies have shown that *N*-glycolylated MDP is highly immunogenic when compared to *N*-acetylated MDP[73,74], suggesting a key contribution of the *N*-glycolylation of PG to the high immunogenicity of the mycobacterial CW. Despite this observation, *Mtb* is still able to thrive inside host macrophages after *namH* disruption[73,74], as it is expected for a nonessential gene.

Nonetheless, the fact that *namH* is conserved in several *Mtb* clinical isolates[157] suggests a possible functional role in TB pathogenesis.

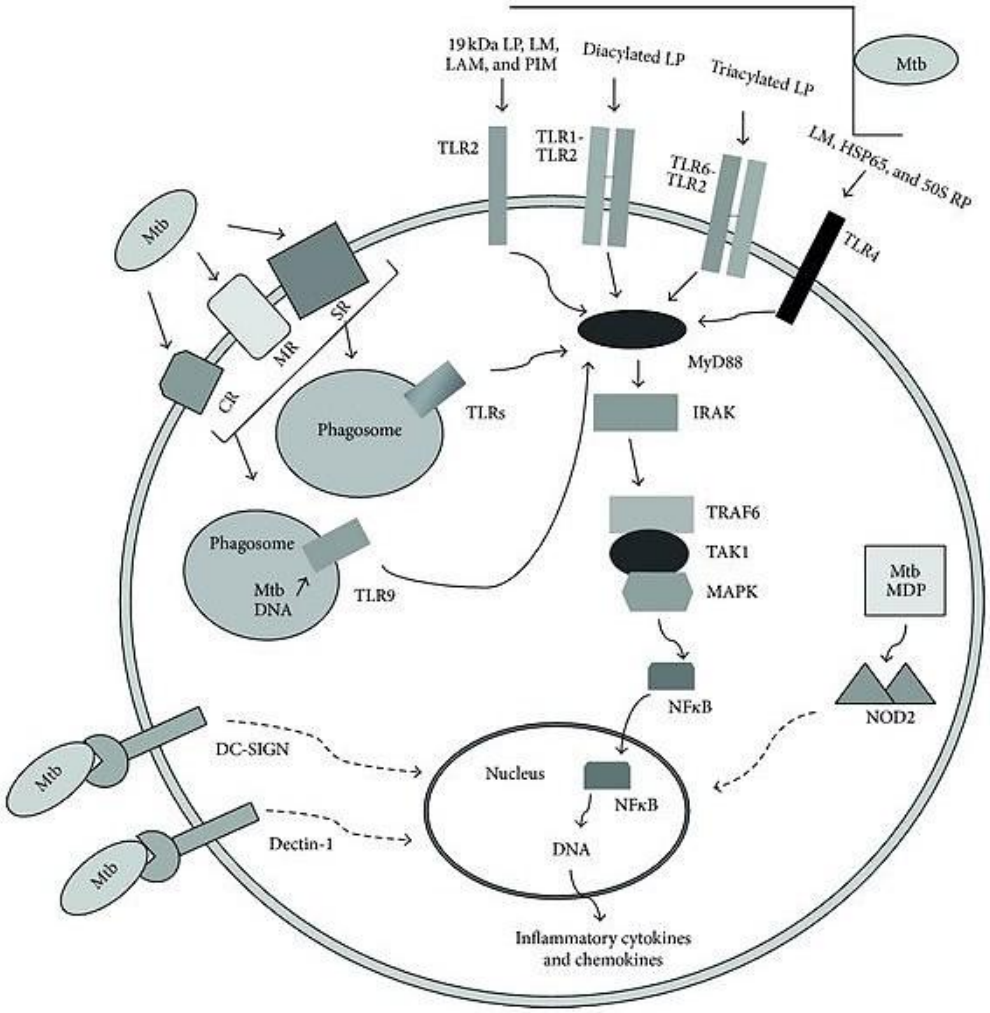

Fig. 20 – Immune recognition of mycobacteria by macrophages is mediated by phagocytosis-inducing complement receptors (CR), mannose receptors (MR) and scavenge receptors (SR). The PRRs that are mainly involved in the immune recognition of mycobacteria are TLRs (mainly TLR2 and TLR4) and NLRs. Adapted from Hossain, M. M. & Norazmi, M. N. *Biomed Res. Int.* **2013,** 1–18 (2013).

5.1.2.3. Immune evasion mechanisms

A hallmark of *Mtb*'s pathogenesis is the ability to evade the immune response and to replicate inside host macrophages[158-161]. *Mtb* employs several mechanisms to subvert the host's immune response and to delay the activation of the adaptive immune system after infection[158-161]. The occurrence of CW virulence factors such as LAM, TDM and phthiocerol dimycocerate have been shown to promote virulence and persistence inside macrophages by scavenging antimicrobial free radicals and by counteracting the action of IFN-γ[158,159]. Moreover, *Mtb* can secrete various highly immunogenic decoy peptides (e.g.: Ag85B) to distract the immune system from recognizing antigens that are essential for virulence[159]. Furthermore, *Mtb* manipulates the host receptors and cell entry routes. Indeed, *Mtb* H37Rv binds mannose receptors while *Mtb* H37Ra does not[158,159,162]. Therefore, interactions with phagocytosis-promoting receptors over TLRs/NLRs might facilitate intracellular survival inside macrophages,

which serve as a reservoir for eventual bacterial dissemination[158,159]. Other major immune evasion mechanisms are: **i)** the blockage of phagosome-lysosome fusion, due to the production of ammonia by *Mtb,* providing an alkaline environment; and **ii)** the inhibition of phagosome maturation by the macrophage's incessant expression of Rab5, induced by virulent *Mtb*[158-161]. The inhibition of lysosomal enzymes production (e.g.: cathepsins) is correlated with the halt of antigen presentation via MHC II[160,161]. The expression of virulence-promoting genes (e.g.: genes present in RD1) is another crucial subversion mechanism[158,159].

What technique can be used to probe the role of the *N*-glycolylation of mycobacterial PG in antibiotic resistance and in host immune recognition?

6. CRISPR

About 45% of bacteria own a CRISPR (Clustered Regularly Interspaced Short Palindromic Repeats) system for defense against foreign DNA elements, such as bacteriophages and plasmids[163-169]. CRISPRs are short palindromic repetitive segments of DNA, usually interpolated by spacers, short segments of foreign DNA[163-168]. Small clusters of *cas* (CRISPR-associated) genes, which encode for Cas proteins, are typically located upstream the CRISPR locus[163-168] (**Figure 21**). Cas proteins contain nuclease and helicase domains and are key players in CRISPR-mediated immunity, which comprises three phases[163-168]: **i)** adaptation, characterized by Cas-mediated cleavage and insertion of the invading protospacer sequence between two CRISPR repeats; **ii)** expression and processing, characterized by the expression of *cas* genes and, the transcription and processing of a precursor crRNA (pre-crRNA) into a mature crRNA, composed of a spacer and a CRISPR repeat; **iii)** interference, characterized by crRNA-guided Cas-mediated cleavage of the complementary target sequence.

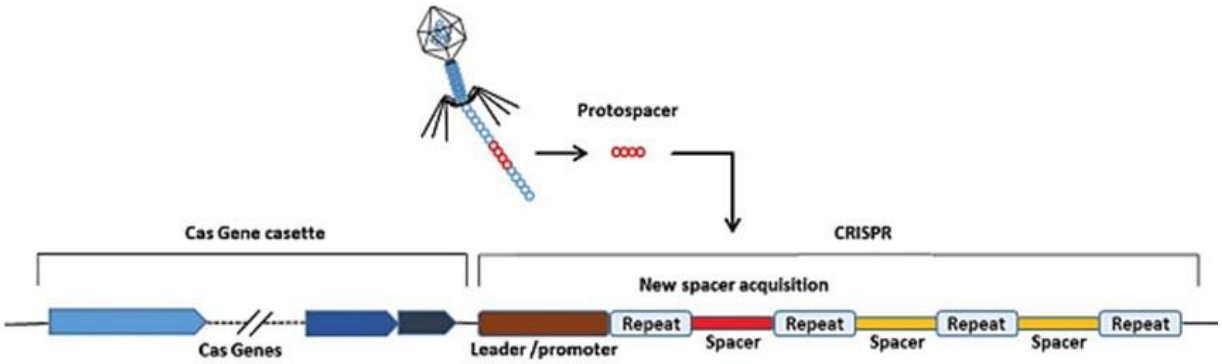

Fig. 21 – The CRISPR locus. Adapted from Lee, S. *et al*. *J. Cell. Biotechnol.* **1,** 95–106 (2015).

The type II CRISPR system from *Streptococcus pyogenes* has been modified to enable precise genome editing and, requires: **i)** a single Cas endonuclease (Cas9); **ii)** a mature CRISPR RNA (crRNA), a 20 bp sequence complementary to the target DNA; **iii)** a trans-acting RNA (tracrRNA), a hairpin structure partially complementary to the crRNA that binds to the Cas endonuclease[165-167]. Recently, the crRNA and the tracrRNA have been fused as a single-guide RNA (sgRNA)[166]. Therefore, CRISPR works as a two-component system, composed of Cas9 and a sgRNA that can be designed to target a specific DNA sequence[166]. The target specificity is not only dependent on the complementarity between the sgRNA and the target sequence

but also on a 2-5 bp DNA motif, found downstream the target sequence, the protospacer adjacent motif (PAM)[165-169].

6.1. CRISPR interference

Although TB remains a global health concern, the lack of efficient gene inactivation tools for *Mycobacterium* has rendered ineffective the identification of new vaccine candidates and drug targets, required for the development of new therapeutics[170-172]. Therefore, potential antibiotic targets, such as genes encoding enzymes involved in CW biosynthesis, remain poorly characterized[170-172]. Thereupon, CRISPR interference can be helpful by enabling the transcriptional regulation of specific genes such as *namH*[170-172].

To repurpose CRISPR for transcription regulation, Cas9 was inactivated by two point mutations within its nuclease domains, generating an endonuclease-deficient Cas9 (dCas9) with retained DNA-binding activity[173-175]. The sgRNA comprises three regions: a 20 bp base-pairing sequence, a 42 bp dCas9-binding hairpin and a 40 bp species-specific transcriptional terminator[173,174]. Thus, CRISPR interference (CRISPRi) employs a dCas9-sgRNA complex to repress any target gene by sterically hindering the transcription of the target sequence[173-175].

The mode of action of CRISPRi (**Figure 22**) depends on the target sequence and can affect transcription elongation, RNA polymerase binding or transcription factor binding[173-175]. When the non-template strand of the gene or the 5'UTR is targeted, the dCas9-sgRNA complex will block the action of RNA polymerase, resulting in transcription abortion[173-175]. When either strand of the promoter region is targeted, the dCas9-sgRNA complex will block the association between *cis*-acting elements and the correspondent *trans*-acting transcription factors, consequently inhibiting transcription initiation[173-175].

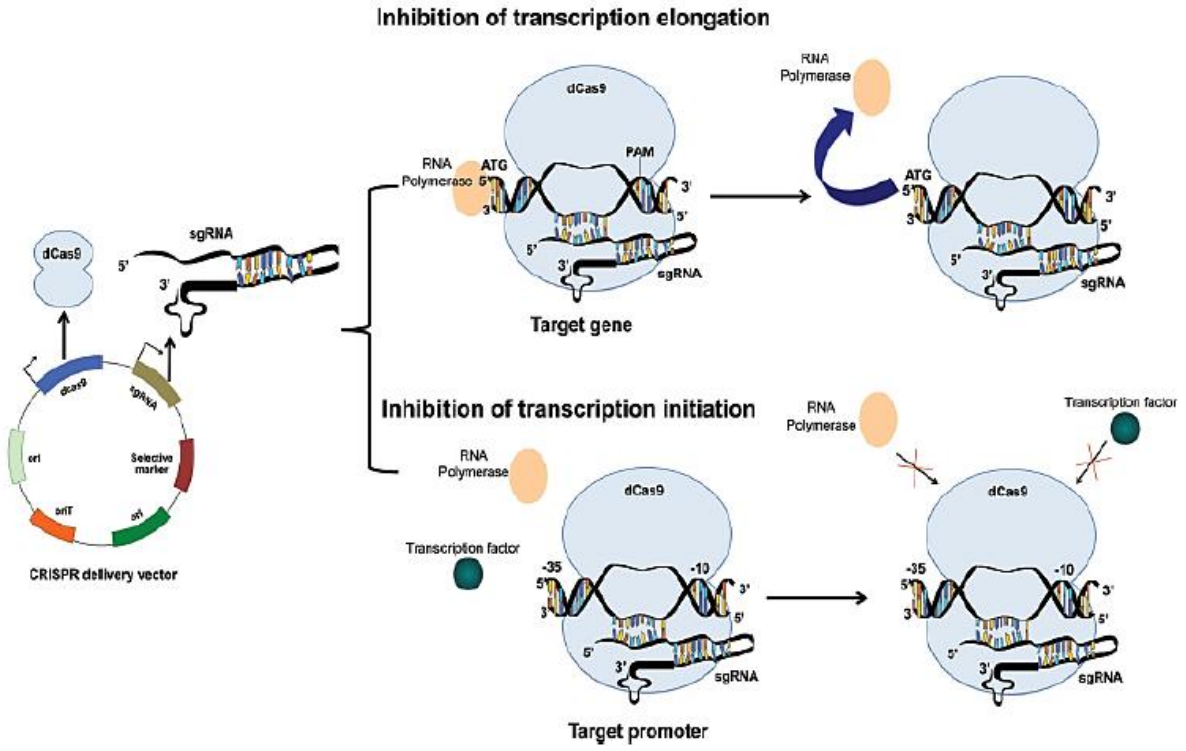

Fig. 22 – Mode of action of CRISPR interference. Adapted from de la Fuente-Núñez, C. & Lu, T. K. *Integr. Biol.* **9,** 109–122 (2017).

6.1.1. Advantages and disadvantages

The CRISPRi system has several advantages: **i)** programmability, since the selected sgRNA is referent to a single target of interest[173-177]; **ii)** inducibility, because CRISPRi can be regulated through the use of inducible promoters[173-179]; **iii)** tunability, since repression strength can be regulated by using different concentrations of inducer, changing the strength of the used PAM or varying the sgRNA:$_{target}$DNA complementarity specificity[173-179]; **iv)** scalability, because it enables the creation of sgRNA vector libraries[173-178]; and **vi)** multiplexing, either by using several sgRNAs to repress the same gene or by using distinct sgRNAs to repress different genes[173-177,179].

The major disadvantages of CRISPRi are: **i)** polar effects, the repression of downstream genes within an operon[176,179]; **ii)** reverse polarity[176,179]; and **iii)** the emergence of suppressor mutations, which inactivate either dCas9 or the sgRNA[176,177].

6.1.2. Optimization of the targeting efficiency

In order to achieve optimal targeting efficiency, several requirements must be attained: **i)** the sgRNA must comprise a specific 20 bp sequence, complementary to the target site[174]; **ii)** the sgRNA must bind to the non-template strand of the ORF of the target gene[174]; **iii)** the dCas9-sgRNA complex requires a PAM sequence downstream the target sequence[174]; **iv)** mismatches in the seed region, a PAM-adjacent 12 bp sequence, result in deficient silencing[174]; **v)** increased silencing efficiency can be obtained when two sgRNAs binding to different sites are used to target the same gene[174].

6.2. CRISPRi in mycobacteria

Choudhary *et al.*[170] and Singh *et al.*[171] were the first to develop a CRISPRi system for mycobacteria. Their systems included two anhydrotetracycline (ATc)-inducible[180] vectors: one for the conditional expression of a codon-optimized dCas9; another for the conditional expression of the sgRNA[170,171]. Both studies demonstrated that: **i)** the use of sgRNAs targeting the non-template strand lead to a higher repression efficiency when the coding region of the gene was targeted[170,171]; **ii)** dCas9 expression levels and, gene repression levels were directly proportional to the concentration of inducer used[170,171]; **iii)** polar effects are common in mycobacteria[170,171].

Nevertheless, Rock *et al.* have found that the silencing efficiency of dCas9 from *S. pyogenes* is poor and toxic in mycobacteria[172,178]. Therefore, they have developed a simpler and more efficient CRISPRi system, based on the employment of dCas9 from *Streptococcus thermophilus* (dCas9$_{Sth1}$)[172]. This system merely requires the cloning of a ~20-25 bp complementary sequence into a sgRNA scaffold[172]. It was developed by constructing a single plasmid system that contains[172]: **i)** a codon-optimized dCas9$_{Sth1}$ under the control of an ATc-inducible promoter; **ii)** a sgRNA under the control of a constitutive or ATc-inducible promoter; **iii)** a Tet repressor; **iv)** a single-copy L5-integrative backbone that includes the integrase gene and an *attP* site; **v)** an *E. coli* derived pBR3222 origin of replication**; vi)** a kanamycin resistance cassette. Since the known PAM sequence (NNAGAAW) for dCas9$_{Sth1}$-mediated gene silencing is not frequently found in the mycobacterial GC rich genome, other PAM variants have been investigated[172,178] (**Figure 23**).

PAM	Fold repression	SD
5'-NNAGAAG-3'	216.7	10.0
5'-NNAGAAT-3'	216.2	10.4
5'-NNAGAAA-3'	158.1	22.8
5'-NNGGAAG-3'	145.2	5.3
5'-NNAGAAC-3'	120.5	7.9
5'-NNGGAAA-3'	110.5	26.4
5'-NNAGCAT-3'	84.6	5.2
5'-NNAGGAG-3'	82.2	9.2
5'-NNAGGAT-3'	64.7	8.7
5'-NNAGCAA-3'	53.4	9.9
5'-NNGGAAC-3'	51.5	6.2
5'-NNGGAAT-3'	47.3	3.3
5'-NNAGCAG-3'	42.2	7.0
5'-NNAGGAA-3'	38.5	5.2
5'-NNAGGAC-3'	25.5	0.8
5'-NNGGGAG-3'	24.7	1.9
5'-NNGGGAT-3'	24.2	3.4
5'-NNGGGAA-3'	12.3	0.8
5'-NNAGCAC-3'	11.9	1.2
5'-NNGGGAC-3'	7.9	1.0
5'-NNGGCAT-3'	6.7	0.9
5'-NNGGCAG-3'	4.0	0.3
5'-NNGGCAA-3'	3.3	0.3
5'-NNGGCAC-3'	2.7	0.3
ctrl sgRNA	1.3	0.1

Fig. 23 - Possible PAM variants for dCas9$_{Sth1}$-mediated gene silencing. Their correspondent silencing efficiency is indicated as "fold repression" and PAMs are organized in descending order. The subsequent reference of PAMX, where X is any number between 1 and 11, in the materials and methods and in the results and discussion, refers to the order by which the PAMs are organized in this table.

This CRISPRi system was found to be very robust and extremely specific in both *Mtb* and *M. smegmatis*[172]. Unlike previous studies, dCas9$_{Sth1}$ was found to produce not only polar effects but also reverse polarity[172]. After the development of this CRISPRi system, several studies have employed it to advance TB research[122,181].

What are the objectives of this thesis?

7. Objectives

The available data shows that a *namH* deletion mutant is hypersusceptible to β-lactams and lysozyme[72], suggesting a role for the *N*-glycolylation of mycobacterial PG in CW integrity. Moreover, *N*-glycolylated MDP is highly immunogenic[73,74] and, although *namH* is not essential for the virulence of *Mtb*, the *N*-glycolylation of PG may have a role in TB pathogenesis. Furthermore, the *namH* gene is highly conserved in clinical isolates[157], implying a vital function for the *N*-glycolylation of PG in antibiotic resistance or/and in host-pathogen interactions. Therefore, the main goal of this thesis is to modulate *namH* expression in order to understand the significance of the *N*-glycolylation of PG in antibiotic resistance and in host immune recognition.

The specific aims of this thesis are:

A) <u>To construct and characterize *namH* knockdown mutants in mycobacteria:</u>

1) Silence the *namH* gene in *M. smegmatis* and *Mtb* H37Ra using CRISPRi.

2) Characterize the *namH* knockdown mutants by performing spotting dilutions and growth curves.

3) Assess the repression of *namH* using quantitative real-time PCR (qRT-PCR).

B) To understand the role of the *N*-glycolylation of PG in antibiotic susceptibility and in host immune recognition:

1) Determine antibiotic resistance differences between WT and *namH* knockdown mycobacteria, by: **i)** determining the minimum inhibitory and minimum bactericidal concentrations (MICs/MBCs) of three different classes of β-lactams (amoxicillin, cefotaxime and meropenem), with and without clavulanate, and of isoniazid (MA biosynthesis inhibitor) and ethambutol (AG biosynthesis inhibitor) in the study model *M. smegmatis*; **ii)** performing disk diffusion assays in the previously mentioned conditions.

2) Study the contribution of the *N*-glycolylation of PG for host immune recognition and pathogenesis, by performing infections of RAW 264.7 murine macrophages with the *namH* knockdown mutants followed by characterization of the resultant immune response:

- Determine the bacterial survival inside macrophages by counting colony forming units (CFUs).

Materials and Methods

1. Bacterial strains and culture conditions

The bacterial strains and plasmids used in this project are listed in **Table 4**. The media were prepared according to the manufacturer's instructions and autoclaved at 121°C for 20 min.

To amplify the CRISPRi backbones, *E. coli* was grown in Luria-Bertani (LB) broth or agar (Merck), overnight (ON), at 37°C with or without shaking (200 rpm). When necessary, the media were supplemented with 25 µg/mL of kanamycin (KAN; Sigma-Aldrich).

M. smegmatis mc^2 155 was grown at 37°C in Middlebrook 7H9 broth medium (BD™ Biosciences) supplemented with 0.22% (v/v) glycerol (ThermoScientific) or in Middlebrook 7H10 agar medium (BD™ Biosciences) supplemented with 0.55% (v/v) glycerol. Both media were supplemented with 0.5% (v/v) glucose (Glu; Sigma-Aldrich), a source of energy, and 0.05% (v/v) tyloxapol (Tyl; Sigma-Aldrich), a detergent used to prevent clump formation.

The avirulent *M. tuberculosis* strain H37Ra (25177™, ATCC) was grown at 37°C in Middlebrook 7H9 or in Middlebrook 7H10 medium supplemented with 0.22% (v/v) glycerol or 0.55% (v/v) glycerol, respectively. Media were supplemented with 10% (v/v) OADC and 0.05% (v/v) Tyl. OADC contains: **O**leic acid, essential for mycobacterial metabolism; **A**lbumin Factor V Bovine, protective against toxic fatty acids; **D**extrose, an energy source; **C**atalase, which neutralizes toxic peroxides; and Sodium Chloride (NaCl), which sustains the osmotic equilibrium. The OADC enrichment medium was prepared as described in **Appendix 1**. Manipulations of *Mtb* H37Ra were performed in a BSL2 laboratory.

When necessary, the media were supplemented with 25 µg/mL of KAN for PLJR962 (*M. smegmatis*; Addgene ID: 115162) or PLJR965 (*M. tuberculosis*; Addgene ID: 115163) selection. To induce sgRNA and $dCas9_{Sth1}$ expression, the media were supplemented with 100 ng/mL of anhydrotetracycline (ATc; Sigma-Aldrich).

Table 4 - Bacterial strains and plasmids used in this study.

Bacterial strain or plasmid	Description	Reference or source
Bacteria		
Escherichia coli		
JM109	*recA1 endA1 gyr96 thi hsdR17 supE44 relA1* Δ(*lac-proAB*) [F´ *traD36 proAB lac*^{q}*Z*ΔM15]	Stratagene
Mycobacterium smegmatis		
$mc^2$155 (WT)	High-transformation-efficiency mutant of *M. smegmatis* ATCC 607	41
PM965	*M. smegmatis* mc^2 155 *ept-1 rpsL4 ΔblaS*	72
PM979/ΔnamH	*M. smegmatis* mc^2 155 *ept-1 rpsL4 ΔblaS ΔnamH*	72
Mycobacterium tuberculosis		
H37Ra	Highly attenuated strain of *M. tuberculosis*	25177™, ATCC
Plasmids		
PLJR962 (8881 bp)	Sth1 *dcas9* Tet^R and Kan^R L5 Int *attP* for *M. smegmatis*	172
PLJR965 (8631 bp)	Sth1 *dcas9* Tet^R and Kan^R L5 Int *attP* for *M. tuberculosis*	172

2. Cell lines

The murine-derived macrophage cell line RAW 264.7 (TIB-71™, ATCC) was grown in DMEM media (GIBCO) supplemented with 10% (v/v) Fetal Bovine Serum (FBS; GIBCO), 1% (v/v) Sodium Pyruvate (NaPyr; GIBCO), 1% (v/v) L-Glutamine (GIBCO), and 1% (v/v) Hepes buffer (GIBCO). The cells were incubated at 37ºC with an atmosphere of 5% carbon dioxide (CO_2).

3. Preparation of *E. coli* chemically competent cells (CCC)

The preparation of *E. coli* CCC was performed as previously described[182]. Briefly, *E. coli* JM109 was grown to an optical density at 600 nm (OD_{600}) of ~0.5, determined by a spectrophotometer (Biophotometer-Eppendorf), and after 30 min of incubation on ice, the cells were pelleted by centrifugation (Centrifuge 5810 - Eppendorf) at 4000 *g* for 5 min at 4°C. The pellet was then ressuspended in ice-cold 0.1 M $CaCl_2$ solution by pipetting for 30 min. The cells were recovered by centrifugation at 4000 *g* for 5 min at 4°C. The pellet was subsequently ressuspended in 2.5 mL of ice-cold 0.1 M $CaCl_2$ plus 375 µL of 10% (v/v) glycerol and, stored in aliquots at -80°C.

4. Preparation of *Mycobacterium* electrocompetent cells (ECC)

M. smegmatis and *M. tuberculosis* H37Ra cells were grown in 7H9 broth medium at 37°C, until an OD_{600} of 0.8-1.0 was reached, as determined by a spectrophotometer[183]. After 90 min of incubation on ice, the cells were pelleted by centrifugation at 4000 *g* for 5 min at 4°C[183]. The pellet was washed four times with ice-cold 10% (v/v) glycerol. The cells were then ressuspended in 1 mL of ice-cold 10% (v/v) glycerol and, stored in aliquots at -80°C[183].

5. Treatment and normalization of *Mycobacterium* cultures

Once the cultures containing *M. smegmatis* or *Mtb* H37Ra reached the log-phase, the bacterial suspensions were centrifuged at 3000 *g* for 5 min. The pellets were ressuspended in the initial volume of media, the suspensions were sonicated for 5 min (Bandelin sonorex RK-52) to dissolve clumps and, centrifuged at 500 *g* for 1 min to separate the remaining cell aggregates. The supernatants were then transferred to new tubes, the OD_{600} was determined and, the cultures were normalized to the desired OD_{600}.

6. Antibiotic and clavulanate stocks

a) MIC assays

Amoxicillin, cefotaxime, meropenem and ethambutol (Sigma-Aldrich) stocks were prepared by dissolving the necessary mass (mg) of antibiotic in a certain volume (mL) of MilliQ water to a final stock concentration of 1.28 mg/mL, having in account the solute purity. After dissolution, the antibiotic solutions were filtered through a sterile 0.2 µM syringe filter (VWR) and, aliquots were stored at -80°C. Isoniazid (Sigma-Aldrich) was prepared in the same way to a final stock concentration of 1 mg/mL and, aliquots were stored at -20°C. Clavulanate (Sigma-Aldrich) was available in the laboratory and was used at the stock concentration of 10 mg/mL.

b) Antibiotic disks

The disk diffusion assays were only optimized for meropenem without clavulanate. The meropenem stock solution was prepared following the previously described protocol to a final concentration of 512 µg/mL and, stored at -80°C.

c) Anhydrotetracycline stocks

The anhydrotetracycline stock solution was prepared by dissolving the necessary mass (mg) of ATc in a certain volume (mL) of DMSO cell culture grade (AppliChem) to a final stock concentration of 10 mg/mL. After dissolution, the ATc stock solution was filtered through a sterile 0.2 µM syringe filter and, aliquots were stored at -20°C.

A) Construction and characterization of *namH* knockdown mutants in mycobacteria

1. Repression of the *namH* gene in *M. smegmatis* and *Mtb* H37Ra using CRISPRi

To silence the expression of *namH* in both *M. smegmatis* (*MSMEG_6410*) and *Mtb* H37Ra (*MRA_3858*), various sgRNAs were designed for each (**Tables 5 and 6**), according to the following strategy (**Figure 24**).

1.1. Design of the sgRNAs (*namH* example):

1. Identification of a PAM sequence on the template strand of the *namH* gene.
2. Extract the sgRNA sequence as the first ~20-25 bps sequence upstream the PAM (**5' - GCTGCCTGCCCGGGACTCGA – 3'**).
3. Make sure to extract a sgRNA with at least 20 bps and that begins with an "A" or "G".

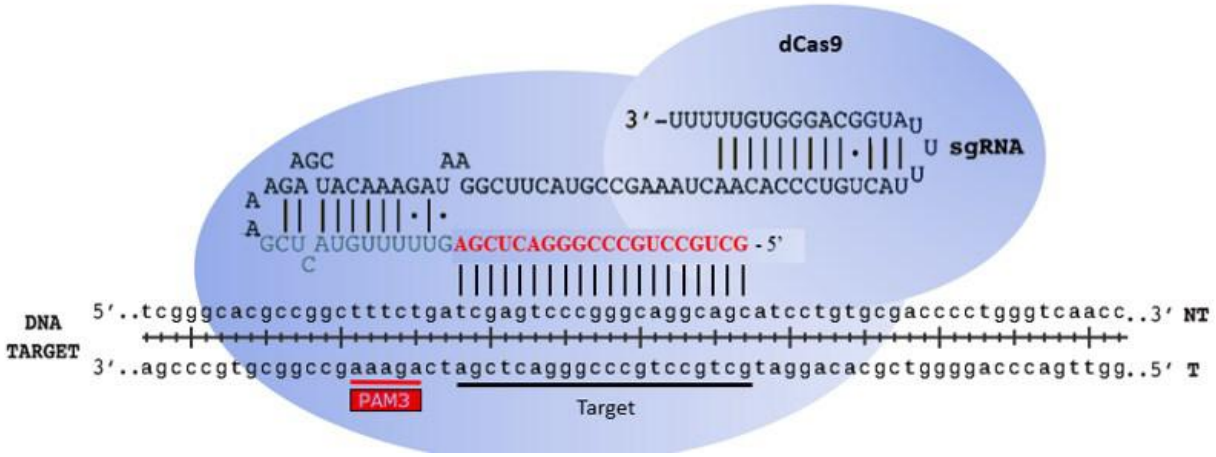

Fig. 24 – Strategy used to design sgRNAs to repress *namH* using CRISPRi in mycobacteria.

A high repression efficiency is known to be obtained when either the non-template strand of a gene of interest or its promoter region are targeted, that is, bound by complementarity to the selected sgRNA[174,175]. Therefore, the extent of the repression efficiency of CRISPRi was assessed by targeting different sites in the non-template strand of *namH*. This required the prior finding of PAMs (**Figure 23**) in the template strand of *namH* and, the posterior extraction

of the sgRNA sequence as the first ~20-25 bps sequence upstream the PAM (**Figure 24**)[166]. Since mycobacterial transcription is more efficient when it starts with an "A" or "G", the sgRNA was selected to begin with an "A" or "G"[166]. A BLAST search was then performed to assure that the base-pairing sequence is unique in the mycobacterial genome, that is, to avoid off-target effects[173].

Table 5 – sgRNAs used to target *namH* in *M. smegmatis*.

***namH* (MSMEG_6410)**					
M. smegmatis mc² 155					
Searched PAM	**Actual PAM**	**Base-pairing region of the sgRNA (the 12 bp seed region is underlined)**	**Size (bps)**	**BLAST (seed region + PAM)**	**Unique in Genome**
5'-NNAGAAG-3'	5' - GAAGAAG - 3'	5' - GCTTCACCGAGTCGGTGGTCTC - 3'	22	GTCGGTGGTCTCGAAGAAG	Yes
5'-NNAGAAT-3'	5' - CAAGAAT - 3'	5' - GCCAGGCCCTGAACCGCGTCGA - 3'	22	GAACCGCGTCGACAAGAAT	Yes
5'-NNAGAAA-3'	5' - TCAGAAA - 3'	5' - GCTGCCTGCCCGGGACTCGA - 3'	20	CCCGGGACTCGATCAGAAA	Yes
5'-NNGGAAG-3'	5' - GTGGAAG - 3'	5' - GTCGGTGGTCTCGAAGAAGTT - 3'	21	CTCGAAGAAGTTGTGGAAG	Yes
	5' - CGGGAAG - 3'	5' - GCTCCAGGAACACCATCTGGTC - 3'	22	CACCATCTGGTCCGGGAAG	Yes
	5' - GGGGAAG - 3'	5' - GGTTCGCGGACAACCCGTTT - 3'	20	GACAACCCGTTTGGGGAAG	Yes
	5' - CTGGAAG - 3'	5' - ATGCGGGCAGCGCCGCTGGAT - 3'	21	GCGCCGCTGGATCTGGAAG	Yes
5' - NNGGAAC - 3'	5' - CTGGAAC - 3'	5' - AGAGTGCTTCGCCAGCCTAG - 3'	20	TCGCCAGCCTAGCTGGAAC	Yes

Table 6 - sgRNAs used to target *namH* in *Mtb* H37Ra.

***namH* (MRA_3858)**					
***M. tuberculosis* H37Ra**					
Searched PAM	**Actual PAM**	**Base-pairing region of the sgRNA (the 12 bp seed region is underlined)**	**Size (bps)**	**BLAST (seed region + PAM)**	**Unique in Genome**
5'-NNAGAAG-3'	5' - TAAGAAG - 3'	5' - GCCATGCCCGAAATCGGGTGGA - 3'	22	AAATCGGGTGGATAAGAAG	Yes
5'-NNAGAAA-3'	5' - TCAGAAA - 3'	5' - GCTGCCGGCCTGGGTCTGGA - 3'	20	CCTGGGTCTGGATCAGAAA	Yes
5'-NNGGAAG-3'	5' - GGGGAAG - 3'	5' - ATCCAGGAACACCATCTGGTC - 3'	21	CACCATCTGGTCGGGGAAG	Yes
	5' - TCGGAAG - 3'	5' - GTGACCTGCACAGCTACCTT - 3'	20	CACAGCTACCTTTCGGAAG	Yes
5'-NNAGAAC-3'	5' - GAAGAAC - 3'	5' - GTTTGACCGAGTCGGTGGTTTC - 3'	22	GTCGGTGGTTTCGAAGAAC	Yes
	5' - GAAGAAC - 3'	5' - GCGTTCGTCGGTCAGACACTT - 3'	21	GGTCAGACACTTGAAGAAC	Yes

1.2. Amplification of the CRISPRi backbones

To amplify the CRISPRi backbones (**Figure 25**), *E. coli* JM109 chemically competent cells were transformed with PLJR962 and PLJR965 using a double heat-shock approach. Briefly, the suspension of DNA and *E. coli* CCC was incubated on ice for 30 min, gently mixed and, heated at 42˚C for 45 seconds. The cells were put on ice for 10 min, 950 µL of LB media at 42°C were added, and the cells were then incubated at 37˚C for 1h, with shaking. Finally, the

cells were spinned-down at 3000 *g* for 5 min, the supernatants were discarded and, the pellets were resuspended in 100 µL of LB. The cells were then spread on pre-heated LB supplemented with kanamycin (LK) plates, incubated ON at 37°C and, kanamycin resistant (KAN^R) transformants were selected. Afterwards, plasmid DNA was extracted using a NZYMiniprep kit (NZYTech) and quantified using Nanodrop® ND-1000 Spectrophotometer (ThermoScientific).

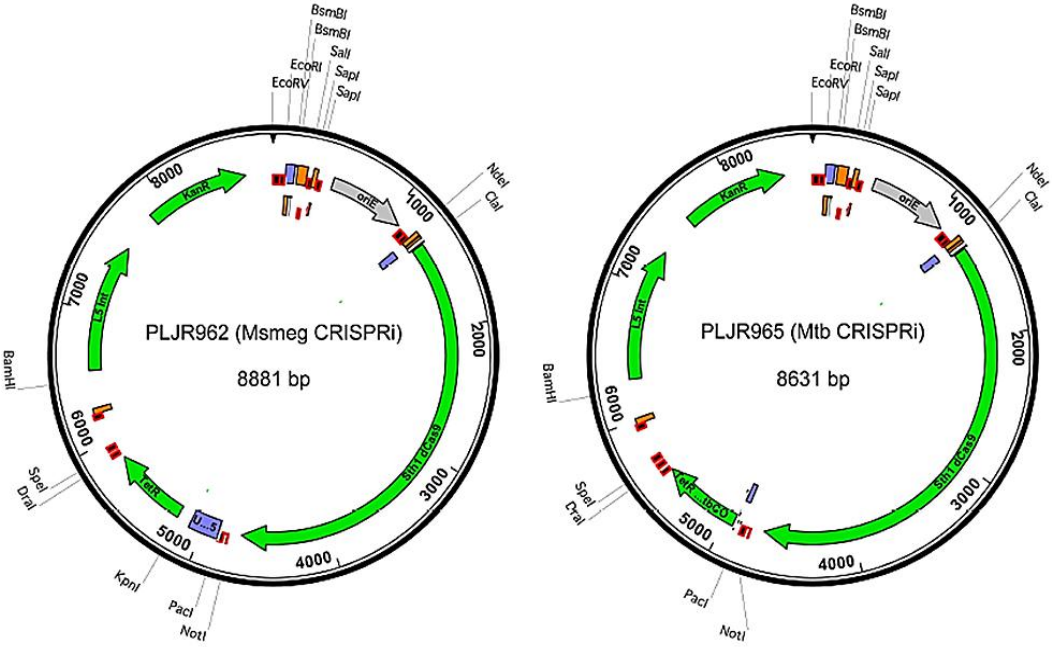

Fig. 25 – The CRISPRi backbones for *M. smegmatis* (PLJR962; 8881bp) **and *M. tuberculosis*** (PLJR965; 8631 bp). Both vectors contain: **1)** $dCas9_{Sth1}$ regulated by an ATc-inducible promoter; **2)** a sgRNA scaffold regulated by an ATc-inducible promoter; **3)** a Tet repressor; **4)** a single-copy L5-integrative backbone; **5)** a pBR3222 origin of replication; **6)** a kanamycin resistance cassette.

Afterwards, 2-5 µg of PLJR962 and PLJR965 were digested with 40 U of the restriction enzyme BsmB*I* (5'-CGTCTC$(N)_1$-3'; ThermoScientific), for at least 4h at 37°C in a PCR block (Applied Biosystems Veriti™ Dx 96-well Thermal Cycler)[172]. After, the reactions were purified using the QIAquick PCR Purification Kit (Qiagen) following the manufacturer's instructions. A minimal volume of the purification products was run on a 0.8% electrophoresis agarose gel with ethidium bromide, using a Bio-Rad apparatus. Molecular masses were estimated with the GeneRuler 1 kb DNA Ladder (ThermoScientific) following visualization on a UV transilluminator to verify the obtainment of the desired DNA bands (8881 bp and 8631bp, respectively). The obtained DNA was quantified using Nanodrop® ND-1000 Spectrophotometer, evaluated in terms of purity (pure DNA → A260/A280=1.8; A260/A230=2) and, stored at -20°C.

1.3. Cloning the sgRNAs into the backbone vectors

To clone the *namH* sgRNA targeting sequence into the sgRNA scaffold, two complementary primers were designed, as previously described[172]. The forward primer corresponds to the sgRNA sequence preceded by 5'-GGGA-3'. The reverse primer is the reverse complement of the sgRNA preceded by 5'-AAAC-3'. The sequences were added to the sgRNAs to regenerate

the sgRNA promoter and the dCas9 handle sequences and, thus, facilitate the ligation between the sgRNA and the backbone vectors. The forward and reverse primers used to clone the sgRNAs into PLJR962 or PLR965 are detailed in **Tables 7 and 8** and the distribution of these along the *namH* gene (*MSMEG_6410*/*MRA_3858*) is present in **Figure 26**. To anneal these primers, 4 µL of each primer (100 µM) was added to 42 µL of annealing buffer (50 mM Tris, pH 7.5; 50 mM NaCl; 1 mM EDTA) in a PCR tube and, the program (95°C for 2 min, 0.1°/sec to 25°C, END) was run on a thermal cycler[172]. The annealed oligos (AO) were ligated into the CRISPRi backbones (PLJR962/PLJR965) using T4 DNA ligase (400 U/µL; NEB), at 22°C for 30 min[172]. The ligation mixtures used for both mycobacteria are present in **Table 9**.

Table 7 – Primers used to clone the sgRNAs into PLJR962.

***M. smegmatis* mc^2 155**						
		Primers		**Length (bps)**	**%GC**	**Tm (°C)**
C1	**PLJR962: :AO1**	Msmeg_namH_PAM11_-24_Fwd	5' - GGGAAGAGTGCTTCGCCAGCCTAG - 3'	24	63	62
		Msmeg_namH_PAM11_-44_Rv	5' - AAACCTAGGCTGGCGAAGCACTCT - 3'	24	54	61
C2	**PLJR962: :AO2**	Msmeg_namH_PAM1_330_Fwd	5' - GGGAGCTTCACCGAGTCGGTGGTCTC - 3'	26	65	63
		Msmeg_namH_PAM1_303_Rv	5' - AAACGAGACCACCGACTCGGTGAAGC - 3'	25	56	60
C3	**PLJR962: :AO3**	Msmeg_namH_PAM2_1267_Fwd	5' - GGGAGCCAGGCCCTGAACCGCGTCGA - 3'	26	73	67
		Msmeg_namH_PAM2_1246_Rv	5' - AAACTCGACGCGGTTCAGGGCCTGGC - 3'	26	65	68
C4	**PLJR962: :AO4**	Msmeg_namH_PAM3_58_Fwd	5' - GGGAGCTGCCTGCCCGGGACTCGA - 3'	24	75	68
		Msmeg_namH_PAM3_37_Rv	5' - AAACTCGAGTCCCGGGCAGGCAGC - 3'	24	67	65
C5	**PLJR962: :AO5**	Msmeg_namH_PAM4_320_Fwd	5' - GGGAGTCGGTGGTCTCGAAGAAGTT - 3'	25	56	60
		Msmeg_namH_PAM4_295_Rv	5' - AAACAACTTCTTCGAGACCACCGAC - 3'	25	48	61
C6	**PLJR962: :AO6**	Msmeg_namH_PAM4_770_Fwd	5' - GGGAGCTCCAGGAACACCATCTGGTC - 3'	26	62	61
		Msmeg_namH_PAM4_747_Rv	5' - AAACGACCAGATGGTGTTCCTGGAGC - 3'	26	54	60
C7	**PLJR962: :AO7**	Msmeg_namH_PAM4_1142_Fwd	5' - GGGAGGTTCGCGGACAACCCGTTT - 3'	24	63	60
		Msmeg_namH_PAM4_1121_Rv	5' - AAACAAACGGGTTGTCCGCGAACC - 3'	24	54	63
C8	**PLJR962: :AO8**	Msmeg_namH_PAM4_1420_Fwd	5' - GGGAATGCGGGCAGCGCCGCTGGAT - 3'	25	72	73
		Msmeg_namH_PAM4_1399_Rv	5' - AAACATCCAGCGGCGCTGCCCGCAT - 3'	25	64	73

Table 8 – Primers used to clone the sgRNAs into PLJR965.

***Mtb* H37Ra**						
		Primers		**Length (bps)**	**%GC**	**Tm (°C)**
C1	**PLJR965: :AO1**	Mra_namH_PAM4_11_Fwd	5' - GGGAGTGACCTGCACAGCTACCTT - 3'	24	58	60
		Mra_namH_PAM4_-9_Rv	5' - AAACAAGGTAGCTGTGCAGGTCAC - 3'	24	50	60
C2	**PLJR965: :AO2**	Mra_namH_PAM1_1261_Fwd	5' - GGGAGCCATGCCCGAAATCGGGTGGA - 3'	26	65	65
		Mra_namH_PAM1_1239_Rv	5' - AAACTCCACCCGATTTCGGGCATGGC- 3'	26	58	63
C3	**PLJR965: :AO3**	Mra_namH_PAM3_57_Fwd	5' - GGGAGCTGCCGGCCTGGGTCTGGA - 3'	24	75	68
		Mra_namH_PAM3_37_Rv	5' - AAACTCCAGACCCAGGCCGGCAGC - 3'	24	67	65
C4	**PLJR965: :AO4**	Mra_namH_PAM4_768_Fwd	5' - GGGAATCCAGGAACACCATCTGGTC - 3'	25	56	59
		Mra_namH_PAM4_746_Rv	5' - AAACGACCAGATGGTGTTCCTGGAT - 3'	25	48	61
C5	**PLJR965: :AO5**	Mra_namH_PAM5_328_Fwd	5' - GGGAGTTTGACCGAGTCGGTGGTTTC - 3'	26	58	60
		Mra_namH_PAM5_305_Rv	5' - AAACGAAACCACCGACTCGGTCAAAC - 3'	26	50	63
C6	**PLJR965: :AO6**	Mra_namH_PAM5_1320_Fwd	5' - GGGAGCGTTCGTCGGTCAGACACTT - 3'	25	60	62
		Mra_namH_PAM5_1298_Rv	5' - AAACAAGTGTCTGACCGACGAACGC - 3'	25	52	64

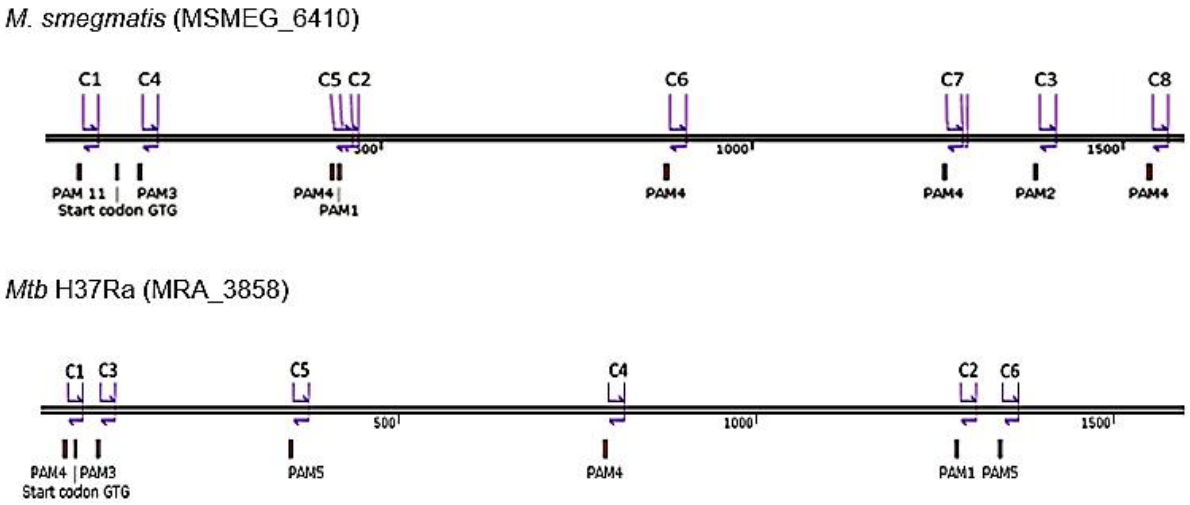

Fig. 26 – Distribution of primer pairs along the *namH* gene in *M. smegmatis* and *Mtb* H37Ra. Different sites were targeted along the *namH* gene to assess the repression efficiency of CRISPRi.

Table 9 – Ligation mixture used to clone the annealed oligos (AO) into each vector (PLJR962/PLJR965) in both mycobacteria.

Ligation Mixture	
1 reaction	
T4 DNA ligase buffer (10X)	1X
T4 DNA ligase (400 U/µL)	500 U
Digested PLJR962 (77 ng/µL) or PLJR965 (63 ng/µL)	9 ng
Annealed oligos (AO)	0.5 µL
Nuclease free water	up to 5 µL

1.4. Selection of sgRNA-containing CRISPRi plasmids

To obtain the sgRNA-containing CRISPRi plasmids, *E. coli* CCC were transformed with the ligation mixture by double heat-shock, streaked on pre-heated LK plates, incubated ON at 37°C and, KAN^R transformants were then selected[172]. Afterwards, plasmid DNA was extracted using the NZYMiniprep kit (NZYTech) and quantified using Nanodrop® ND-1000 Spectrophotometer. Recombinant clones were verified by Sanger sequencing (Eurofins Genomics), using the following primer: 5' - TTCCTGTGAAGAGCCATTGATAATG - 3'[172]. The employed cloning strategy is exemplified in **Figure 27**.

Afterwards, *M. smegmatis* or *M. tuberculosis* H37Ra ECC were transformed with 500 ng of the obtained clones by electroporation in the presence of 10% (v/v) glycerol (using 2 mm cuvettes and a Bio-Rad Gene Pulser™ Electroporation System, with pulse settings of 2.5 kV, 1000 Ω resistance and 25 µF capacitance)[183]. The cells were recovered in supplemented 7H9 for 2 hours (*M. smegmatis*) or 2 days (*Mtb*) and, later plated in 7H10+OADC supplemented with KAN for selection of KAN^R transformants. The mycobacteria harboring the CRISPRi systems were grown in 7H9+Glu/OADC+Tyl at 37°C with (*M. smegmatis*) or without shaking (*Mtb*).

As an example, a summary of the step-by-step methodology applied in the construction of the *namH* knockdown mutants in *M. smegmatis* is depicted in **Figure 28**.

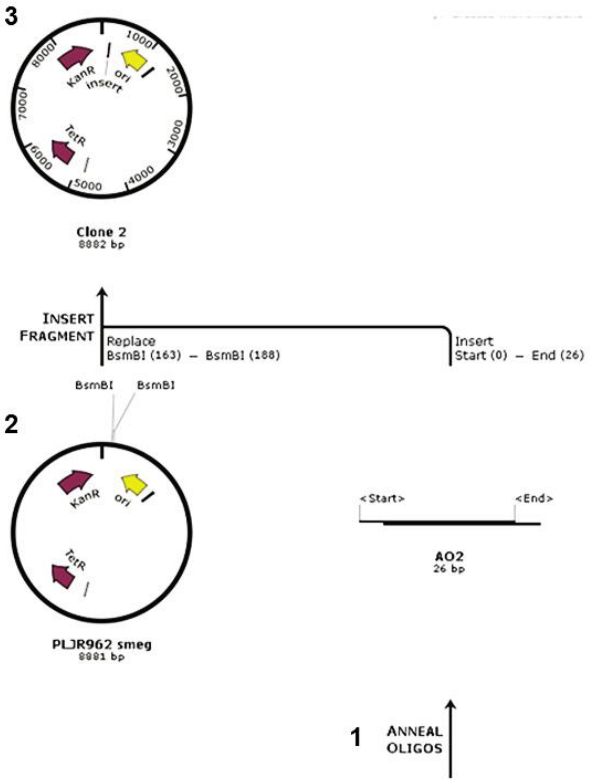

Fig. 27 – The employed cloning strategy. The first step was to design the sgRNAs and the correspondent primers. These oligos were annealed (**1**) and the backbone vectors were digested (**2**) with BsmB*I*. The annealed oligos were then ligated to the digested vectors aided by T4 DNA ligase (**3**).

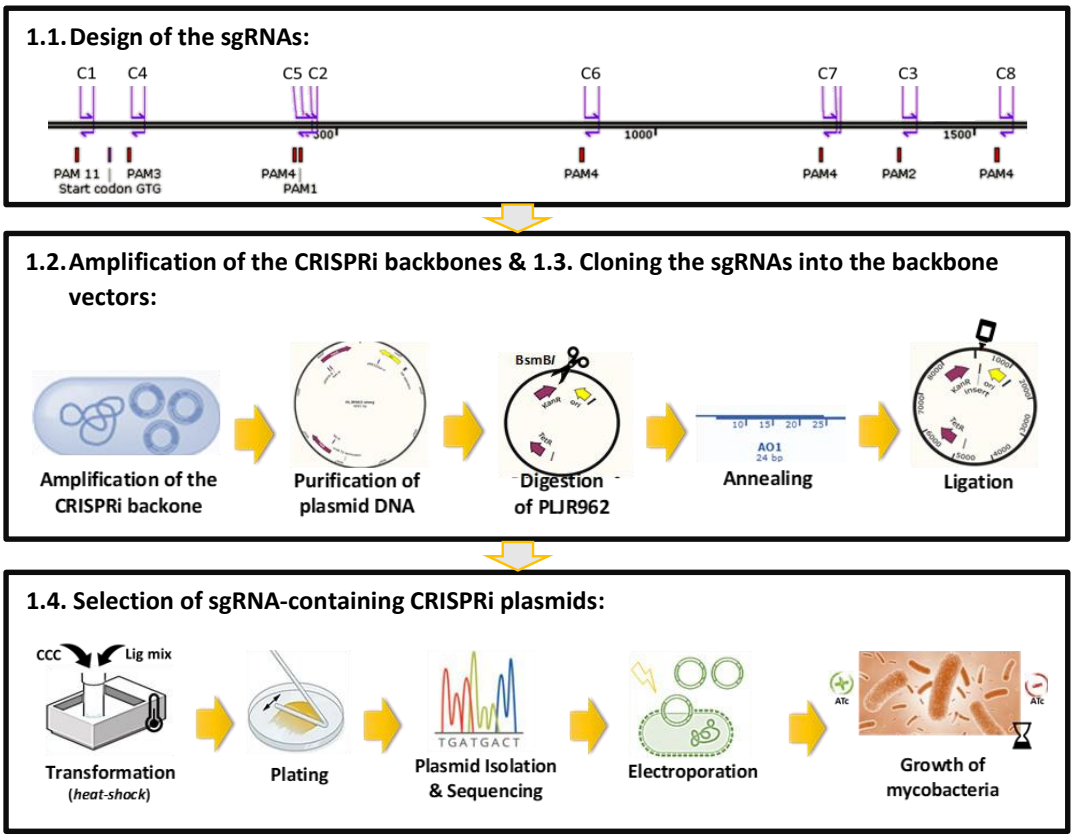

Fig. 28 – Step-by-step construction of the *namH* knockdown mutants (*M. smegmatis*): design of the sgRNAs (**1.1.**), amplification of the CRISPRi backbones (**1.2.**), cloning the sgRNAs into the backbone vectors (**1.3.**) and selection of sgRNA-containing CRISPRi plasmids (**1.4.**).

2. Characterization of the *namH* knockdown mutants

The *namH* knockdown mutants (*namH*$^{-}$) were initially characterized by phenotypical assays: growth curves and spotting dilutions.

To assess the growth differences between WT and *namH*$^{-}$ bacteria, growth curves were performed. Briefly, *M. smegmatis* containing PLJR962::sgRNA were grown to log phase and, after treatment, the cultures were normalized to an OD_{600} of 0.001 and, further incubated at 37°C in the absence (uninduced) or in the presence (induced) of 100 ng/mL of ATc. The culture growth evaluation was performed for ~45 hours, by plotting OD_{600} versus the incubation time[171]. This assay was performed at least three times for each culture of interest and, the average and the standard error of the mean (SEM) were calculated.

To evaluate WT vs. *namH*$^{-}$ differences in cell survival, spotting dilutions were performed[172]. Briefly, cultures of *M. smegmatis* were grown to log phase, treated and, normalized to an OD_{600} of 0.001. Two-fold serial dilutions were performed in a 96-well plate and, 5 µL of each suspension were transferred into 7H10 or 7H10+ATc plates. These plates were then incubated at 37°C for ~2 days. This assay was performed at least three times.

3. Assessment of the repression of *namH* using qRT-PCR

The relative quantification of the mRNA expression levels of *namH* (*MSMEG_6410*), downstream operonic gene (*MSMEG_6411*), neighboring genes (*MSMEG_6409; MSMEG_6412*) and chosen reference housekeeping gene *dnaK* (*MSMEG_0709*) was assessed by qRT-PCR in a selected *namH* knockdown mutant (*M. smegmatis* C2). Briefly, cultures were grown to log phase, treated, normalized to an OD_{600} of 0.001 and, incubated with shaking at 37°C until an OD_{600} of 0.1-0.2 was reached. At this timepoint (0h), cultures were split into uninduced and induced (ATc was added to a final concentration of 100 ng/mL) and, further incubated at 37°C for 6 hours. At chosen time points (0h, 3h, 6h), cultures were retrieved for RNA extraction. The cells were harvested by centrifugation at 3000 *g* for 5 min at 4°C, ressuspended in 500 µL of RNAprotect Bacteria Reagent (Qiagen) and, stored at -20°C. When convenient, the cells were thawed, centrifuged at 5000 *g* for 5 min at 4°C and, the supernatant was discarded. Then, lysis was promoted by the addition of 350 µL of buffer NR (NZYTech) and 3.5 µL of β-mercaptoethanol (Merck), followed by vortexing. The bacterial suspension was transferred to 2 mL screw-cap tubes containing 0.5 mL zirconia beads (Sigma-Aldrich) and bead-beated (BeadBug) four times at maximum speed for 1 min, with 1 min intervals on ice. The beads were spinned-down and, the lysate was applied into the NZYSpin Homogenization column (NZYTech). The next steps were performed according to the NZYTotal RNA Isolation Kit's instructions. In the elution step, yield was optimized by adding 40 µL of DEPC water (Invitrogen) at 70°C, followed by 5 min incubation, centrifugation and, repetition of the elution-incubation step for 1 min. Genomic DNA contamination was avoided by performing a rigorous treatment with TurboDNase (Invitrogen). The quantity and purity of the obtained RNA was determined using Nanodrop. Pure RNA is indicated by a A260/280 ratio of ~2.0 and a A260/230 ratio of ~2.0-2.2. The presence of DNA contamination was assessed by performing a PCR on a housekeeping gene using NZYTaq DNA polymerase (NZYTech), followed by 1.5% agarose (NZYTech) gel electrophoresis with GreenSafe Premium (NZYTech). Molecular masses were estimated with the GeneRuler 100 bp Plus DNA Ladder (ThermoScientific), following visualization on a ChemiDoc Gel Imaging System (Bio-Rad).

Afterwards, purified RNA was used to synthesize 200 ng of cDNA, by reverse transcription (RT) on a PCR-block (Bio-Rad) using the NZY First-Strand cDNA Synthesis Kit (NZYTech), following the manufacturer's instructions. Subsequently, the cDNA levels were quantified by qPCR using the NZY qPCR Green Master Mix (2x), ROX plus (NZYTech), a QuantStudio™ 7 Flex Real-Time PCR System (Applied Biosystems) and different sets of primers (Eurofins Genomics; **Table 10**). The primers were chosen to amplify a specific product between 100 - 200 bps, have at least 50% GC, avoid primer secondary structures and sequence repeats and, have a melting temperature between 55°-65°C. The PCR reaction (40 cycles) proceeded as follows: 95°C for 10 min (polymerase activation), 95°C for 15 s (denaturation), 60°C for 30 s (annealing/extension). For each run, three technical replicates and one negative control (without template) were produced and, afterwards, the average C_T was calculated. The mRNA expression levels of the genes of interest were then normalized to the reference gene (*dnaK*), and the relative expression of each gene was quantified using the Comparative C_T method ($\Delta\Delta C_T$ method) with the following formula: $\Delta C_T = C_T$ (Target gene) - C_T (Reference gene). As required for this method, a calibration curve was performed to guarantee that the amplification efficiency of the used primers ranged 90-110%. This assay was performed using three biological replicates for the culture of interest and, the average of the relative gene expression (RGE) and the standard error of the mean (SEM) were calculated. The statistical significance of the differences between control cultures and induced cultures were determined at t=6h using a two-tailed t-test (Excel), with the following confidence intervals (CIs): CI_1 = 98%; CI_2 = 99%; CI_3 = 99,9%.

Table 10 – Sets of primers used to quantify the expression of *namH* and neighboring genes by qRT-PCR in *M. smegmatis*.

Primers						
Species	**Target**	**Sequence**		**Length (bps)**	**% GC**	**Tm (°C)**
M. smegmatis	*dnaK (MSMEG_0709)*	PFwd	5' - CGACGAACTTCTCCGTCTGG - 3'	20	58	60
		PRv	5' - CAAGATCCAGGAAGGCTCCG - 3'	20	58	60
	namH (MSMEG_6410)	PFwd	5' - CGTTCTTCAAGTGCCTCACC - 3'	20	55	57
		PRv	5' - GTTGCCTTCCACCACACC - 3'	18	61	58
	MSMEG_6409	PFwd	5' - CCGGTACAGGTTCTTCGGAC - 3'	20	58	60
		PRv	5' - CCGCAGCTTCGAGATCAAGG - 3'	20	59	60
	MSMEG_6411	PFwd	5' - GTGCCAGAAGCTGTGACCG - 3'	19	59	63
		PRv	5' - GGGATCACCTTCGATGTGCC - 3'	20	59	60
	MSMEG_6412	PFwd	5' - CAGAGGCGTATCGTCGGAAC - 3'	20	60	58
		PRv	5' - CCATGCGTCTGGTGTGCTA - 3'	19	58	58

B) Deciphering the role of the *N*-glycolylation of PG in antibiotic susceptibility and in host immune recognition

1. Determination of WT vs. *namH*⁻ antibiotic susceptibility

1.1. Minimum inhibitory concentrations (MICs)

To assess antibiotic susceptibility differences between WT and *namH*⁻ mycobacteria, the protocol from Singh *et al*[171] was modified. The MICs of β-lactams amoxicillin, cefotaxime and

meropenem, with and without clavulanate, and of isoniazid and ethambutol were determined for *M. smegmatis* in 7H9+Glu+Tyl media, as depicted in **Figure 29**.

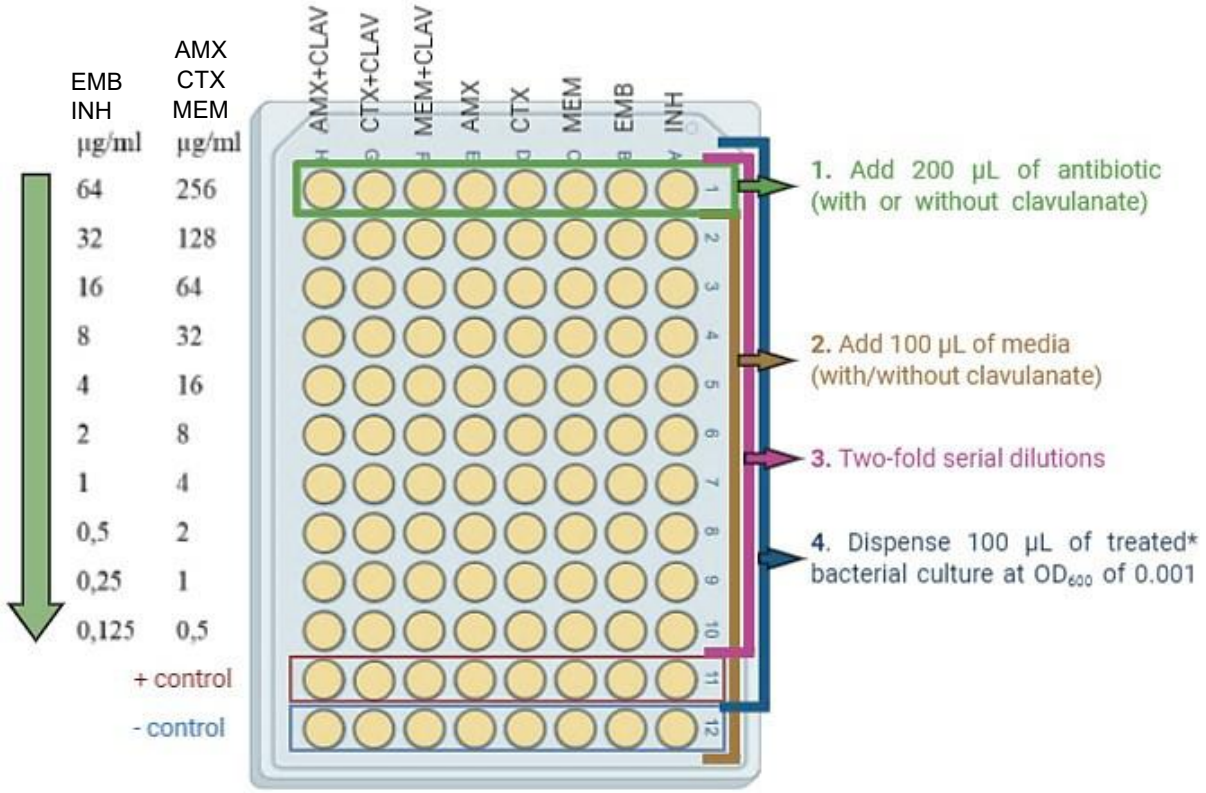

Fig. 29 – Antibiotic susceptibility testing by MICs assessment. This protocol was performed with *M. smegmatis*. Three β-lactams (amoxicillin – AMX; cefotaxime-CTX; and meropenem - MEM) with and without clavulanate (CLAV), and two anti-TB agents (isoniazid – INH; ethambutol - EMB) were tested. All plates were incubated at 37°C for the adequate time.

First, antibiotics were diluted in media to achieve the desired initial concentration. β-lactams were prepared at an initial concentration of 512 µg/mL and, clavulanate was added to β-lactams at 5 µg/mL. Moreover, ethambutol and isoniazid were prepared at an initial concentration of 128 µg/mL. After, 96-well plates (Sarstedt) were prepared by adding 100 µL of media, from the second to the 11th row of the plate, with or without clavulanate (5 µg/mL). In the last row, 200 µL of media with or without clavulanate were added. Then, 200 µL of each antibiotic was added to the first row. Two-fold serial dilutions were performed, except in the last two rows, in which were the positive (media with bacteria) and negative (only media) controls, respectively.

M. smegmatis cultures were grown to log phase, treated and, normalized to an OD_{600} of 0.002, which corresponds to approximately 2x10^5 CFU/mL. The bacterial suspensions were divided into two equal volumes, without and with 100 ng/mL of ATc and, distributed in a 96-well MegaBlock (VWR). Subsequently, 100 µL of each well were transferred to 96-well plates, starting in the antepenult row until the first one. The plates were then sealed in individual bags and, incubated at 37°C for ~2 days. Following this period, the plates were observed for evidence of growth and the MIC was annotated as the minimum concentration of antibiotic capable of preventing visible bacterial growth. This assay was performed at least three times for each culture of interest and the median values were calculated.

1.2. Minimum bactericidal concentrations (MBCs)

The MBCs to different antibiotics were determined for *M. smegmatis*, as depicted in **Figure 30**. After MIC determination, a 50 µL sample of the MIC and two wells above (2-fold MIC and 4-fold MIC) were transferred to a new 96-well plate and, 5 µL of each sample were pipetted into 7H10 or into 7H10+ATc square plates (Corning). These were incubated at 37°C for two days. The MBC was defined as the lowest concentration of antibiotic capable of eradicating the tested bacteria. The tested antibiotics were considered bactericidal if the MBC was no more than four times the MIC. On the contrary, if the MBC was more than four times the MIC, the antibiotics were considered bacteriostatic. The MBCs were performed for each MIC assay and, medians were also calculated.

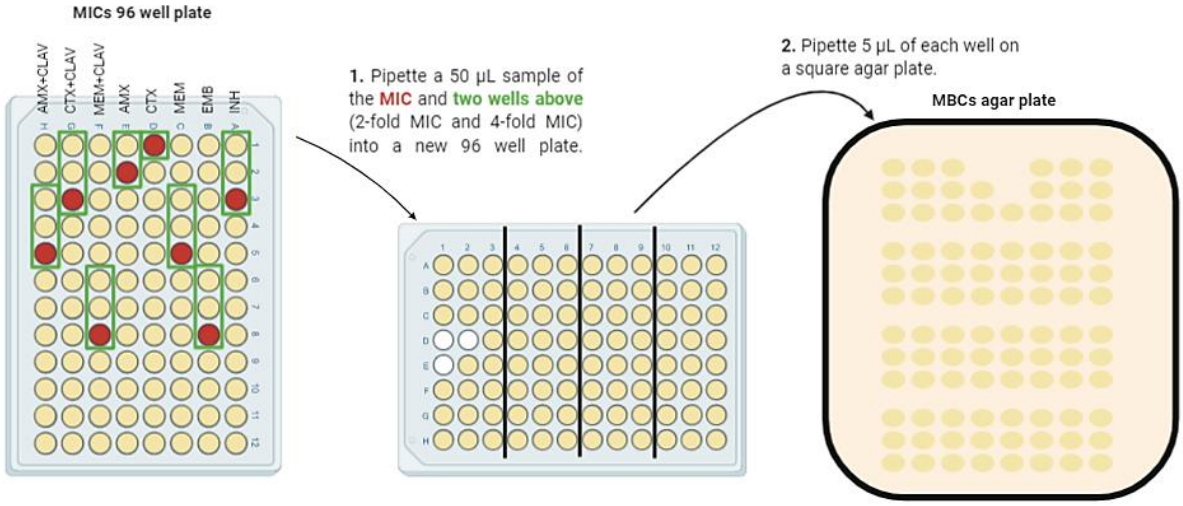

Fig. 30 – Antibiotic bactericidal testing by MBCs assessment. This protocol was performed with *M. smegmatis*. Three β-lactams (amoxicillin – AMX; cefotaxime-CTX; and meropenem - MEM) with and without clavulanate (CLAV), and two anti-TB agents (isoniazid – INH; ethambutol - EMB) were tested. All plates were incubated at 37°C for the adequate time.

1.3. Disk diffusion assays

To assess antibiotic susceptibility differences between WT and *namH*$^{-}$ mycobacteria, disk diffusion assays were performed as previously described[126]. *M. smegmatis* cultures were grown to log phase and treated. After, a pour-plate technique was employed to create a uniformly distributed layer of mycobacteria: the cultures were normalized to an OD_{600} of 0.05 in a total volume of 4 mL, where at least 3.5 mL were molten Top Agar (**Appendix 1**). This mixture was then poured onto 7H10 or 7H10+ATc plates, which were dried for 20 min in a laminar airflow hood. Subsequently, four two-fold dilutions of meropenem (512 µg/mL) were prepared, 20 µL of each were pipetted into the correspondent disks and, the impregnated disks were dried for 20 min. Afterwards, the plates were divided in four quadrants and five 9 mm filter paper disks (**Figure 31**) were placed on top of the uniform layer of Top Agar and mycobacteria with a sterile needle. The plates were then incubated at 37°C for ~2 days. Subsequently, the diameters of the inhibition zones were registered in mm and pictures were taken. This assay was performed once.

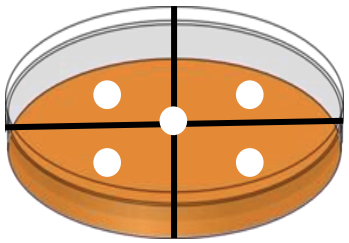

Fig. 31 – Plate disposition for antibiotic susceptibility testing by disk diffusion.

2. Assessing the contribution of the *N*-glycolylation of PG in host immune recognition

2.1. Infections of RAW 264.7 murine macrophages with the *namH* knockdown mutants

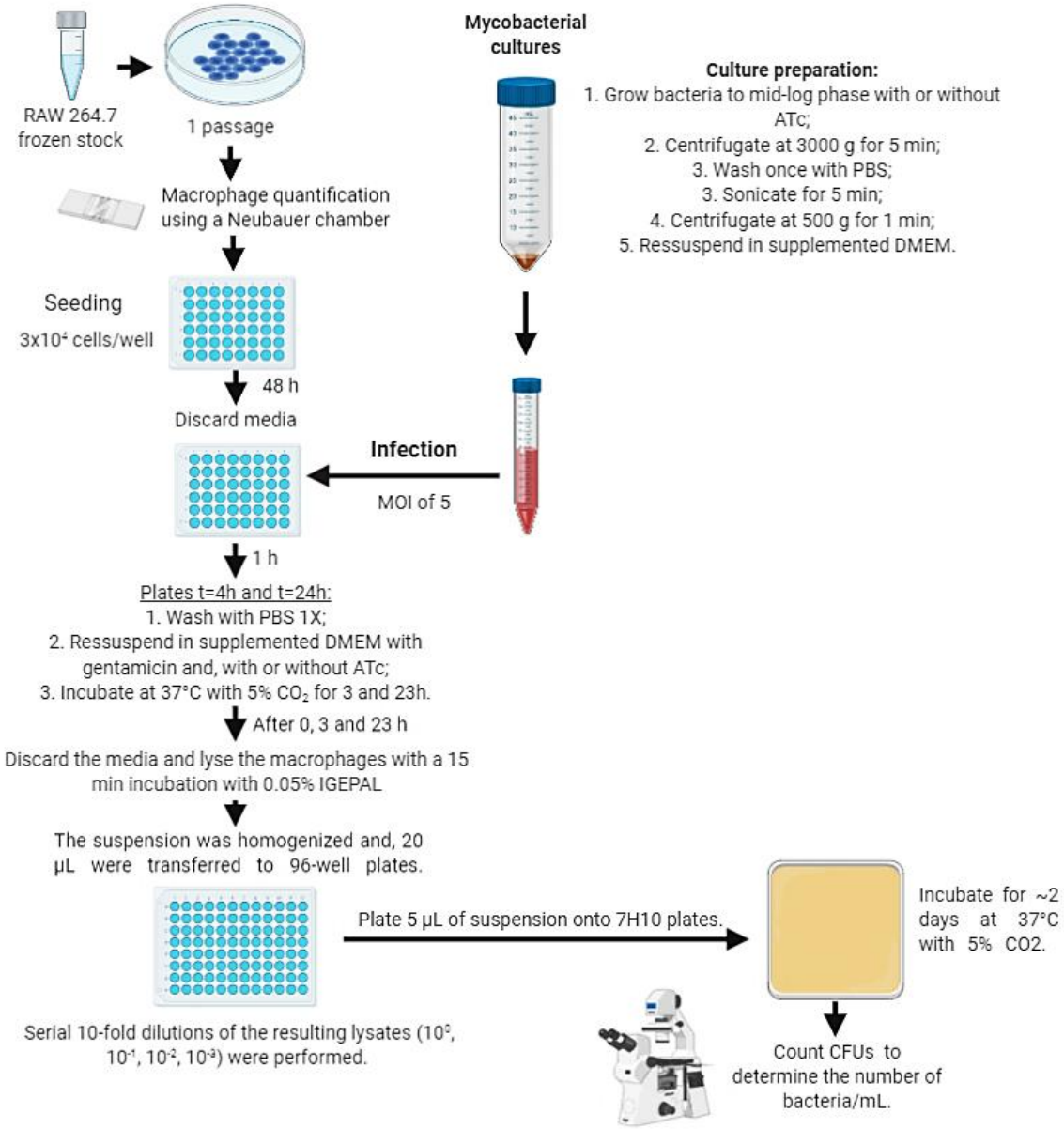

Fig. 32 – Protocol used for infection of RAW 264.7 macrophages with *M. smegmatis*. Macrophages were infected with WT, PLJR962 and a selected *namH* knockdown mutant (*M. smegmatis* C2).

To study differences in pathogenesis between WT and *namH*- mycobacteria, infections of the RAW 264.7 murine macrophages (**Figure 32**) with a selected *namH*- mutant (*M. smegmatis* C2) were performed, as previously described[160,161].

First, the stock of RAW 264.7 cells was rapidly defrosted in warm supplemented DMEM media, centrifuged at 450 *g* for 5 min to remove the DMSO used in the freezing process, the supernatant was discarded, cells were ressuspended in warm supplemented DMEM, plated in a TC-petri dish and, incubated at 37°C with 5% CO_2 (P_0). The cell culture was maintained with the addition of new supplemented DMEM media after 2 days (P_1). After 48 h, RAW 264.7 macrophages were seeded in 48-well-plates at a density of $3x10^4$ cells/well and, quantified using a Neubauer chamber.

In the day of infection, mycobacterial cultures were grown to mid-log phase in the presence or absence of 100 ng/mL of ATc, centrifuged at 3000 *g* for 5 minutes, and washed with 5 mL of Phosphate buffer saline (PBS) 1X. To avoid clumps and obtain a single-cell suspension, the bacterial culture was subsequently sonicated for 5 min, centrifuged at 500 *g* for 1 min and, resuspended in supplemented DMEM media[160,161]. To infect RAW 264.7 macrophages, the media was discarded, and the macrophages were infected with a single-cell suspension of mycobacteria at a multiplicity of infection (MOI; ratio of bacteria/cells) of 5 and, incubated at 37°C with 5% CO_2 for different timepoints (1h; 4h; 24h)[160,161].

2.1.1. Assessing bacterial survival inside macrophages by counting CFUs

After defined incubation timepoints (1h; 4h; 24h), differences in bacterial intracellular survival between macrophages infected with either *M. smegmatis* WT, PLJR962 or a selected *namH*- mutant (C2) were assessed.

At t=1h, the TC-plates from t=4h and t=24h were further prepared. The media with bacteria was discarded from these plates, macrophages were washed once with PBS 1X and, further ressuspended in supplemented DMEM media[160,161], with or without 100 ng/mL of ATc. Gentamicin (50 mg/mL; Sigma-Aldrich) was also added to the cell media at a final concentration of 5 µg/mL to kill extracellular bacteria.

At timepoints 1h, 4h and 24h, the media was discarded, and macrophages were lysed after 15 min incubation with a 0.05% (v/v) IGEPAL (Sigma-Aldrich) solution in water[160,161]. The suspension was homogenized and, 20 µL were transferred to 96-well plates. Serial 10-fold dilutions of the resulting lysates (10^0, 10^{-1}, 10^{-2}, 10^{-3}) were performed in sterile water, 5 µL of these were transferred onto 7H10 plates, which were incubated for ~2 days at 37°C with 5% CO_2. After this period, CFUs were counted using an optical microscope[160,161]. The number of CFUs was calculated using the following formula: [number of colonies x dilution factor] / volume of inoculum. Two biological replicates, each counting three technical replicates, were performed. The average of the CFUs and the standard error of the mean (SEM) were calculated. The statistical significance of the differences in CFUs between control cultures and induced cultures at different timepoints (1h; 4h; 24h) was determined using a two-tailed t-test (Excel), with the following confidence intervals (CIs): CI1 = 90%; CI2 = 95%; CI3 = 99%.

Results and Discussion

The success of *Mtb* as an intracellular pathogen derives from its highly complex CW, its ability to subvert the immune system of the host and, its ability to survive inside macrophages in a state of dormancy. As opposed to most bacteria, mycobacterial PG has several distinctive characteristics, of which the predominance of *N*-glycolylated muramic acid residues is the most striking[71,72]. The *N*-glycolylation of muramic acid residues, catalyzed by the *N*-acetyl muramic acid hydroxylase (NamH), is an evolutionary advantage characteristic of *Mycobacterium*[72]. Previous studies showed that mycobacteria lacking *namH* are hypersusceptible to β-lactams/lysozyme and less immunogenic[72,73,74]. Despite the non-essentiality of *namH*[81], the *N*-glycolylation of PG is hypothesized to increase CW integrity[72] and, to have a undetermined role in pathogenesis, by either enabling immune evasion or by facilitating the persistence of *Mtb* inside host macrophages and eventual disease transmission[73,74]. Moreover, the *namH* gene is highly conserved in *Mtb* clinical isolates[157], implying a vital function for the *N*-glycolylation of PG in antibiotic resistance or/and in immune response. Therefore, the main goal of this thesis is to modulate the expression of *namH* in order to understand the role of the *N*-glycolylation of mycobacterial PG in antibiotic resistance and in host immune recognition.

A) Construction and characterization of *namH* knockdown mutants in mycobacteria

1. Repression of the *namH* gene in *M. smegmatis* and *Mtb* H37Ra using CRISPRi

The first step to construct the *namH* knockdown mutants in mycobacteria was to design various sgRNAs (**Tables 5 and 6**), with different PAM strengths and different targeting sites, either in the *namH* gene or in the promoter region (**Figure 26**). After, the cloning procedures were completed as optimized by Rock *et al*[172]. The CRISPRi backbones were first amplified in *E. coli* yielding the following concentration after purification: PLJR962 at 368 ng/µL and PLJR965 at 328.5 ng/µL. The plasmids were then digested with BsmB*I*, purified and quantified: PLJR962 at 77 ng/µL and PLJR965 at 63 ng/µL. Gel electrophoresis (**data not shown**) confirmed that both PLJR962 (*M. smegmatis*) and PLJR965 (*Mtb*) were completely digested since the digestion products had the expected size (8881 bp and 8631bp, respectively). To clone the *namH* sgRNA targeting sequences into the sgRNA scaffold, two complementary primers (**Tables 7 and 8**) were designed and annealed, generating several annealed oligos (*M. smegmatis*: AO1-AO8; *Mtb*: AO1-AO6; **Appendix 2**). The sequences 5'-GGGA-3' and 5'-AAAC-3' were added to the forward and reverse primers to regenerate the sgRNA promoter and the dCas9 handle sequences, thus facilitating the ligation of the annealed oligos to the CRISPRi vectors by complementarity, aided by T4 DNA ligase. To obtain the sgRNA-containing CRISPRi plasmids, *E. coli* JM109 CCC were transformed with the ligation mixture, KAN^R transformants were selected and the obtained plasmid DNA was extracted. Typically, the obtainment of desired clones after transformation is performed by restriction analysis. However, this CRISPRi system was designed so that BsmB*I* (5'- $CGTCTC(N)_1$ -3') restriction sites disappear after digestion to avoid the religation of vector ends. In this way, the obtainment of the desired recombinant clones was confirmed by Sanger sequencing. The sequencing results (**Appendix 3**) demonstrate the successful construction of all desired recombinant vectors (**Appendix 4**), as verified by AO search for every sequencing output. The obtained concentrations of the CRISPRi clones after plasmid purification are detailed in **Tables 12 and 13**.

Table 12 - Obtained concentrations of the CRISPRi recombinant vectors for *M. smegmatis*.

Mutant	Plasmid	[ ] (ng/µL)	260/280	260/230
C1	**PLJR962::AO1**	123.2	1.9	2.2
C2	**PLJR962::AO2**	190.8	1.9	2.4
C3	**PLJR962::AO3**	47.5	1.9	2.2
C4	**PLJR962::AO4**	44.1	1.9	2.3
C5	**PLJR962::AO5**	202.6	1.9	2.4
C6	**PLJR962::AO6**	116.7	1.9	2.2
C7	**PLJR962::AO7**	288.8	1.9	2.2
C8	**PLJR962::AO8**	44.3	1.9	2.2

Table 13 – Obtained concentrations of the CRISPRi recombinant vectors for *Mtb* H37Ra.

Mutant	Plasmid	[ ] (ng/µL)	260/280	260/230
C1	**PLJR965::AO1**	180.8	1.9	2.3
C2	**PLJR965::AO2**	137.4	1.9	2.3
C3	**PLJR965::AO3**	174.0	1.9	2.3
C4	**PLJR965::AO4**	189.5	1.9	2.2
C5	**PLJR965::AO5**	203.8	1.9	2.2
C6	**PLJR965::AO6**	205.1	1.9	2.2

To obtain mycobacteria harboring the CRISPRi systems, *M. smegmatis* or *M. tuberculosis* H37Ra ECCs were transformed with the recombinant clones and, after a recovery period, KAN^R transformants were selected. To silence the *namH* gene, mycobacteria were grown in 7H9 media supplemented with 100 ng/mL of ATc.

2. Characterization of the *namH* knockdown mutants

2.1. Growth curves

2.1.1. *M. smegmatis*

To perform growth curves, various cultures of *M. smegmatis* (WT, PLJR962, control strain PM965, ΔnamH, C1-C8) were incubated with and without inducer for 45 hours, during which the OD_{600} was registered at pre-determined time points (0h; 18h; 21h; 24h; 42h; 45h), as described in **Materials and Methods, section A) 2.1.**. The obtained results for the tested cultures are detailed in **Figure 33**.

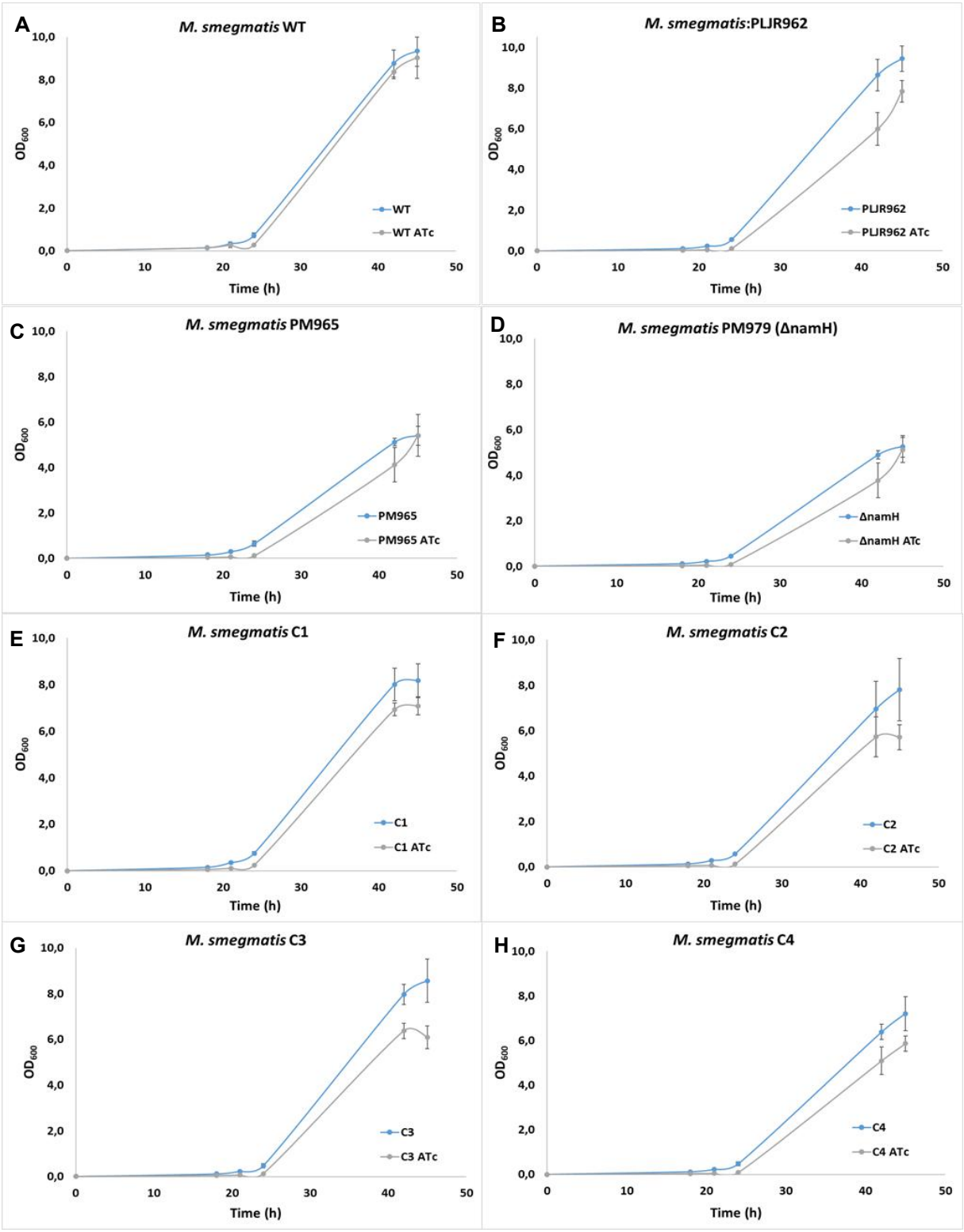
A
M. smegmatis WT
WT
WT ATc
B
M. smegmatis:PLJR962
PLJR962
PLJR962 ATc
C
M. smegmatis PM965
PM965
PM965 ATc
D
M. smegmatis PM979 (ΔnamH)
ΔnamH
ΔnamH ATc
E
M. smegmatis C1
C1
C1 ATc
F
M. smegmatis C2
C2
C2 ATc
G
M. smegmatis C3
C3
C3 ATc
H
M. smegmatis C4
C4
C4 ATc
OD600
Time (h)

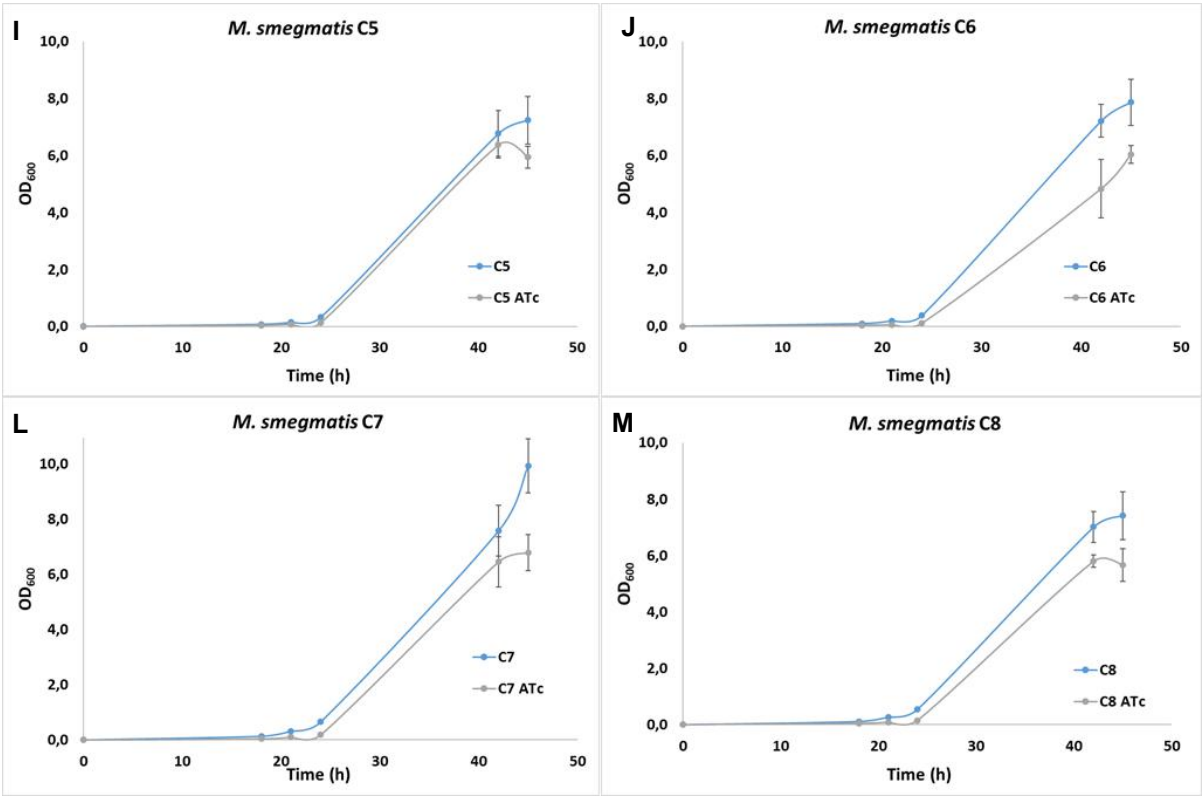

Fig. 33 – Growth curves of *M. smegmatis* cultures in the absence or presence of 100 ng/mL of ATc: (A-C) the negative controls *M. smegmatis* WT, PLJR962 and PM965; **(D)** *M. smegmatis* PM979/ΔnamH; **(E-M)** the *namH* knockdown mutants C1-C8. The growth of each culture in function of the incubation time was evaluated in at least three different experiments (n=3), after which the average was calculated. The error bars represent the standard error of the mean (SEM).

The obtained results show that the negative controls *M. smegmatis* WT (**Fig. 33 A**) and *M. smegmatis* control strain PM965 (**Fig. 33 C**) are growing properly. Moreover, the growth curve of both negative controls is similar with and without ATc induction. This observation, consistent with previous studies[180], suggests that ATc is not toxic to mycobacteria. When compared, *M. smegmatis* WT and PM965 present distinct growth curves possibly due to genomic differences (**Table 4**). *M. smegmatis* PM979/ΔnamH (**Fig. 33 D**) grows similarly to PM965 with and without inducer (ATc), therefore confirming the non-essentiality of the *namH* gene, as reported by previous studies[72,81]. On another hand, the negative control *M. smegmatis*:PLJR962 (**Fig. 33 B**) presents a delayed growth curve when incubated in the presence of 100 ng/mL of ATc, suggesting a residual level of $dCas9_{Sth1}$ toxicity following the induced expression of $dCas9_{Sth1}$ in the CRISPRi backbone (PLJR962). This conclusion is in accordance with previous publications, which have reported the lethality of a high-level expression of $dCas9_{Spy}$ with a non-genome targeting control sgRNA in *M. smegmatis*[172] and, the toxicity of the overexpression of dCas9 in *E. coli*[184-187]. Moreover, the knockdown mutants (*M. smegmatis* C1-C8; **Fig. 33 E-M**) grow similarly to PLJR962 when incubated without ATc. Following CRISPRi induction, no major growth differences were observed between the knockdown mutants and the control vector PLJR962. Therefore, the obtained results indicate that *namH* knockout or repression does not produce severe growth defects, as it is expected for a non-essential gene and, as has been previously reported in *Mtb*[74].

2.2. Spotting dilutions

2.2.1. *M. smegmatis*

Spotting dilutions were performed as described in **Materials and Methods, section A) 2.2.** to evaluate differences in cell viability after normalization of all tested cultures of *M. smegmatis* (WT, PLJR962, PM965, ΔnamH, C1-C8) to a starting OD_{600} of 0.001. The obtained results (**Figure 34**) show that the negative controls WT and control strain PM965 do not display any significant differences in cell viability in the presence of inducer, confirming that CRISPRi induction with 100 ng/mL of ATc is not toxic to mycobacteria. In fact, Ehrt *et al*. have established the MIC of ATc for *M. smegmatis* to be approximately 500 ng/mL and, that maximal induction was achieved with ATc concentrations 10-fold below the MIC[180]. Still, all bacteria seemed to grow less in ATc supplemented agar when compared to 7H10. Even though ATc may have a very low degree of toxicity, as described by Gossen *et al*[188], this effect is most likely caused by some degree of $dCas9_{Sth1}$ toxicity.

Although the strongest PAMs lead to maximal gene repression[172], **Figure 34** does not show any cell viability differences between the tested mutants (*M. smegmatis* C1-C8). This is easily explained since: **i)** the assessment of PAM strength by repressing a non-essential gene is not optimal; **ii)** most sgRNAs, except for C1, were designed upstream of strong PAMs (PAM1-PAM4), which produce a similar fold repression. In conclusion, all *namH* knockdown mutants survive in the presence of ATc, confirming the non-essentiality of the *namH* gene[72,81].

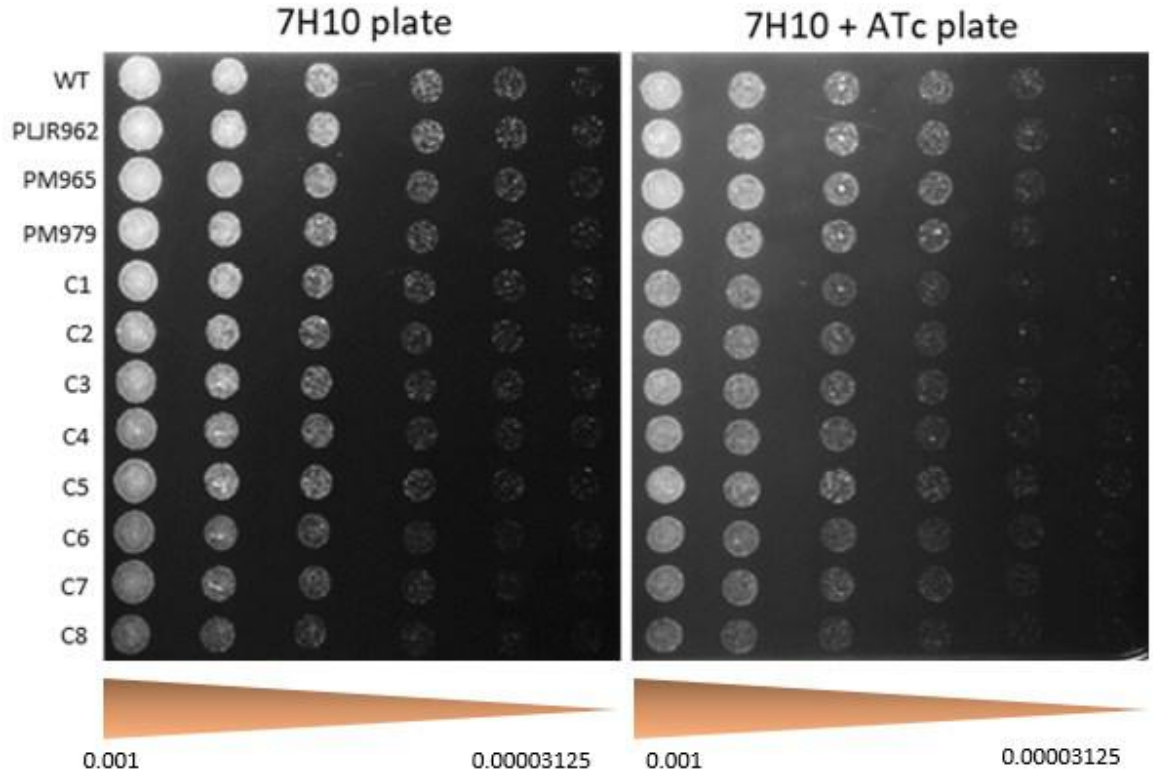

Fig. 34 - Spotting dilutions of all *M. smegmatis* cultures (n=3): negative controls (WT, PLJR962, PM965), positive control (PM979/ΔnamH) and the knockdown mutants (C1-C8). The first spots were normalized to an OD_{600} of 0.001 and the next ones were performed by preparing 2-fold serial dilutions.

3. Assessment of the repression of *namH* in a selected mutant using qRT-PCR

The mRNA expression levels of *namH* at 6 hours post-induction were assessed by qRT-PCR in several samples (*M. smegmatis* WT, PLR962 and C2) to confirm the repression of the target gene (*namH*) in a selected knockdown mutant, *M. smegmatis* C2, as described in **Materials and Methods, section A) 3.1.**.

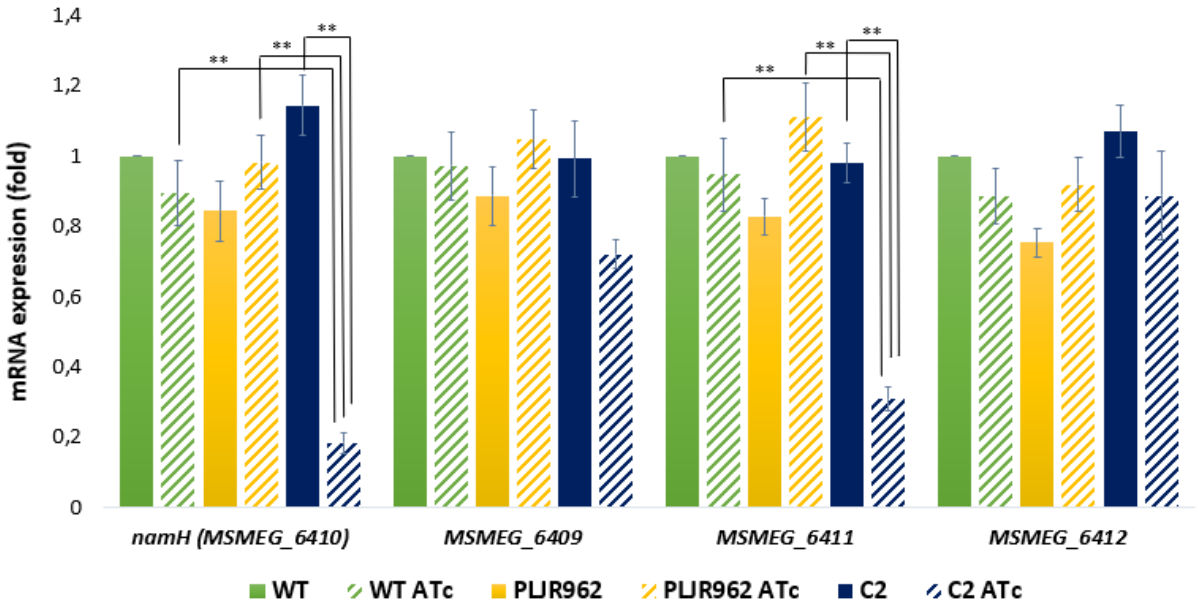

Fig. 35 - Graphical representation of the differences in the average of the relative gene expression of mRNA sequences *MSMEG_6410*, *MSMEG_6409*, *MSMEG_6411* and *MSMEG_6412* normalized to the reference gene *dnaK*, between samples (*M. smegmatis* WT, PLJR962, C2) with and without 100 ng/mL of ATc, at 6 hours post-induction (n=3). Error bars indicate the standard error of the mean. The significance of the differences between averages was calculated using a two-tailed unpaired t-test with different variances: * when p-value < 0.02; ** when p-value < 0.01.

As expected, **Figure 35** shows that the relative fold expression of *namH* is approximately 1 in all controls (*M. smegmatis* WT, WT ATc, PLJR962, PLJR962 ATc and the uninduced knockdown mutant C2). The obtained results for the induced knockdown mutant C2 ATc demonstrate a highly significant decrease in the mRNA expression levels of *namH* when compared to WT ATc (~4.8-fold; p-value = 0.0034), the control vector PLJR962 in the presence of ATc (~5.3-fold; p-value = 0.004) or the uninduced mutant C2 (~6.2-fold; p-value = 0.0034). These observations confirm that *namH* was successfully repressed in the induced knockdown mutant C2 ATc. Rock *et al.* have previously demonstrated that the $dCas9_{Sth1}$ CRISPRi system generated a robust level of knockdown (11–226 fold) of several target genes in *M. smegmatis*[172]. Despite using the same CRISPRi system, the obtained level of knockdown is not nearly as robust as expected[172] and, is more comparable with the level of knockdown achieved by Choudhary *et al.* and Singh *et al.* using first-generation $dCas9_{Spy}$ CRISPRi systems (~4-fold)[170,171]. This difference is even more astonishing since the knockdown mutant C2 uses the strongest available PAM to $dCas9_{Sth1}$, which is the reason why it was chosen as a study model.

The *namH* gene is part of a multicistronic operon (**Figure 36**) which comprises both *MSMEG_6410* and *MSMEG_6411*. Indeed, previous studies have reported that repressing

operonic genes can lead to the occurrence of downstream polar effects or of reverse polarity[172,176].

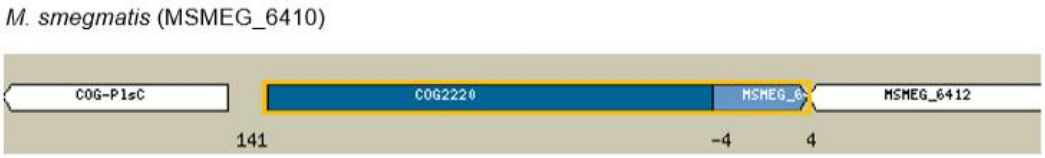

Fig. 36 – The local context of the *namH* gene in *M. smegmatis*. The *namH-msmeg_6411* operon is underlined in yellow.

Thus, the mRNA expression levels of the gene downstream of *namH*, *MSMEG_6411* (encodes a conserved small protein with unknown functional significance), at 6 hours post-induction were assessed by qRT-PCR. The results (**Figure 35**) show that the relative fold expression of *MSMEG_6411* is approximately 1 in all controls. The obtained results for the induced knockdown mutant C2 ATc demonstrate a highly significant decrease in the mRNA expression levels of *MSMEG_6411* when compared to WT ATc (~3.1-fold; p-value = 0.004), PLJR962 ATc (~3.6-fold; p-value = 0.0019) or the uninduced knockdown mutant C2 (~3.2-fold; p-value = 0.0039). As was previously described[170,171,172], these observations confirm that CRISPRi is polar in mycobacteria: targeting *namH,* using a sgRNA that targets a site between the beginning and the middle of the gene (**Figure 26**), leads to repression of transcription of the downstream gene *MSMEG_6411*. To better evaluate the concept of CRISPRi polarity, the mRNA expression levels of the remaining knockdown mutants (C1, C3-C8) should also be assessed.

To confirm that the repression of *namH* does not affect the transcription of neighboring genes, the mRNA expression levels of *MSMEG_6409* (encodes an acetyltransferase) and of *MSMEG_6412* (encodes a conserved hypothetical protein) at 6 hours post-induction were also assessed by qRT-PCR. The obtained results (**Figure 35**) show that the relative fold expression of both *MSMEG_6409* and MSMEG_6412 is approximately 1 in all controls. Moreover, the induced knockdown mutant C2 ATc presents a slight decrease in the mRNA expression levels of *MSMEG_6409* when compared to WT ATc (~1.3-fold; p-value = 0.1502), PLJR962 ATc (~1.4-fold; p-value = 0.0486) or the uninduced knockdown mutant C2 (~1.4-fold; p-value = 0.1265). In addition, the induced knockdown mutant C2 ATc also presents a slight decrease in the mRNA expression levels of *MSMEG_6412* when compared to WT ATc (~0.98-fold; p-value = 0.9497), PLJR962 ATc (~1.0-fold; p-value = 0.8123) or the uninduced knockdown mutant C2 (~1.2-fold; p-value = 0.3617). No significant differences were observed as it was expected since both these genes are transcribed in the opposite direction of *namH*.

The generality of our data (**data not shown**) points toward the existence of a residual level (< 5%) of leaky expression of $dCas9_{Sth1}$, as expected[172].

Previous studies have stated three determinants of CRISPRi efficacy: **i)** PAM strength; **ii)** targeting strand; and **iii)** PAM position along the targeted gene[170,171,173,174]. These studies have showed that repression efficiency is directly correlated with PAM strength and, that effective gene silencing is achieved when either strand of the promoter or the non-template strand of the gene are targeted[170,171,173,174]. In addition, some studies have revealed that repression efficiency was higher when the targeted sequence distanced less from the transcription start site (TSS)[170,173,174]. Nonetheless, Rock *et al*. have showed that the $dCas9_{Sth1}$ CRISPRi system can mediate robust gene knockdown irrespective of PAM distance from the TSS[166].

To probe these determinants, various sgRNAs targeting the same strand, but with different PAMs and target sites, were employed to produce the knockdown mutants used in this work (**Figure 26**). However, there was no chance to assess the mRNA expression levels of all generated CRISPRi mutants due to prolonged protocol fine-tuning. Since most employed sgRNAs target the non-template strand of *namH*, no differences in the level of knockdown of the constructed knockdown mutants are expected at that level. In terms of PAM strength, stronger PAMs are expected to produce a higher level of knockdown but it is important to note that the fold repression discrepancy between strong PAMs (PAM1-PAM4) is minimal[172] and, consequently, the efficacy of targeted gene knockdown is expected to be similar for every tested mutant. In the case of the knockdown mutant C1, which uses a considerable weaker PAM (PAM11), a high level of knockdown is still expected because the employed sgRNA targets the promoter zone of the *namH* gene and, this type of repression inhibits transcription initiation by RNA polymerase[173,174]. Differences in the level of knockdown of the constructed knockdown mutants due to the targeted site in the *namH* gene cannot be predicted.

B) Deciphering the role of the *N*-glycolylation of PG in antibiotic susceptibility and in host immune recognition

1. Determination of WT vs. *namH*$^-$ antibiotic susceptibility

1.1. Minimum inhibitory concentrations (MICs)

One of the main goals of this thesis is to understand the role of the *N*-glycolylation of PG in antibiotic resistance, mainly focused on β-lactams resistance, which have recently been repurposed to treat MDR-TB. To do that, the MIC values of three β-lactams (amoxicillin, cefotaxime and meropenem), with and without the β-lactamase inhibitor clavulanate, and two anti-TB agents (ethambutol, isoniazid) were determined for *M. smegmatis*. The MICs were annotated as the minimum concentration of antibiotic capable of preventing visible bacterial growth. This assay was performed at least three times for each culture of interest and, the median values were calculated. The median was preferred over the mean since: **i)** the tested antibiotic concentrations were pre-defined discrete values; **ii)** the median is not as skewed by outliers as the mean.

Since the assessment of β-lactams susceptibility does not follow a recognized reference methodology, the EUCAST non-species related PK-PD breakpoints (**Table 14**) were used to classify mycobacteria as either susceptible or resistant to β-lactams.

Table 14 - EUCAST non-species related PK-PD breakpoints for β-lactams. S – susceptible; R – resistant.

MIC breakpoints (µg/mL)		
	S ≤	R >
Amoxicillin	2	8
AMX+Clav	2	8
Cefotaxime	1	2
Meropenem	2	8

The assessment of antibiotic susceptibility differences between distinct cultures was performed as described in **Materials and Methods, section B) 1.1.** After 48 h of incubation in the presence of the tested antibiotics, 96-well plates containing distinct cultures of *M. smegmatis* were observed for any evidence of growth and the MICs were annotated. The MIC determination process was simple since there was often a clear distinction between wells evidencing mycobacterial growth and wells where mycobacterial growth was visually undetectable. Nevertheless, the occurrence of some experimental variability between assays existed due to culture asynchrony, characterized by the presence of bacteria at different growth stages. The obtained medians of the minimum inhibitory concentrations for each antibiotic are systematized in **Table 15** and represented in **Figure 37**.

Table 15 – Systematic representation of the median of the minimum inhibitory concentrations (MICs; µg/mL) for the tested antibiotics: Amoxicillin (AMX), Amoxicillin + Clavulanate (AMX+CLAV), Cefotaxime (CTX), Cefotaxime + Clavulanate (CTX+CLAV), Meropenem (MEM), Meropenem + Clavulanate (MEM+CLAV), Ethambutol (EMB) and Isoniazid (INH). The distinct cultures were classified as susceptible (orange), intermediate (yellow) or resistant (blue) to β-lactams according to the EUCAST non-species related PK-PD breakpoints.

Median of MIC values								
	AMX	**AMX+ CLAV**	**CTX**	**CTX + CLAV**	**MEM**	**MEM+ CLAV**	**EMB**	**INH**
WT	64	4 - 8	64 - 128	64	4	4	0.5 - 1	16 - 32
WT ATc	64	4	128 - 256	64	2	2 - 4	0.5	16
PLJR962	64	8	256	128	4	4	0.5	16
PLJR962 ATc	128	8	128	32	4	4	0.5	16
C1	64	8	128	32	2	4	1	32
C1 ATc	64	2	16	8	1	1	1	16
C2	64	8	64	64	4	4	0.5	16
C2 ATc	64	4	32	16	1	2	0.5	16
C3	32 - 64	8	64	64 - 128	2 - 4	2 - 4	0.5	16 - 32
C3 ATc	64	2 - 4	16	8 - 16	2	1	0.5	8 - 16
C4	64	4	64	64	4	2	1	16
C4 ATc	32	4	8	8	2	1	0.5	16
C5	32	8	64	32	4	4	1	16
C5 ATc	32	4	8	16	2	2	1	16
C6	64	8	256	64	4	4	0.5	16
C6 ATc	64	4	16	16	2	2	1	16
C7	128	8	128	128	4	4	1	16
C7 ATc	64	8	16	16	2	1	0.5	32
C8	128	4	128	128	4	4	1	32
C8 ATc	128	4	16	16	2	2	1	32
Δ namH	1 - 2	2	4	4	1	0.5 - 1	0.5 - 1	16 - 32
Δ namH ATc	1	2	2 - 4	4	0.5	1	0.5	16
PM965	4	4	32	32	2 - 4	2 - 4	0.5 - 1	8 - 16
PM965 ATc	2 - 4	4	16 - 32	32	2	2 - 4	0.5	16 - 32

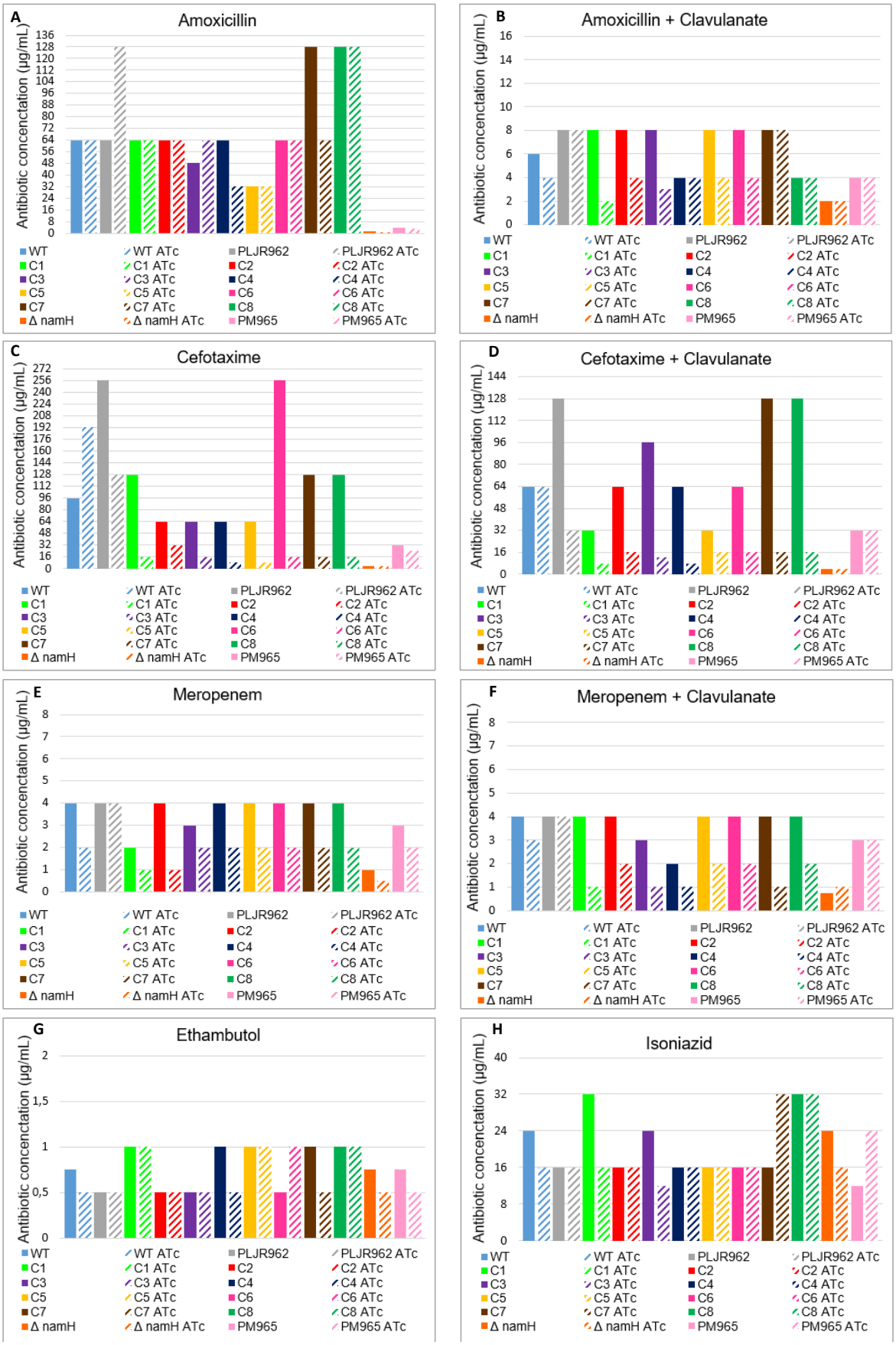

Fig. 37 – **Graphical representation of the median of the minimum inhibitory concentrations (MICs; µg/mL) for antibiotics**: **A)** Amoxicillin; **B)** Amoxicillin + Clavulanate; **C)** Cefotaxime; **D)** Cefotaxime + Clavulanate; **E)** Meropenem; **F)** Meropenem + Clavulanate; **G)** Ethambutol and; **H)** Isoniazid.

Generally, the MIC of amoxicillin was found to be about 64 μg/mL, as the value obtained by Viswanathan *et al.* with *M. smegmatis* WT[189]. The MIC of amoxicillin-clavulanate was found to be 4-8 μg/mL, demonstrating that the addition of clavulanate leads to an 8-fold reduction in the MIC, also verified with *M. smegmatis* WT by Flores *et al*[126]. Most times, the MIC of cefotaxime was found to be 64-128 μg/mL, in accordance with the work of Viswanathan *et al.* using *M. smegmatis* WT[189]. The addition of clavulanate to cefotaxime did not lead to evident changes in the MICs. In the case of meropenem, the MIC was often found to be 4-8 μg/mL, as was also observed by Viswanathan *et al*[189]. Generally, the addition of clavulanate to meropenem did not lead to changes in the MICs. The MIC of ethambutol was usually around 0.5-1 μg/mL, in agreement with the results obtained with *M. smegmatis* WT by Wolff *et al*[190]. Moreover, the MIC of isoniazid was often about 16 μg/mL, as observed by Viswanathan *et al*[189].

Comparing the tested β-lactams, meropenem generally presents the lowest MICs (**Table 15/Figure 37**). This means that a lower concentration of meropenem, in comparison to amoxicillin or cefotaxime, is necessary to inhibit mycobacterial growth. The reasons for the higher efficiency of meropenem at inhibiting bacterial growth are the following: **i)** meropenem inhibits the action of mycobacterial Ldts, the most active transpeptidases during PG cross-linking[55,76,77,101,106,107]; **ii)** meropenem also targets some PBPs of *Mtb*[55,77,106,107,122]; **iii)** meropenem is especially resistant to hydrolysis by β-lactamases, being a poor substrate and even an inhibitor of BlaS and BlaC[55,123]. Hence, meropenem efficiently inhibits the cross-linking of PG by targeting several proteins involved in this process. This explains why meropenem has been repurposed to treat MDR-TB. In contrast, amoxicillin and cefotaxime only target some PBPs. The obtained results (**Table 15/Figure 37**) also show that the amoxicillin-clavulanate combination can also efficiently inhibit bacterial growth, suggesting that amoxicillin may target proteins with relevant roles in the maintenance of CW integrity. However, this effect is only seen in the presence of a β-lactamase inhibitor such as clavulanate.

As expected, the observed MICs for the negative controls (*M. smegmatis* WT, PLJR962 and PM965) and the positive control (*M. smegmatis* PM979/ΔnamH) are not considerably influenced by the addition of ATc. Most MICs remain unaltered after ATc addition and, in case of variations, these are most likely 2-fold differences, which can occur due to experimental errors and are, therefore, not considerable[50].

When compared with WT or PLJR962, *M. smegmatis* PM965 presents lower MIC values for all β-lactams (AMX, CTX, MEM) without the β-lactamase inhibitor clavulanate. This increased susceptibility to β-lactams is expected since PM965 lacks the major β-lactamase enzyme of *M. smegmatis*, BlaS[72,126] (**Table 4**).

Unlike *M. smegmatis* WT, PLJR962 or the knockdown mutants, the addition of clavulanate to β-lactams (AMX+CLAV, CTX+CLAV, MEM+CLAV) does not influence the MICs of both *M. smegmatis* PM965 and PM979/ΔnamH, which lack BlaS[72] (**Table 4**). In contrast to previous studies[126], no synergy between *blaS1* deletion and clavulanate treatment was found. This may occur because the addition of the β-lactamase inhibitor clavulanate has a similar effect to the deletion of the *blaS1* gene.

As expected[72], the positive control *M. smegmatis* PM979/ΔnamH exhibits lower MIC values for all β-lactams, with or without clavulanate, when compared to any of the negative controls. Hence, the annotated values indicate that the ΔnamH mutant is hypersusceptible to β-lactams, suggesting a role for the *N*-glycolylation of PG in β-lactams resistance[72]. To understand the increased susceptibility of ΔnamH to β-lactams, an analysis of the NamH protein was

performed using BLASTp. The NCBI system classifies NamH as an "uncharacterized MBL fold metallo-hydrolase containing a Rieske (2Fe-2S) domain". The obtained graphical summary (**Figure 38**) presents several conserved domains in the architecture of NamH, of which the N-terminal UlaG (COG2220) and the C-terminal Rieske (cl00938) domains are the main representatives.

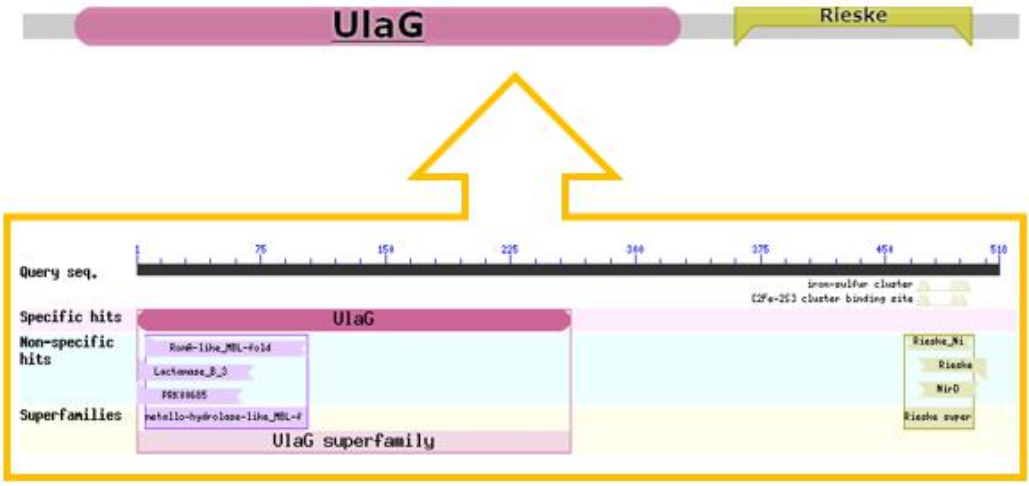

Fig. 38 – Graphical representation of the conserved domains of NamH (*M. smegmatis*).

The UlaG domain has several metabolic functions, belongs to the β-lactamase superfamily, contains two MBL-fold metallo-hydrolase domains (cd16283, PRK00685) and one β-lactamase domain (pfam13483). Metallo-β-lactamases (MBLs) are known to confer resistance to all β-lactams except monobactams, by using the zinc ions at their active site to activate a nucleophilic water molecule, which hydrolyses the β-lactam ring[191,192]. Therefore, it is inferable that the UlaG domain could contribute to the intrinsic β-lactams resistance phenotype of wild-type mycobacteria. Whether the NamH protein has any β-lactamase activity, it is not yet known and needs further assessment. However, a recent study has demonstrated that a novel esterase Rv1497 has both esterase and β-lactamase activities[193]. Similarly, other proteins with predicted metallo-hydrolase domains (e.g.: NamH) could indeed exhibit MBL activity.

In another scope, the ferredoxin-type Rieske iron-sulfur clusters contain three domains (cd03530, pfam00355, COG2146) involved in the metal-dependent acquisition of oxygen and, a NirD domain (COG2146) involved in reduction reactions. Indeed, the Rieske iron-sulfur clusters are common in electron transfer chains (e.g.: bc1 complex) and in non-heme iron oxygenases. Hence, the Rieske domain is implicated in the main catalytic activity of NamH, the *N*-glycolylation of PG via the hydroxylation of the *N*-acetyl group at carbon 2 of the muramic acid residues of mycobacterial PG. The *N*-glycolylation of PG is believed to strengthen CW stability through hydrogen bonding interactions[72]. Furthermore, previous studies argued that the lack of *N*-glycolylated PG residues could disturb the recognition of the glycan backbone by flippases and/or transpeptidases and, eventually, influence further transglycosylation and transpeptidation reactions[72]. These hypotheses could also explain the weakened PG layer and the β-lactams hypersusceptibility phenotype of ΔnamH.

In this way, the β-lactams hypersusceptibility phenotype displayed by ΔnamH could be explained by the "deletion" of: **i)** the activity of NamH as a metallo-β-lactamase; **ii)** the activity of NamH as a monooxygenase, which modifies PG sugars; **iii)** both activities, enabling a synergy between the inhibition of metallo-β-lactamase activity and the inhibition of the *N*-

glycolylation of PG. In fact, the lack of *N*-glycolylated residues leads to decreased PG integrity[72], which can be further accentuated by the action of β-lactams, as they inhibit PG cross-linking[95,96]. Consequently, *namH* deletion/inhibition can synergize with β-lactams treatment to weaken the mycobacterial CW[55].

Nevertheless, Raymond *et al.*[72] have posed another hypothesis that could explain the β-lactams hypersusceptibility phenotype of ΔnamH: "Only *N*-glycolylated muramic acid residues are linked to the AG layer through hydrogen bonding". If this were true, the lack of NamH would lead to defects in the assembly of both the AG and the MA layers, leading to a phenotype of hypersusceptibility to antibiotics that target these layers (e.g.: ethambutol and isoniazid, respectively). However, the observed MICs of both ethambutol and isoniazid remain constant for all cultures (WT, PLJR962, PM965, ΔnamH and the knockdown mutants C1-C8), with and without ATc. Therefore, the obtained results are not in favor of this hypothesis and, suggest that *namH* knockout/repression does not affect ethambutol or isoniazid susceptibility, as had been previously determined[72].

In the absence of inducer, the knockdown mutants C1-C8 present similar MICs to the negative controls WT and PLJR962. In case of variations, these are minor 2-fold differences, which can occur due to experimental errors and, therefore, are not considerable[50]. In the presence of ATc, the knockdown mutants C1 - C8 present lower MICs for all β-lactams when compared to WT or PLJR962. This effect is particularly strong for cefotaxime or cefotaxime-clavulanate (**Figure 39**), indicating a strong link between the *N*-glycolylation of PG and the mechanism of action of cefotaxime.

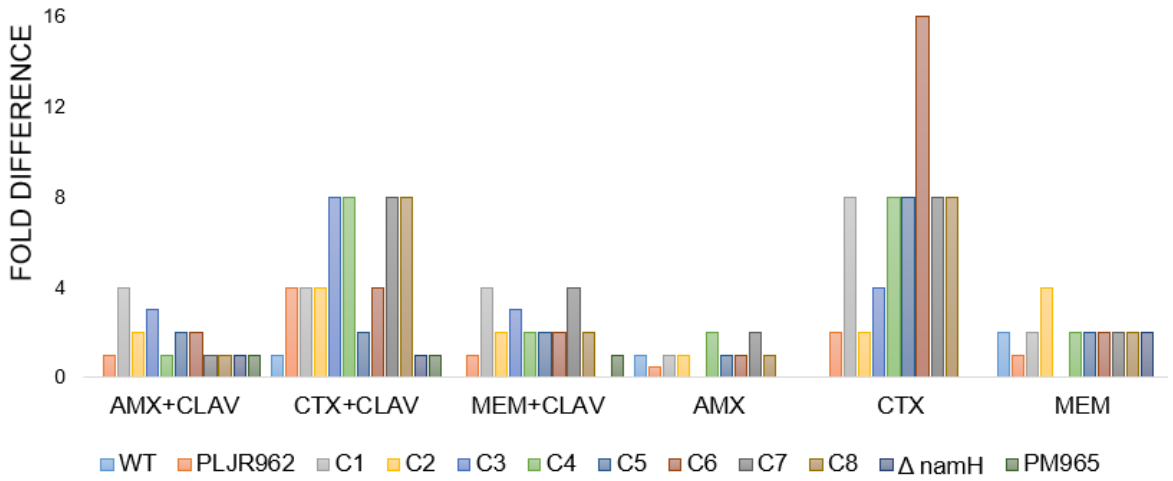

Fig. 39 – ATc fold differences for the MIC values of amoxicillin (AMX), cefotaxime (CTX), meropenem (MEM), amoxicillin + clavulanate (AMX+CLAV), cefotaxime + clavulanate (CTX+CLAV) and meropenem + clavulanate (MEM+CLAV) in *M. smegmatis*.

Thus, a BLASTp analysis (**Table 16**) was performed to determine the targets of cefotaxime in *M. smegmatis*. From this bioinformatics analysis, we can infer that cefotaxime targets the major PBPs of *M. smegmatis*, with higher confidence for class A PBPs PonA1, PonA2 and PonA3. Even though these enzymes are not essential for the viability of mycobacteria, class A transpeptidases catalyze transpeptidation and transglycosylation reactions, contributing to the maintenance of shape and integrity of the CW[95,96]. The induced knockdown mutants have an increased susceptibility to cefotaxime, which could be explained by a synergy between β-lactam inhibition of class A PBPs and decreased PG integrity, due to inhibited NamH activity.

Table 16 – Targets of cefotaxime in *M. smegmatis*, as determined by a BLASTp comparison analysis of annotated DrugBank targets. Percentages in brackets indicate the extent of amino acid sequence identity.

Cefotaxime (DrugBank + BLASTp analysis)	Targets				
			M. smegmatis		
	S. pneumoniae	PBP1B	PonA2 (30,8%)	PonA3 (31,5%)	PbpB (24,7%)
		PBP2A	PonA1 (28,6%)	PonA2 (24,8%)	PonA3 (24,8%)
		PBP1A	PonA2 (27%)	PonA3 (27%)	PonA1 (25,8%)
		PBP2B	PbpB (26,6%)	PbpA (23,7%)	
	B. subtilis	PBP3	PbpA (25,6%)		

The addition of clavulanate to β-lactams (**Figure 40**) considerably decreases the MIC of amoxicillin (in 4-, 8-, 16- or 32- fold) but rarely decreases the MICs of cefotaxime or of meropenem. The excellent synergy between amoxicillin and clavulanate can be explained by the formation of an inactive clavulanate-BlaS complex, which inhibits the hydrolysis of amoxicillin[118-120]. Indeed, the amoxicillin-clavulanate combination treatment has been previously shown to be bactericidal for *Mtb in vitro*[118-120]. The lack of synergy between cefotaxime/meropenem and clavulanate could be explained by differences in the hydrolytic efficiency of BlaS and BlaC to various β-lactams[126-128,194]. In fact, BlaC was described to have 10 to 100-fold lower catalytic affinity for cephalosporins and carbapenems, when compared to penicillins[194].

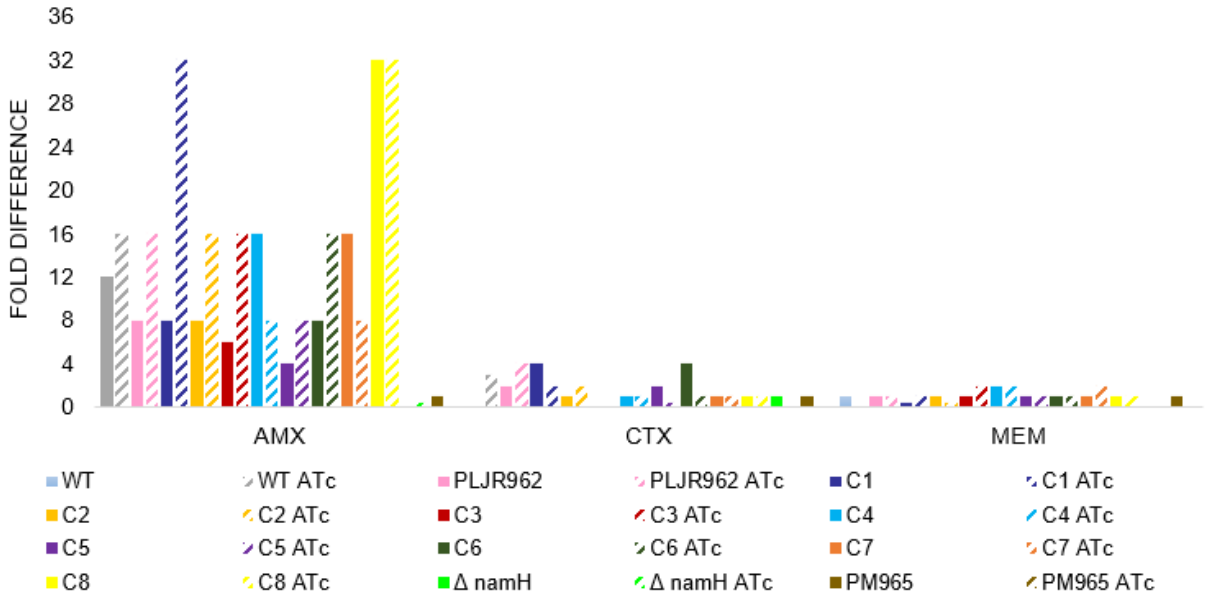

Fig. 40 – Clavulanate fold differences for the MIC values of amoxicillin (AMX), cefotaxime (CTX) and meropenem (MEM) in *M. smegmatis*.

To analyze which knockdown mutants resulted in a higher β-lactam susceptibility phenotype, the number of significant fold differences (> 4-fold) in the MIC of all tested antibiotics between cultures with and without inducer was calculated (**Figure 41**).

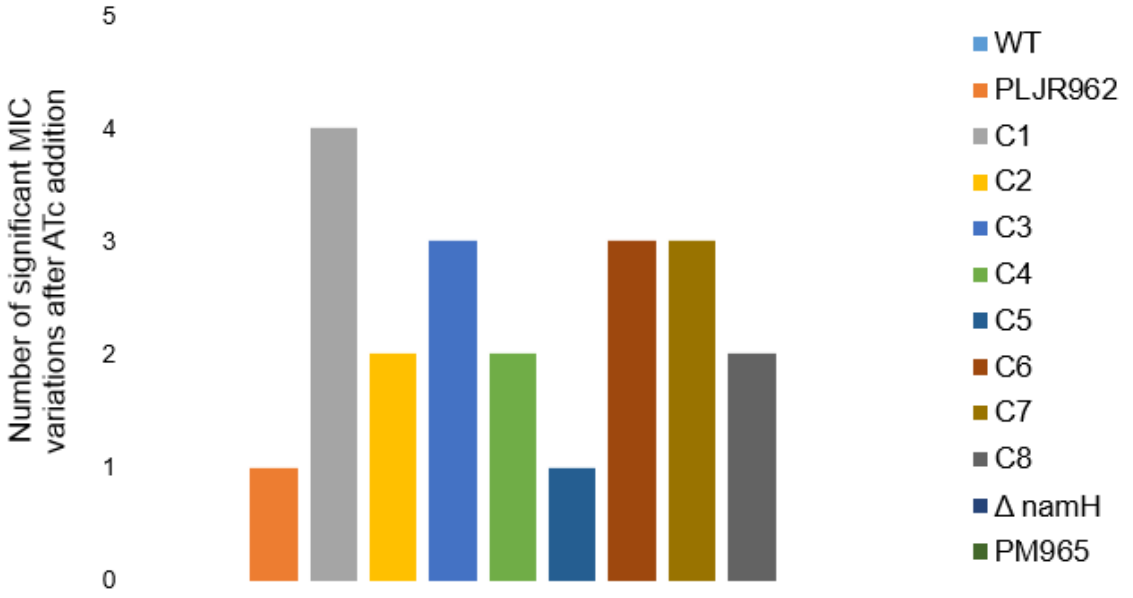

Fig. 41 – Graphical representation of the number of significant (>=4 fold) MIC value variations in all tested antibiotics after ATc addition. The negative and positive controls have constant MIC values while the knockdown mutants have variations in the MIC values after ATc addition.

Figure 41 shows that *M. smegmatis* WT, control strain PM965 and ΔnamH present constant MIC values, without any significant alterations after ATc addition. Both PLJR962 and the knockdown mutant C5 (PAM4) display minimal variations in the MIC values after ATc addition. The knockdown mutants C2 (PAM1), C4 (PAM3) and C8 (PAM4) display considerable variations in the MIC values of several β-lactams after ATc addition. Nonetheless, the knockdown mutants C1 (PAM11), C3 (PAM2), C6 (PAM4) and C7 (PAM4) were found to display increased susceptibility to most β-lactams after ATc addition. Surprisingly, the obtained results could not be explained by PAM strength. Despite the weak PAM of C1, this mutant was found to suffer the greatest number of significant MIC value variations. Perhaps, this may have occurred because the knockdown mutant C1 targets the promoter zone of *namH*, leading to complete inhibition of transcription initiation by RNA polymerase[173,174]. Nevertheless, the correlation between PAM strength, targeting site and knockdown level should be assessed by qRT-PCR.

In terms of targeting position (**Figure 27**), C1 targets the promoter zone, C6 targets the middle of the gene (containing the UlaG domain) and C3 and C7 target the end of the gene (containing the Rieske domain). It is noteworthy that, in the presence of inducer, C1 theoretically halts transcription at its very start while the other knockdown mutants only lead to transcription abortion. From this, it is possible to presume that targeting either the beginning, middle or the end of the gene leads to a phenotype of increased susceptibility to β-lactams. The induced knockdown mutants display increased susceptibility to β-lactams despite the targeting site because no matter how, interfering with the transcription of *namH* will decrease the amount of available NamH protein. Consequently, the *namH*$^{-}$ mutants will be more susceptible to antibiotic pressure, either due to a reduction in the MBL activity of NamH, the hydroxylase activity of NamH or, both. The reduced hydroxylase activity of NamH can lead to: **i)** decreased PG integrity due to a lower availability of *N*-glycolyl groups to establish hydrogen bonds; **ii)** altered PG polymerization due to a lower availability of *N*-glycolylated PG precursors.

Considering the non-species related EUCAST PD-PK breakpoints for β-lactams (**Table 14**),

Amoxicillin:

- WT, PLJR962 and all the uninduced and induced knockdown mutants are classified as resistant to amoxicillin.
- PM965, with and without ATc, is classified as intermediate, being neither resistant nor susceptible to amoxicillin. Nevertheless, it is worth recalling that these bacteria lack BlaS, thus preventing the hydrolysis of amoxicillin.
- ΔnamH, with and without ATc, is classified as susceptible to amoxicillin, further demonstrating that the NamH protein has a role in amoxicillin resistance.

Amoxicillin-clavulanate:

- Every culture except C1 ATc and ΔnamH, with and without ATc, is classified as intermediate, neither as susceptible nor resistant to amoxicillin-clavulanate. The addition of clavulanate significantly lowers MIC values because clavulanate inhibits the hydrolytic activity of BlaS.
- C1 ATc and ΔnamH, with and without ATc, are classified as susceptible to amoxicillin-clavulanate. Therefore, the induced knockdown mutant that produces the most comparable hypersusceptibility phenotype to the one produced by ΔnamH is C1 ATc.

Cefotaxime:

- Every culture without exception is classified as resistant to cefotaxime. Nonetheless, ΔnamH displays the lowest MIC values observed for cefotaxime, indicating a considerable significance of NamH in cefotaxime resistance.
- Whether the breakpoints for cefotaxime-clavulanate are equal to the EUCAST breakpoints for cefotaxime alone, the addition of clavulanate to cefotaxime does not change this classification.

Meropenem:

- In the case of the negative controls, only WT ATc and PM965 ATc are classified as susceptible to meropenem. The rest (WT, PLJR962, PLJR962 ATc, PM965) are neither susceptible nor resistant.
- The ΔnamH mutant and C1 are classified as susceptible to meropenem, with and without ATc, further demonstrating the strength of C1 ATc as a knockdown mutant of *namH*.
- All the other uninduced knockdown mutants are classified as intermediate. The addition of inducer leads to *namH* knockdown and, consequently, makes them susceptible to meropenem, further demonstrating the role of NamH in meropenem resistance.
- Whether the breakpoints for meropenem-clavulanate are equal to the EUCAST breakpoints for meropenem alone, the addition of clavulanate to meropenem may produce some minor 2-fold changes in the MICs. So, mycobacteria are classified between intermediate and susceptible to meropenem-clavulanate.

1.2. Minimum bactericidal concentrations (MBCs)

After MIC determination, the MBCs for *M. smegmatis* were performed for each MIC assay as described in **Materials and Methods, section B) 1.2.** The MBC value was defined as the lowest concentration of antibiotic capable of eradicating mycobacteria. The MBC/MIC ratio was determined in at least three assays and, medians were calculated. When the median of the MBC was no more than four times the median of the MIC, that is if the MBC/MIC ratio was <=4, the tested antibiotics were considered bactericidal[195]. On the contrary, when the median of the MBC/MIC ratio was higher than four, said antibiotics were considered bacteriostatic[195].

The obtained median of the MBC/MIC ratios are displayed in **Table 17**.

Table 17 – Median of the MBC/MIC ratio. The green background indicates the cases where the MBC is equal to the MIC and the red background indicates bacteriostatic conditions.

Median of the ratio between MBCs and MICs								
	AMX	AMX+ CLAV	CTX	CTX + CLAV	MEM	MEM+ CLAV	EMB	INH
WT	1	3	>4	>4	1	2	>4	2
WT ATc	1	3	>4	4	2	1-2	4	1-2
PLJR962	2	2	2	3	1	2	>4	4
PLJR962 ATc	1	2	4	2	4	2	4	2
C1	4	2	2	4	2	1	4	2
C1 ATc	1	2	1	2	1	2	4	2
C2	1	2	4	4	2	1	4	>4
C2 ATc	2	2	1	4	2	1	4	2
C3	>4	1	>4	2-3	3	3	>4	1-2
C3 ATc	1	1	1	4	1-2	2	4	1-2
C4	1	2	>4	4	1	4	>4	1
C4 ATc	1	1	1	1	1	1	4	1
C5	1	2	4	4	1	2	4	1
C5 ATc	1	2	2	1	1	1	2	1
C6	1	2	2	4	1	1	4	2
C6 ATc	1	4	1	2	1	1	2	2
C7	1	1	4	1	2	1	3	1
C7 ATc	2	1	1	1	2	>4	>4	1
C8	1	2	2	2	1	1	2	4
C8 ATc	1	1	2	2	1	2	2	1
Δ namH	2	1-2	2	2	2	2	4	1
Δ namH ATc	2	1-2	1-2	1-2	3	1	>4	2-3
PM965	2	1-2	3	2	2	1-2	>4	4
PM965 ATc	4	1-2	2	3	3	1	4	2-3

It is crucial to note that an antibiotic is not classified as purely bactericidal or bacteriostatic, even more because some antibiotics have both activities[195]. As a matter of fact, the effect of an antibiotic depends on the strain being tested and on the conditions of the experiment[195]: **i)** inoculum size; **ii)** incubation time; **iii)** culture growth phase; **iv)** growth conditions, such as oxygenation, temperature, osmolarity and pH of the medium; **v)** the quantities of antibiotic transferred to subcultures and; **vi)** experimental error.

The obtained results (**Table 17**) show that all β-lactams are bactericidal against most of the tested *M. smegmatis* samples. This observation is in accordance with previous work in *Mtb*, where all β-lactams were found to be highly bactericidal[194]. Both amoxicillin-clavulanate and meropenem are bactericidal against all the tested conditions. Moreover, amoxicillin seems to be highly bactericidal against all the tested samples, except in the case of the uninduced knockdown mutant C3, where it exerts a bacteriostatic effect. Interestingly, the addition of clavulanate to amoxicillin results in total eradication of the uninduced knockdown mutant C3. In addition, meropenem-clavulanate displays a similar bactericidal activity to meropenem against all the tested samples, except for the induced knockdown mutant C7 ATc. Furthermore, cefotaxime is moderately bactericidal in most conditions, but it exerts a bacteriostatic effect against WT, with and without ATc, and against the uninduced knockdown mutants C3 and C4. Likewise, cefotaxime-clavulanate only exerts a bacteriostatic effect against WT in the absence of inducer. Additionally, ethambutol exerts a bacteriostatic effect in the growth of *M. smegmatis* WT, PLJR962, PM965, ΔnamH ATc, the uninduced knockdown mutants C3 and C4 and the induced knockdown mutant C7 ATc. It would be expected for ethambutol to be bacteriostatic against most of the tested samples, as its bacteriostatic activity has been previously demonstrated in several mycobacteria[196]. Generally, isoniazid displayed a high bactericidal activity, except in the case of the uninduced knockdown mutant C2. This observation is in accordance with previous studies in several mycobacteria[196].

As expected, the observed MBC/MIC ratios of the negative controls (*M. smegmatis* WT, PLJR962 and PM965) and the positive control (*M. smegmatis* PM979/ΔnamH) are not considerably influenced by the addition of inducer. Nevertheless, the activity of cefotaxime-clavulanate against WT is altered from bacteriostatic to bactericidal in the presence of inducer. Likewise, the activity of ethambutol against all controls changes with the addition of ATc.

In the presence of inducer, all β-lactams display an increased or constant bactericidal activity against the *M. smegmatis namH* knockdown mutants. Indeed, β-lactams seem to have an increased bactericidal activity against the knockdown mutants C1 (PAM11), C3 (PAM2), C4 (PAM3) and C5 (PAM4) in the presence of inducer. This effect seems unrelated to PAM strength or target site. In the case of C3, the activity of both amoxicillin and cefotaxime changes from bacteriostatic to bactericidal with ATc addition. In the case of C4, the activity of cefotaxime changes from bacteriostatic to bactericidal in the presence of inducer. On another hand, the bactericidal activity of β-lactams against C2 (PAM1), C6 (PAM4), C7 (PAM4) and C8 (PAM4) remains somewhat constant with the addition of inducer. In the case of C7, the activity of meropenem-clavulanate changes from bactericidal to bacteriostatic with ATc addition.

In conclusion, the *N*-glycolylation of PG does not severely affect the killing activity of β-lactams, as these exert a bactericidal effect against most of the tested samples. However, the induction of CRISPRi seems to increase the bactericidal activity of β-lactams in some cases, as various *namH* knockdown bacteria seem to be more easily eradicated by these antibiotics in the presence of inducer.

1.3. Disk diffusion assays

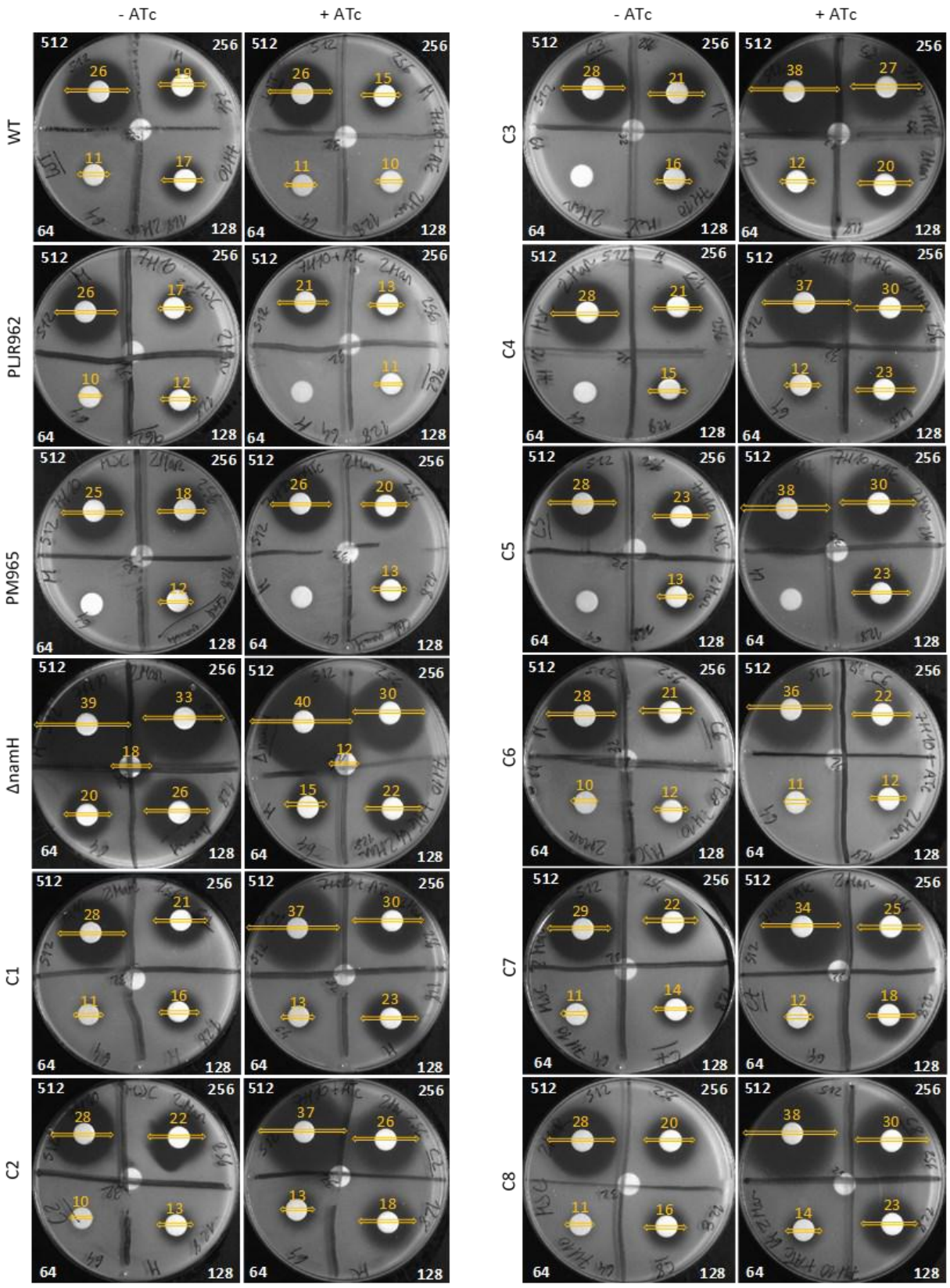

Fig. 42 – **The sensitivity of all *M. smegmatis* cultures to serial concentrations of meropenem** (512, 256, 128, 64 and 32 µg/mL), **in the presence or absence of ATc, as represented by the diameter of the obtained zones of inhibition** (in mm) **after disk diffusion** (n=1): negative controls (WT, PLJR962, PM965), positive control (PM979/ΔnamH) and the knockdown mutants (C1-C8).

The sensitivity of all *M. smegmatis* cultures (WT, PLJR962, PM965, ΔnamH, C1-C8) to meropenem, in the presence or absence of ATc, was assessed by a disk diffusion assay, as described in **Materials and Methods, section A) 3.1.**. The utilized protocol does not follow a recognized reference methodology, but it has been previously applied to study antibiotic susceptibility in mycobacteria[72,126,127]. Briefly, the cultures were grown to log phase, normalized to an OD_{600} of 0.05 in Top Agar, and poured onto either 7H10 or 7H10+ATc plates to create a uniformly distributed layer of mycobacteria. The 9 mm paper disks were impregnated with the following serial final quantities of meropenem (10.24; 5.12; 2.56; 1.28 and 0.64 µg) and, subsequently, placed on top of this layer. After 2 days of incubation, a suspension of bacteria, known as lawn, and a circular region around the meropenem disk in which there is no bacterial growth, the zone of inhibition, become visible through the agar. The diameters (registered in mm) of the zones of inhibition indicate the lethality of meropenem on the tested cultures, with and without ATc.

In this disk diffusion assay, the Top Agar method was used instead of the streak method because it enables a precisely uniform distribution of the mycobacteria along the agar, which will in turn affect the diameter of the zone of inhibition. This is a particularly important factor to monitor when performing disk diffusion assays with mycobacteria since they tend to display distinct colony morphology variants on solid media, classified as smooth or rough[197]. Furthermore, it is imperative to note that the zone of inhibition can be influenced by other factors[198] such as: **i)** the thickness and hydration of the agar layer; **ii)** the characteristics of diffusion of meropenem; **iii)** the growth rate of bacteria; **iv)** the preparation and plating of the bacterial suspension, e.g.: the temperature of Top Agar; **v)** disk positioning, e.g.: if the disks are too close to each other; **vi)** media and materials, e.g.: if the plates are new enough so that ATc is not degraded.

It is relevant to pinpoint that the final concentrations of meropenem (512, 256, 128, 64 and 32 µg/mL) used in this disk diffusion assay are at least 32-fold higher than the correspondent MIC. These differences can be explained by distinct inoculum size between these assays, distinct growth on liquid and solid media, the efficiency of the diffusion of both meropenem and ATc through the lawn, or a combination of these factors[126].

The obtained results (**Figure 42**) show that the diameter of the meropenem zones of inhibition of the negative controls (*M. smegmatis* WT, PLJR962 and PM965) and the knockdown mutants (*M. smegmatis* C1-C8) is similar in the absence of inducer. The only exception is the positive control *M. smegmatis* PM979/ΔnamH, which displays an exacerbated meropenem hypersusceptibility phenotype. These results are in accordance with the MIC values obtained for meropenem (**Table 15**/**Figure 37**), where the negative controls have similar MICs (2-4 µg/mL) and *M. smegmatis* PM979/ΔnamH presents 4-fold lower MIC value (0.5-1 µg/mL). These observations suggest that NamH plays a role in meropenem resistance since the only genomic difference between *M. smegmatis* PM965 and PM979/ΔnamH is the knockout of *namH* (**Table 4**).

As expected, the diameter of the meropenem zones of inhibition of the negative controls (*M. smegmatis* WT, PLJR962 and PM965) and of the positive control *M. smegmatis* PM979/ΔnamH is constant in the absence and presence of inducer. As anticipated, the addition of ATc only affects the knockdown mutants (*M. smegmatis* C1-C8), which have approximately the same diameter of meropenem zones of inhibition as the positive control *M. smegmatis* PM979/ΔnamH, therefore, exhibiting a meropenem hypersusceptibility phenotype. Even though the effects of repressing *namH* are more pronounced on solid media than in liquid

media, the obtained results corroborate those of the MICs (**Table 15**/**Figure 37**), which classify all the induced knockdown mutants as susceptible to meropenem. These observations further highlight the role of NamH in meropenem resistance, albeit with an unknown mechanism. Even though meropenem is especially resistant to hydrolysis by class A β-lactamases[55,123], the same might not be true for class B β-lactamases, where MBLs such as NamH are included. In fact, MBLs are accountable for the increasing resistance of gram-negative bacteria to carbapenems[192]. Thereupon, the meropenem hypersusceptibility phenotype displayed by the induced *namH* knockdown mutants may have been caused by: **i)** the inhibition of the metallo-β-lactamase activity of NamH; **ii)** downregulated NamH hydroxylase activity or; **iii)** the inhibition of both activities. In fact, a reduced hydroxylase activity of NamH can cause: **i)** a lower availability of *N*-glycolyl groups to establish hydrogen interactions, resulting in decreased PG integrity[72]; **ii)** a lower availability of *N*-glycolylated PG precursors, which might result in an altered PG polymerization profile and, in turn, affect the antibiotic sensitivity of bacteria[72]. These events can be further accentuated by the action of β-lactams, as they inhibit PG cross-linking[95,96].

Besides, the addition of inducer does not affect the mutants in the same way. For example, the knockdown mutant C7 (PAM4) does not suffer any substantial changes in the meropenem zone of inhibition. Moreover, the knockdown mutants C2 (PAM1) and C6 (PAM4) only display an increased zone of inhibition for the maximal concentration of meropenem used (512 μg/mL) with ATc addition. On the contrary, the knockdown mutants C1 (PAM11), C3 (PAM2), C4 (PAM3), C5 (PAM4) and C8 (PAM4) display increased zones of inhibition for several concentrations of meropenem (128, 256 and 512 μg/mL) with the addition of inducer. The observed differences in the zones of inhibition do not correspond to any significant differences in the MIC values of meropenem (**Table 15/Figure 37**). Intriguingly, the mutants that display a higher increase in the meropenem zones of inhibition after ATc addition seem to be more easily eradicated at their correspondent MIC for meropenem (**Table 17**). Moreover, this effect does not seem to be correlated with PAM strength or with the target site (**Figure 26**).

Having in mind that antibiotic susceptibility testing using MICs/MBCs or disk diffusion assays are complementary strategies which provide different sorts of information, the susceptibility of all tested *M. smegmatis* cultures to amoxicillin, cefotaxime, amoxicillin-clavulanate, cefotaxime-clavulanate, meropenem-clavulanate, ethambutol and isoniazid should also be assessed using disk diffusion assays.

2. Assessing the contribution of the *N*-glycolylation of PG in host immune recognition

2.1. Infections of RAW 264.7 murine macrophages with the *namH* knockdown mutants

2.1.1.3. Assessing bacterial survival inside macrophages by counting CFUs

One of the goals of this thesis was to elucidate the contribution of the *N*-glycolylation of PG in host immune recognition. To assess differences in intracellular bacterial survival, infections of the RAW 264.7 murine macrophages with WT mycobacteria and with a selected *namH*$^{-}$ mutant, *M. smegmatis* C2, were performed as described in **Materials and Methods, section B) 2.1.**.

Even though *Mtb* H37Ra cultures would be ideal to study the mechanisms of infection of mycobacteria, *M. smegmatis* cultures were used due to time constraints. It is widely known that *M. smegmatis* has a low ability to survive and multiply inside macrophages when a MOI of 1:1 is utilized[199]. However, when a MOI of 5:1 is used, *M. smegmatis* has been shown to have a limited ability to grow and multiply inside host macrophages and is, therefore, considered a suitable model to evaluate intracellular mycobacterial survival[199].

Furthermore, it is relevant to note that bacteria were grown in the absence and presence of 100 ng/mL of ATc for 24h preceding macrophage infection, as maximal induction has been reported to occur 4h after the addition of ATc[180]. During the infection procedure, induction was maintained by using media supplemented with 100 ng/mL ATc. Since Ehrt *et al.* have previously showed that ATc is able to enter macrophages and regulate mycobacterial gene expression intracellularly[180], we did not confirm that ATc was indeed reaching mycobacteria residing inside RAW 264.7 macrophages. This experiment could have been performed with a *M. smegmatis*:pEGFP strain that presents abrogated *gfp* expression in the presence of an ATc-inducible CRISPRi system containing a sgRNA designed to target the *gfp* gene.

The variations in the average of the intracellular survival of the tested samples (*M. smegmatis* WT, PLJR962, C2), in the absence and presence of 100 ng/mL of ATc, are depicted in **Figure 43**.

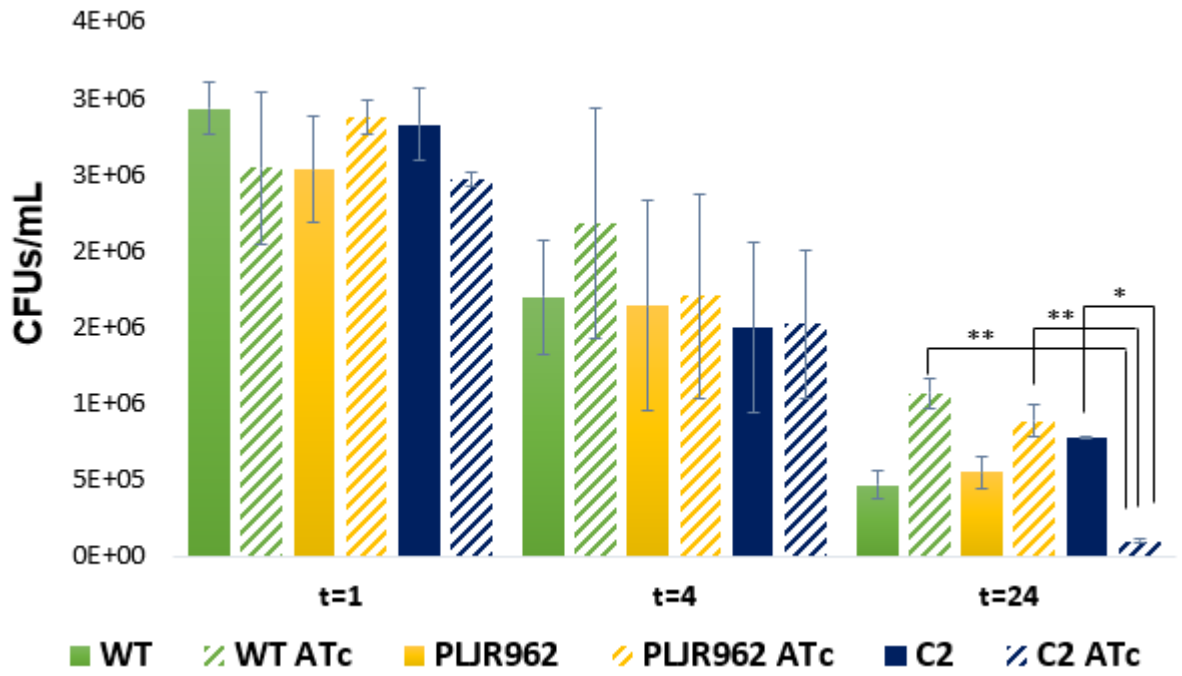

Fig. 43 - Graphical representation of the variations in the average of bacterial survival inside RAW 264.7 macrophages between the tested samples (*M. smegmatis* WT, PLJR962, C2), in the absence and presence of 100 ng/mL of ATc (n=2). Error bars indicate the standard error of the mean. The significance of the differences between averages was calculated using a two-tailed unpaired t-test, considering different variances: * when p-value < 0.1; ** when p-value < 0.05.

As expected[199], the obtained results (**Figure 43**) show that the intracellular survival of all tested *M. smegmatis* samples decreases overtime. In t=1h and t=4h, the intracellular survival of all tested samples is somewhat similar, and no significant differences were found between

samples. In this case, all bacteria seem to be able to survive rather similarly inside macrophages. Nevertheless, this observation is not true for t=24h, where significant differences were found between the intracellular survival of the induced knockdown mutant C2 ATc and the intracellular survival of the negative controls WT ATc (~10.8-fold; p-value = 0.025), PLJR962 ATc (~8.9-fold; p-value = 0.022) and, the uninduced knockdown mutant C2 (~7.8-fold; p-value = 0.071). Therefore, it appears that RAW 264.7 macrophages are more effective at killing the induced knockdown mutant C2 ATc than any other bacteria, suggesting that the presence of *N*-glycolylated PG promotes intracellular survival. Indeed, the *N*-glycolylation of PG is crucial to CW stability[72] and may, therefore, have a role in the fitness of mycobacteria inside macrophages. However, these results should be further corroborated and, an analysis of macrophage viability by flow cytometry should be performed prior to lysis and CFU counting.

These observations cannot be compared with those of other studies. Coulombe *et al.* have revealed that there were no significant differences in the number of CFUs/mL in the spleens of mice infected with either *M. smegmatis* WT or *M. smegmatis* ΔnamH[73]. On another hand, Hansen *et al.* have demonstrated that both *Mtb* WT and *Mtb* ΔnamH thrive inside host macrophages, while displaying an equal intracellular survival profile[74]. In addition, Hansen *et al.* have showed that mice infected with NamH-disrupted *Mtb* survived longer than those which were infected with WT mycobacteria[74]. Furthermore, both authors have stated *N*-glycolylated PG to be more immunogenic than *N*-acetylated PG at promoting NMHR, which include the activation of the transcription factor NF-κB and increased production of pro-inflammatory cytokines (e.g.: TNF-α, IL-6, IL-1β)[73,74]. Despite not having assessed either event, the obtained results (**Figure 43**) show that the induced knockdown mutant C2 ATc seems to elicit an enhanced immune response when compared to other bacteria, as it is more efficiently eradicated by macrophages. This interpretation is not supported by the findings of previously mentioned publications, but Wang *et al.* have reported the stimulatory activity of *N*-glycolylated PG to be lower than that of *N*-acetylated PG[92]. Therefore, the role of NamH in the context of immune recognition and host-pathogen interactions remains unknown and needs further assessment. Nonetheless, the fact that *namH* is conserved in several *Mtb* clinical isolates[157] suggests a key role in TB pathogenesis. Perhaps, the *N*-glycolylation of PG acts as an immune evasion mechanism by concealing PG and refining lysozyme resistance or, on the contrary, acts to make mycobacterial PG more immunogenic as a way for *Mtb* to recruit macrophages, replicate and persist inside them and, later, facilitate disease transmission.

Concluding Remarks and Future Perspectives

In the past decades, TB has become a global health concern due to: **i)** the emergence and spread of multi-drug and extensively-drug resistant strains of *Mtb*, which is accentuated by an intrinsic resistance to β-lactams and lysozyme; **ii)** the relative ineffectiveness of the BCG vaccine and of currently known antimycobacterial agents, which is accentuated by the lack of new effective therapeutics. With nearly two million people dying from TB annually, it is urgent to find a new TB vaccine, to develop rapid diagnostic tools and, to create improved treatment regimens. Therefore, it is imperative to enlighten the mechanism of TB pathogenesis.

The success of *Mtb* as an intracellular pathogen derives from its highly complex CW and its ability to subvert the immune system of the host. The mycobacterial PG is characterized by the predominance of *N*-glycolylated muramic acid residues, which are thought to increase β-lactams/lysozyme resistance and the immunogenic capacity of the CW. Despite not being essential, the *namH* gene is highly conserved in clinical isolates, implying a vital function for the *N*-glycolylation of PG in antibiotic resistance or/and in pathogenesis. Therefore, the main goal of this thesis was to modulate *namH* expression in order to understand the significance of the *N*-glycolylation of mycobacterial PG in antibiotic resistance and in host immune recognition.

To start, the construction of several *namH* knockdown mutants in *M. smegmatis* (C1-C8) and in *Mtb* H37Ra (C1-C6) was successful. The characterization of the *M. smegmatis namH* knockdown mutants was completed by performing growth curves and spotting dilutions. These experiments showed that *namH* knockout or repression does not produce severe growth defects, thus, confirming the non-essentiality of *namH*. Moreover, these experiments indicated a residual level of $dCas9_{Sth1}$ toxicity. Unfortunately, it was not possible to confirm the repression of *namH* in all knockdown mutants. However, the repression of *namH* in the induced knockdown mutant *M. smegmatis* C2 ATc was confirmed, as demonstrated by a highly significant decrease in the mRNA expression levels of *namH*, when compared to the control vector PLJR962 in the presence of ATc and the uninduced mutant C2. Furthermore, the polarity of CRISPRi was also inquired and verified, as the gene downstream of *namH* was also shown to be repressed. Nevertheless, it was not possible to probe the determinants of CRISPRi efficacy due to time constraints.

Then, the role of the *N*-glycolylation of PG in antibiotic susceptibility was inquired by performing MIC and MBC assays for all *M. smegmatis namH* knockdown mutants, with and without ATc.

First, meropenem was found to be more efficient at inhibiting the growth of mycobacteria, when compared to amoxicillin or cefotaxime. This effect is allegedly caused by its characteristic resistance to β-lactamases and, the simultaneous inhibition of L,D-transpeptidases and some PBPs. A role for the *N*-glycolylation of PG in β-lactams resistance was revealed, as both *M. smegmatis* ΔnamH and the induced knockdown mutants exhibited lower MIC values for all β-lactams, with or without clavulanate, when compared to any of the negative controls. Likewise, a strong link between the *N*-glycolylation of PG and the mechanism of action of cefotaxime was also uncovered, as the *namH* knockdown mutants displayed a particularly significant decrease in the MIC values of cefotaxime or cefotaxime-clavulanate in the presence of inducer. This may be caused by a synergy between the inhibition of class A PBPs, which catalyze PG cross-linking, and decreased PG integrity due to inhibited NamH activity. Furthermore, differences in the hydrolytic efficiency of BlaS to various β-lactams were verified as the addition

of clavulanate to β-lactams considerably decreased the MIC of amoxicillin, as opposed to cefotaxime and meropenem.

All β-lactams were found to be bactericidal against most of the tested *M. smegmatis* samples, indicating that the *N*-glycolylation of PG does not severely affect the killing activity of β-lactams. Meropenem and amoxicillin, with and without clavulanate, were found to be more bactericidal than cefotaxime. Moreover, ethambutol was found to be bacteriostatic or bactericidal depending on the experimental conditions and, isoniazid typically displayed a highly bactericidal activity.

Although disk diffusion assays were intended to be performed for all previously mentioned antibiotics, it was only possible to determine the meropenem zones of inhibition for all *M. smegmatis* knockdown mutants, with and without inducer. These experiments suggested that NamH plays a role in meropenem resistance as both *M. smegmatis* ΔnamH and the induced *namH* knockdown mutants displayed an exacerbated meropenem hypersusceptibility phenotype.

These experiments demonstrated that the *namH* knockout/knockdown mutants display increased susceptibility to most β-lactams. To understand the reason for this "β-lactams hypersusceptibility phenotype", an analysis of the NamH protein was performed using BLASTp and, NamH was found to be classified as an "uncharacterized MBL fold metallo-hydrolase containing a Rieske (2Fe-2S) domain". This finding raised the question: What if the NamH protein has any β-lactamase activity, which could contribute to the intrinsic β-lactams resistance phenotype of wild-type mycobacteria? In this way, the observed phenotype could be explained by the inhibition of: **i)** the hydrolytic activity of NamH as a β-lactamase; **ii)** the activity of NamH as a monooxygenase, which modifies PG sugars; **iii)** both activities, enabling a synergy between the inhibition of β-lactamase activity and the inhibition of the *N*-glycolylation of PG. Indeed, the reduced hydroxylase activity of NamH can lead to: **i)** decreased PG integrity due to a lower availability of *N*-glycolyl groups to establish hydrogen bonds; **ii)** altered PG polymerization due to a lower availability of *N*-glycolylated PG precursors. Even though *namH* is not considered as a key target for anti-TB therapy, targeting NamH (using chemical inhibitors or CRISPR antimicrobials) will decrease the integrity of the mycobacterial CW, which can be further accentuated by β-lactams treatment.

The determination of the contribution of the *N*-glycolylation of PG for host immune recognition, assessed by performing infections of RAW 264.7 macrophages with the *namH* knockdown mutants was only partially achieved. The effective killing of *M. smegmatis* by RAW 264.7 macrophages over time was verified. In addition, macrophages were found to be more effective at killing the induced knockdown mutant C2 ATc than any other bacteria at t=24h. This observation indicates that the presence of *N*-glycolylated PG promotes intracellular survival, possibly by increasing the fitness of mycobacteria inside macrophages. This inference is not in accordance with the findings of previous studies and, needs to be further corroborated.

Given the results obtained in this thesis and all the questions that remain to be answered, future perspectives should focus on:

- Characterizing the *Mtb namH* knockdown mutants, by performing growth curves and spotting dilutions, and confirming *namH* repression in both mycobacteria using qRT-PCR. This will enable the confirmation of the non-essentiality of *namH* in *Mtb*, the

confirmation that *namH* is being silenced in all mutants, the study of CRISPRi polarity and, the probing of the determinants of CRISPRi efficacy.

- Evaluating whether NamH displays any β-lactamase activity, by performing a β-lactamase assay with a purified NamH protein.
- Assessing the antibiotic and lysozyme susceptibility of mycobacteria by performing MIC and MBC assays in the *Mtb namH* knockdown mutants using the nitrocefin method and, optimizing disk diffusion assays in *M. smegmatis* for the following antibiotics - amoxicillin, amoxicillin-clavulanate, cefotaxime, ethambutol, isoniazid – and, for lysozyme.
- Performing infections of RAW 264.7 murine macrophages with selected *M. smegmatis namH* knockdown mutants followed by characterization of the resultant immune response: quantification of the mRNA expression levels of several immune receptors (NOD1, NOD2, TLR1, TLR2, TLR4), pro-inflammatory cytokines (TNF-α, IL-6, IL-1β), anti-inflammatory cytokines (IL-10) and, of the nitric oxide synthase 2 (Nos2) by qRT-PCR.
- Performing infections of THP-1 derived macrophages with selected *Mtb namH* knockdown mutants followed by characterization of the resultant immune response: quantification of the expression of immune receptors and cytokines by qRT-PCR and, assessment of intracellular survival by counting CFUs.
- Determining the host innate immune response to purified glycolylated vs. acetylated PG muropeptides by performing pull-down binding assays with fluorescent derivatives of *D. melanogaster*'s PGRPs and with fluorescent recombinant human immune receptors (TLR2-mCherry-His_6 and TLR4-mCherry-His_6), followed by microscopy analysis of the resulting mCherry fluorescence.

To conclude, the work presented in this thesis helped implement CRISPRi as a technique in the lab, enlighten the role of the *N*-glycolylation of PG in antibiotic susceptibility by posing new hypothesis as to how NamH enables β-lactams resistance and raised intriguing questions about the role of *N*-glycolylated PG in host immune recognition. These findings may give an important contribution to the future understanding of mycobacterial pathogenesis and to the future development of alternative TB therapeutics.

Bibliography

1. World Health Organization. *Global Health TB Report*. (2019).

2. MacNeil, A. *et al*. Global Epidemiology of Tuberculosis and Progress Toward Achieving Global Targets — 2017. *MMWR. Morb. Mortal. Wkly. Rep.* **68,** 263–266 (2019).

3. Floyd, K. *et al*. The global tuberculosis epidemic and progress in care, prevention, and research: an overview in year 3 of the End TB era. *Lancet Respir. Med.* **6,** 299–314 (2018).

4. PORTUGAL - Ministério da Saúde - Direcção-Geral da Saúde. Infeção por VIH, SIDA e Tuberculose em números – 2015. *Direção Geral de Saúde*. (2015).

5. Gagneux, S. Ecology and evolution of *Mycobacterium tuberculosis*. *Nat. Rev. Microbiol.* **16,** 202–213 (2018).

6. Forbes, B. A. *et al.* Practice Guidelines for Clinical Microbiology Laboratories: Mycobacteria. *Clin. Microbiol. Rev.* **31,** 1–66 (2018).

7. Silva Miranda, M. *et al*. The tuberculous granuloma: An unsuccessful host defence mechanism providing a safety shelter for the bacteria? *Clin. Dev. Immunol.* **2012,** 1-14 (2012).

8. Brites, D. & Gagneux, S. Co-evolution of *Mycobacterium tuberculosis* and *Homo sapiens*. *Immunol. Rev.* **264,** 6–24 (2015).

9. Russell, D. G. Who puts the tubercle in tuberculosis? *Nat. Rev. Microbiol.* **5,** 39–47 (2007).

10. Daniel, T. M. The history of tuberculosis. *Respir. Med.* **100,** 1862–1870 (2006).

11. Rothschild, B. M. *et al. Mycobacterium tuberculosis* Complex DNA from an Extinct Bison Dated 17,000 Years before the Present. *Clin. Infect. Dis.* **33,** 305–311 (2001).

12. Hershkovitz, I. *et al.* Detection and Molecular Characterization of 9000-Year-Old *Mycobacterium tuberculosis* from a Neolithic Settlement in the Eastern Mediterranean. *PLoS One* **3,** e3426 (2008).

13. Zink, A. R. *et al.* Characterization of *Mycobacterium tuberculosis* complex DNAs from Egyptian mummies by spoligotyping. *J. Clin. Microbiol.* **41,** 359–67 (2003).

14. Zink, A. R. *et al.* Molecular history of tuberculosis from ancient mummies and skeletons. *Int. J. Osteoarchaeol.* **17,** 380–391 (2007).

15. Taylor, G. M. *et al*. Genotypic Analysis of the Earliest Known Prehistoric Case of Tuberculosis in Britain. *J. Clin. Microbiol.* **43,** 2236–2240 (2005).

16. Laennec, R.T.H *et al*. A treatise on the disease of the chest. *New York, NY: Hafner Publishing Company*. (1962).

17. Koch, R. *et al*. Die aetiologie der tuberculose. *Am Rev Tuberc.* **25,** 285–323 (1932).

18. Calmette A. On preventive vaccination of the new-born against tuberculosis by B.C.G. *Br J Tuberc* **22,**161–165 (1928).

19. Barbier, M. & Wirth, T. The Evolutionary History, Demography, and Spread of the *Mycobacterium tuberculosis* Complex. *Microbiol. Spectr.* **4,** 1–21 (2016).

20. Ernst, J. D. *et al*. Genomics and the evolution, pathogenesis, and diagnosis of tuberculosis. *J. Clin. Invest.* **117,** 1738–1745 (2007).

21. Hett, E. C. & Rubin, E. J. Bacterial Growth and Cell Division: a Mycobacterial Perspective. *Microbiol. Mol. Biol. Rev.* **72,** 126–156 (2008).

22. Rue-Albrecht, K. *et al.* Comparative Functional Genomics and the Bovine Macrophage Response to Strains of the *Mycobacterium* Genus. *Front. Immunol.* **5,** 1–14 (2014).

23. Smith, N. H. *et al*. Myths and misconceptions: the origin and evolution of *Mycobacterium tuberculosis*. *Nat. Rev. Microbiol.* **7,** 537–544 (2009).

24. Comas, I. *et al.* Out-of-Africa migration and Neolithic coexpansion of *Mycobacterium tuberculosis* with modern humans. *Nat. Genet.* **45,** 1176–1182 (2013).

25. Gagneux, S. *et al.* Variable host-pathogen compatibility in *Mycobacterium tuberculosis*. *Proc. Natl. Acad. Sci. U. S. A.* **103,** 2869–2873 (2006).

26. Pasipanodya, J. G. *et al.* Allopatric tuberculosis host–pathogen relationships are associated with greater pulmonary impairment. *Infect. Genet. Evol.* **16,** 433–440 (2013).

27. Brosch, R. *et al.* A new evolutionary scenario for the *Mycobacterium tuberculosis* complex. *Proc. Natl. Acad. Sci.* **99,** 3684–3689 (2002).

28. Supply, P. *et al.* Genomic analysis of smooth tubercle bacilli provides insights into ancestry and pathoadaptation of *Mycobacterium tuberculosis*. *Nat. Genet.* **45,** 172–179 (2013).

29. Wirth, T. *et al.* Origin, Spread and Demography of the *Mycobacterium tuberculosis* Complex. *PLoS Pathog.* **4,** e1000160 (2008).

30. Pym, A. S., *et al*. Loss of RD1 contributed to the attenuation of the live tuberculosis vaccines *Mycobacterium bovis* BCG and *Mycobacterium microti*. *Mol. Microbiol.* **46,** 709–717 (2002).

31. Coscolla, M. & Gagneux, S. Consequences of genomic diversity in *Mycobacterium tuberculosis*. *Semin. Immunol.* **26,** 431–444 (2014).

32. Bañuls, A.-L., *et al*. *Mycobacterium tuberculosis*: ecology and evolution of a human bacterium. *J. Med. Microbiol.* **64,** 1261–1269 (2015).

33. Ford, C. B. *et al. Mycobacterium tuberculosis* mutation rate estimates from different lineages predict substantial differences in the emergence of drug-resistant tuberculosis. *Nat. Genet.* **45,** 784–790 (2013).

34. de Jong, B. C. *et al.* Progression to Active Tuberculosis, but Not Transmission, Varies by *Mycobacterium tuberculosis* Lineage in The Gambia. *J. Infect. Dis.* **198,** 1037–1043 (2008).

35. Comas, I. *et al.* Human T cell epitopes of *Mycobacterium tuberculosis* are evolutionarily hyperconserved. *Nat. Genet.* **42,** 498–503 (2010).

36. Blouin, Y. *et al.* Progenitor '*Mycobacterium canettii*' Clone responsible for lymph node tuberculosis epidemic, Djibouti. *Emerg. Infect. Dis.* **20,** 21–28 (2014).

37. Sharma, S. & Dheda, K. What is new in the WHO consolidated guidelines on drug-resistant tuberculosis treatment? *Indian J. Med. Res.* **149,** 309 (2019).

38. Public Notice: Guideline Development Group meeting to update the WHO guidelines on drug-resistant tuberculosis. *World Health Organization* (2019). Available at: https://www.who.int/tb/areas-of-work/drug-resistant-tb/treatment/drug-resistant-tb-gdg/en/. (Accessed: 25th April 2020).

39. Shiloh, M. U. & DiGiuseppe Champion, P. A. To catch a killer. What can mycobacterial models teach us about *Mycobacterium tuberculosis* pathogenesis? *Curr. Opin. Microbiol.* **13,** 86–92 (2010).

40. Jacobs, Jr., W. R. Gene Transfer in *Mycobacterium tuberculosis*: Shuttle Phasmids to Enlightenment. *Microbiol. Spectr.* **2,** 1–22 (2014).

41. Snapper, S. B. *et al.* Lysogeny and transformation in mycobacteria: stable expression of foreign genes. *Proc. Natl. Acad. Sci.* **85,** 6987–6991 (1988).

42. Labidi, A., *et al*. Restriction endonuclease mapping and cloning of *Mycobacterium fortuitum var. fortuitum* plasmid pAL5000. *Ann. l'Institut Pasteur / Microbiol.* **136,** 209–215 (1985).

43. Snapper, S. B., *et al*. Isolation and characterization of efficient plasmid transformation mutants of *Mycobacterium smegmatis*. *Mol. Microbiol.* **4,** 1911–1919 (1990).

44. Zheng, H. *et al.* Genetic Basis of Virulence Attenuation Revealed by Comparative Genomic Analysis of *Mycobacterium tuberculosis* Strain H37Ra versus H37Rv. *PLoS One* **3,** e2375 (2008).

45. Steenken, W. Lysis of Tubercle Bacilli in Vitro. *Exp. Biol. Med.* **33,** 253–255 (1935).

46. Middlebrook, G., *et al*. Virulence and Morphological Characteristics of Mammalian Tubercle Bacilli. *J. Exp. Med.* **86,** 175–184 (1947).

47. Heplar, J. Q., *et al*. Virulence of the Tubercle Bacillus: I. Effect of Oxygen Tension upon Respiration of Virulent and Avirulent Bacilli. *J. Infect. Dis.* **94,** 90–98 (1954).

48. Hart, P. D. & Armstrong, J. A. Strain Virulence and the Lysosomal Response in Macrophages Infected with *Mycobacterium tuberculosis*. *Infect. Immun.* **10,** 742–746 (1974).

49. Larson, C. L. & Wicht, W. C. Infection of Mice with *Mycobacterium tuberculosis*, Strain H37Ra. *Am. Rev. Respir. Dis.* **90,** 742–748 (1964).

50. Heinrichs, M. *et al. Mycobacterium tuberculosis* Strains H37ra and H37rv have equivalent minimum inhibitory concentrations to most antituberculosis drugs. *Int. J. Mycobacteriology* **7,** 156 (2018).

51. Brennan, P. J. & Nikaido, H. The Envelope of Mycobacteria. *Annu. Rev. Biochem.* **64,** 29–63 (1995).

52. Jankute, M. *et al*. Assembly of the Mycobacterial Cell Wall. *Annu. Rev. Microbiol.* **69,** 405–423 (2015).

53. Abrahams, K. A. & Besra, G. S. Mycobacterial cell wall biosynthesis: a multifaceted antibiotic target. *Parasitology* **145,** 116–133 (2018).

54. Alderwick L.J. *et al*. The Mycobacterial Cell Wall—Peptidoglycan and Arabinogalactan. *Cold Spring Harbor Perspectives in Medicine*. **5,** 1-15 (2015).

55. Catalão, M. J. *et al*. Revisiting anti-tuberculosis therapeutic strategies that target the peptidoglycan structure and synthesis. *Front. Microbiol.* **10,** 1–11 (2019).

56. Nasiri, M. J. *et al.* New insights in to the intrinsic and acquired drug resistance mechanisms in mycobacteria. *Front. Microbiol.* **8,** 681 (2017).

57. Duan, X. *et al*. Crucial components of mycobacterium type II fatty acid biosynthesis (Fas-II) and their inhibitors. *FEMS Microbiol. Lett.* **360,** 87–99 (2014).

58. Lea-Smith, D. J. *et al.* The reductase that catalyzes mycolic motif synthesis is required for efficient attachment of mycolic acids to arabinogalactan. *J. Biol. Chem.* **282,** 11000–11008 (2007).

59. Liu, J. & Nikaido, H. A mutant of *Mycobacterium smegmatis* defective in the biosynthesis of mycolic acids accumulates meromycolates. *Proc. Natl. Acad. Sci.* **96,** 4011–4016 (1999).

60. Vilchèze, C. & Jacobs, W. R. The Isoniazid Paradigm of Killing, Resistance, and Persistence in *Mycobacterium tuberculosis*. *J. Mol. Biol.* **431,** 3450–3461 (2019).

61. Crick, D. C. *et al*. Structure and Biosynthesis of the Mycobacterial Cell Wall. in *Comprehensive Natural Products II* **38,** 381–406 (Elsevier, 2010).

62. Jin, Y. *et al*. *Mycobacterium tuberculosis* Rv1302 and *Mycobacterium smegmatis* MSMEG-4947 have WecA function and MSMEG-4947 is required for the growth of *M. smegmatis*. *FEMS Microbiol. Lett.* **310,** 54–61 (2010).

63. Alderwick, L. J. *et al.* Expression, purification and characterisation of soluble GlfT and the identification of a novel galactofuranosyltransferase Rv3782 involved in priming GlfT-mediated galactan polymerisation in *Mycobacterium tuberculosis*. *Protein Expr. Purif.* **58,** 332–341 (2008).

64. Kremer, L. *et al.* Galactan Biosynthesis in *Mycobacterium tuberculosis*. *J. Biol. Chem.* **276,** 26430–26440 (2001).

65. Alderwick, L. J. *et al*. Identification of a Novel Arabinofuranosyltransferase (AftA) Involved in Cell Wall Arabinan Biosynthesis in *Mycobacterium tuberculosis*. *J. Biol. Chem.* **281,** 15653–15661 (2006).

66. Birch, H. L. *et al.* Biosynthesis of mycobacterial arabinogalactan: Identification of a novel α(1→3) arabinofuranosyltransferase. *Mol. Microbiol.* **69,** 1191–1206 (2008).

67. Škovierová, H. *et al.* AftD, a novel essential arabinofuranosyltransferase from mycobacteria. *Glycobiology* **19,** 1235–1247 (2009).

68. Seidel, M. *et al.* Identification of a Novel Arabinofuranosyltransferase AftB Involved in a Terminal Step of Cell Wall Arabinan Biosynthesis in *Corynebacterianeae*, such as *Corynebacterium glutamicum* and *Mycobacterium tuberculosis*. *J. Biol. Chem.* **282,** 14729–14740 (2007).

69. Harrison, J. *et al.* Lcp1 Is a Phosphotransferase Responsible for Ligating Arabinogalactan to Peptidoglycan in *Mycobacterium tuberculosis*. *MBio* **7,** 1–12 (2016).

70. Cui, Z. *et al.* Mutations in the embC-embA intergenic region contribute to *Mycobacterium tuberculosis* resistance to ethambutol. *Antimicrob. Agents Chemother.* **58,** 6837–6843 (2014).

71. Mahapatra, S. *et al*. *N* Glycolylation of the Nucleotide Precursors of Peptidoglycan Biosynthesis of *Mycobacterium spp*. Is Altered by Drug Treatment. *J. Bacteriol.* **187,** 2341–2347 (2005).

72. Raymond, J. B. *et al*. Identification of the *namH* Gene, Encoding the Hydroxylase Responsible for the *N*-Glycolylation of the Mycobacterial Peptidoglycan. *J. Biol. Chem.* **280,** 326–333 (2005).

73. Coulombe, F. *et al.* Increased NOD2-mediated recognition of *N*-glycolyl muramyl dipeptide. *J. Exp. Med.* **206,** 1709–1716 (2009).

74. Hansen, J. M. *et al. N*-Glycolylated Peptidoglycan Contributes to the Immunogenicity but Not Pathogenicity of *Mycobacterium tuberculosis*. *J. Infect. Dis.* **209,** 1045–1054 (2014).

75. Kieser, K. J. *et al.* Peptidoglycan synthesis in *Mycobacterium tuberculosis* is organized into networks with varying drug susceptibility. *Proc. Natl. Acad. Sci.* **112,** 13087–13092 (2015).

76. Lavollay, M. *et al.* The peptidoglycan of stationary-phase *Mycobacterium tuberculosis* predominantly contains cross-links generated by L,D-transpeptidation. *J. Bacteriol.* **190,** 4360–4366 (2008).

77. Wivagg, C. N. *et al*. Mechanisms of β-lactam killing and resistance in the context of *Mycobacterium tuberculosis*. *J. Antibiot. (Tokyo).* **67,** 645–654 (2014).

78. Figueiredo, T. A. *et al.* Identification of Genetic Determinants and Enzymes Involved with the Amidation of Glutamic Acid Residues in the Peptidoglycan of *Staphylococcus aureus*. *PLoS Pathog.* **8,** e1002508 (2012).

79. Münch, D. *et al.* Identification and in vitro Analysis of the GatD/MurT Enzyme-Complex Catalyzing Lipid II Amidation in *Staphylococcus aureus*. *PLoS Pathog.* **8,** e1002509 (2012).

80. Morlot, C. *et al.* Structure of the essential peptidoglycan amidotransferase MurT/GatD complex from *Streptococcus pneumoniae*. *Nat. Commun.* **9,** 3180 (2018).

81. Sassetti, C. M. *et al*. Genes required for mycobacterial growth defined by high density mutagenesis. *Mol. Microbiol.* **48,** 77–84 (2003).

82. Figueiredo, T. A. *et al*. Contribution of Peptidoglycan Amidation to Beta-Lactam and Lysozyme Resistance in Different Genetic Lineages of *Staphylococcus aureus*. *Microb. Drug Resist.* **20,** 238–249 (2014).

83. Mir, M. *et al.* The Extracytoplasmic Domain of the *Mycobacterium tuberculosis* Ser/Thr Kinase PknB Binds Specific Muropeptides and Is Required for PknB Localization. *PLoS Pathog.* **7,** e1002182 (2011).

84. Pidgeon, S. E. *et al.* L,D-Transpeptidase Specific Probe Reveals Spatial Activity of Peptidoglycan Cross-Linking. *ACS Chem. Biol.* **14,** 2185−2196 (2019).

85. Mahapatra, S. *et al*. Mycobacterial Lipid II Is Composed of a Complex Mixture of Modified Muramyl and Peptide Moieties Linked to Decaprenyl Phosphate. *J. Bacteriol*. **187,** 2747–2757 (2005).

86. Bernard, E. *et al*. Identification of the amidotransferase AsnB1 as being responsible for meso-Diaminopimelic acid amidation in *Lactobacillus plantarum* peptidoglycan. *J. Bacteriol.* **193,** 6323–6330 (2011).

87. Levefaudes, M. *et al.* Diaminopimelic Acid Amidation in *Corynebacteriales*. *J. Biol. Chem.* **290,** 13079–13094 (2015).

88. Mitani, Y. *et al*. Characterization of LtsA from *Rhodococcus erythropolis*, an Enzyme with Glutamine Amidotransferase Activity. *J. Bacteriol.* **187,** 2582-2591 (2005).

89. Dajkovic, A. *et al.* Hydrolysis of peptidoglycan is modulated by amidation of meso-diaminopimelic acid and Mg 2+ in *Bacillus subtilis*. *Mol. Microbiol.* **104,** 972–988 (2017).

90. Ren, H. & Liu, J. AsnB Is Involved in Natural Resistance of *Mycobacterium smegmatis* to Multiple Drugs. *Antimicrob. Agents Chemother.* **50,** 250–255 (2006).

91. Ngadjeua, F. *et al.* Critical Impact of Peptidoglycan Precursor Amidation on the Activity of l,d-Transpeptidases from *Enterococcus faecium* and *Mycobacterium tuberculosis*. *Chem. -A Eur. J.* **24,** 5743–5747 (2018).

92. Wang, Q. *et al.* Synthesis of characteristic *Mycobacterium* peptidoglycan (PGN) fragments utilizing with chemoenzymatic preparation of meso-diaminopimelic acid (DAP), and their modulation of innate immune responses. *Org. Biomol. Chem.* **14,** 1013–1023 (2016).

93. Maitra, A. *et al.* Cell wall peptidoglycan in *Mycobacterium tuberculosis*: An Achilles' heel for the TB-causing pathogen. *FEMS Microbiol. Rev.* **43,** 548–575 (2019).

94. Pavelka, Jr. *et al*. Genetics of Peptidoglycan Biosynthesis. *Microbiol. Spectr.* **2,** 1–20 (2014).

95. Sauvage, E., *et al*. The penicillin-binding proteins: Structure and role in peptidoglycan biosynthesis. *FEMS Microbiol. Rev.* **32,** 234–258 (2008).

96. Machowski, E. *et al*. Comparative genomics for mycobacterial peptidoglycan remodelling enzymes reveals extensive genetic multiplicity. *BMC Microbiol.* **14,** 75 (2014).

97. Billman-Jacobe, H. *et al*. Characterization of a *Mycobacterium smegmatis* Mutant Lacking Penicillin Binding Protein 1. *Antimicrob. Agents Chemother.* **43,** 3011–3013 (1999).

98. Patru, M.-M. & Pavelka, M. S. A Role for the Class A Penicillin-Binding Protein PonA2 in the Survival of *Mycobacterium smegmatis* under Conditions of Nonreplication. *J. Bacteriol.* **192,** 3043–3054 (2010).

99. Dubée, V. *et al.* Inactivation of *Mycobacterium tuberculosis* L,D-transpeptidase LdtMt1 by carbapenems and cephalosporins. *Antimicrob. Agents Chemother.* **56,** 4189–4195 (2012).

100. Lavollay, M. *et al.* The β-lactam-sensitive D,D-carboxypeptidase activity of Pbp4 controls the L,D and D,D transpeptidation pathways in *Corynebacterium jeikeium*. *Mol. Microbiol.* **74,** 650–661 (2009).

101. Cordillot, M. *et al.* In Vitro Cross-Linking of *Mycobacterium tuberculosis* Peptidoglycan by L,D-Transpeptidases and Inactivation of These Enzymes by Carbapenems. *Antimicrob. Agents Chemother.* **57,** 5940–5945 (2013).

102. Sanders, A. N. *et al*. Genetic characterization of mycobacterial L,D-transpeptidases. *Microbiology* **160,** 1795–1806 (2014).

103. Gupta, R. *et al.* The *Mycobacterium tuberculosis* protein LdtMt2 is a nonclassical transpeptidase required for virulence and resistance to amoxicillin. *Nat. Med.* **16,** 466–469 (2010).

104. Schoonmaker, M. *et al*. Nonclassical transpeptidases of *Mycobacterium tuberculosis* alter cell size, morphology, the cytosolic matrix, protein localization, virulence, and resistance to β-lactams. *J. Bacteriol.* **196,** 1394–1402 (2014).

105. Rullas, J. *et al.* Combinations of β-Lactam Antibiotics Currently in Clinical Trials Are Efficacious in a DHP-I-Deficient Mouse Model of Tuberculosis Infection. *Antimicrob. Agents Chemother.* **59,** 4997–4999 (2015).

106. Bianchet, M. A. *et al.* Structural insight into the inactivation of *Mycobacterium tuberculosis* non-classical transpeptidase LdtMt2 by biapenem and tebipenem. *BMC Biochem.* **18,** 8 (2017).

107. Kumar, P. *et al.* Non-classical transpeptidases yield insight into new antibacterials. *Nat. Chem. Biol.* **13,** 54–61 (2017).

108. Fleming, A. On the antibacterial action of cultures of a penicillium, with special reference to their use in the isolation of *B. influenzae*. *Br J Exp Pathol* **10,** 226–236 (1929).

109. Kong, K. F. *et al*. Beta-lactam antibiotics: From antibiosis to resistance and bacteriology. *Apmis* **118,** 1–36 (2010).

110. Zaffiri, L. *et al*. History of antibiotics. from salvarsan to cephalosporins. *J. Investig. Surg.* **25,** 67–77 (2012).

111. Bush, K. & Bradford, P. A. β-Lactams and β-Lactamase Inhibitors: An Overview. *Cold Spring Harb. Perspect. Med.* **6,** a025247 (2016).

112. Wang, F. *et al*. Crystal structure and activity studies of the *Mycobacterium tuberculosis* β-lactamase reveal its critical role in resistance to β-lactam antibiotics. *Antimicrob. Agents Chemother.* **50,** 2762–2771 (2006).

113. Fisher, J. F. & Mobashery, S. β-Lactam resistance mechanisms: Gram-positive bacteria and *Mycobacterium tuberculosis*. *Cold Spring Harb. Perspect. Med.* **6,** 1–20 (2016).

114. Sotgiu, G. *et al.* Carbapenems to Treat Multidrug and Extensively Drug-Resistant Tuberculosis: A Systematic Review. *Int. J. Mol. Sci.* **17,** 373 (2016).

115. Jaganath, D. *et al*. Carbapenems against *Mycobacterium tuberculosis*: A review of the evidence. *Int. J. Tuberc. Lung Dis.* **20,** 1436–1447 (2016).

116. Fernandes, R. *et al*. β-Lactams: Chemical structure, mode of action and mechanisms of resistance. *Rev. Med. Microbiol.* **24,** 7–17 (2013).

117. Lobanovska, M. & Pilla, G. Penicillin's discovery and antibiotic resistance: Lessons for the future? *Yale J. Biol. Med.* **90,** 135–145 (2017).

118. Nadler, J. P. *et al*. Amoxicillin-clavulanic acid for treating drug-resistant *Mycobacterium tuberculosis*. *Chest* **99,** 1025–1026 (1991).

119. Cohen, K. A. *et al.* Paradoxical Hypersusceptibility of Drug-resistant *Mycobacterium tuberculosis* to β-lactam Antibiotics. *EBioMedicine* **9,** 170–179 (2016).

120. Pagliotto, A. D. F. *et al.* Anti-*Mycobacterium tuberculosis* activity of antituberculosis drugs and amoxicillin/clavulanate combination. *J. Microbiol. Immunol. Infect.* **49,** 980–983 (2016).

121. Kahan, J. S. *et al*. Thienamycin, a new β-lactam antibiotic. I. Discovery, taxonomy, isolation and physical properties. *J. Antibiot.* **32,** 1–12 (1979).

122. Baranowski, C. *et al.* Maturing *Mycobacterium smegmatis* peptidoglycan requires non-canonical crosslinks to maintain shape. *Elife* **7,** 1–24 (2018).

123. Tremblay, L. W. *et al*. Biochemical and structural characterization of *Mycobacterium tuberculosis* β-lactamase with the carbapenems ertapenem and doripenem. *Biochemistry* **49,** 3766–3773 (2010).

124. Gygli, S. M. *et al*. Antimicrobial resistance in *Mycobacterium tuberculosis*: Mechanistic and evolutionary perspectives. *FEMS Microbiol. Rev.* **41,** 354–373 (2017).

125. Hackbarth, C. J. *et al*. Cloning and sequence analysis of a class A β-lactamase from *Mycobacterium tuberculosis* H37Ra. *Antimicrob. Agents Chemother.* **41,** 1182–1185 (1997).

126. Flores, A. R. *et al*. Genetic analysis of the β-lactamases of *Mycobacterium tuberculosis* and *Mycobacterium smegmatis* and susceptibility to β-lactam antibiotics. *Microbiology* **151,** 521–532 (2005).

127. Flores, A. R. *et al*. Characterization of novel *Mycobacterium tuberculosis* and *Mycobacterium smegmatis* mutants hypersusceptible to β-lactam antibiotics. *J. Bacteriol.* **187,** 1892–1900 (2005).

128. Hugonnet, J. E. & Blanchard, J. S. Irreversible inhibition of the *Mycobacterium tuberculosis* β-lactamase by clavulanate. *Biochemistry* **46,** 11998–12004 (2007).

129. Li, G. *et al.* Efflux Pump Gene Expression in Multidrug-Resistant *Mycobacterium tuberculosis* Clinical Isolates. *PLoS One* **10,** e0119013 (2015).

130. Lamichhane, G. *et al*. Designer Arrays for Defined Mutant Analysis To Detect Genes Essential for Survival of *Mycobacterium tuberculosis* in Mouse Lungs. *Infect. Immun.* **73,** 2533–2540 (2005).

131. Wivagg, C. N. *et al*. Loss of a Class A Penicillin-Binding Protein Alters β-Lactam Susceptibilities in *Mycobacterium tuberculosis*. *ACS Infect. Dis.* **2,** 104–110 (2016).

132. Hugonnet, J. E. *et al*. Meropenem-clavulanate is effective against extensively drug-resistant *Mycobacterium tuberculosis*. *Science (80-.).* **323,** 1215–1218 (2009).

133. Kumar, P. *et al.* Meropenem inhibits D,D-carboxypeptidase activity in *Mycobacterium tuberculosis*. *Mol. Microbiol.* **86,** 367–381 (2012).

134. Horita, Y. *et al*. In vitro susceptibility of *Mycobacterium tuberculosis* isolates to an oral carbapenem alone or in combination with β-Lactamase inhibitors. *Antimicrob. Agents Chemother.* **58,** 7010–7014 (2014).

135. Zhang, D. *et al*. In Vitro Activity of β-Lactams in Combination with β-Lactamase Inhibitors against *Mycobacterium tuberculosis* Clinical Isolates. *Biomed Res. Int.* **2018,** 1–8 (2018).

136. Forsman, L. D. *et al.* Meropenem-clavulanic acid has high in vitro activity against multidrug-resistant *Mycobacterium tuberculosis*. *Antimicrob. Agents Chemother.* **59,** 3630–3632 (2015).

137. Gonzalo, X. & Drobniewski, F. Is there a place for β-lactams in the treatment of multidrug-resistant/extensively drug-resistant tuberculosis? Synergy between meropenem and amoxicillin/clavulanate. *J. Antimicrob. Chemother.* **68,** 366–369 (2013).

138. England, K. *et al.* Meropenem-Clavulanic Acid Shows Activity against *Mycobacterium tuberculosis* In Vivo. *Antimicrob. Agents Chemother.* **56,** 3384–3387 (2012).

139. Veziris, N. *et al*. Activity of carbapenems combined with clavulanate against murine tuberculosis. *Antimicrob. Agents Chemother.* **55,** 2597–2600 (2011).

140. Payen, M. C. *et al.* Clinical use of the meropenem-clavulanate combination for extensively drug-resistant tuberculosis. *Int. J. Tuberc. Lung Dis.* **16,** 558–560 (2012).

141. De Lorenzo, S. *et al.* Efficacy and safety of meropenem–clavulanate added to linezolid-containing regimens in the treatment of MDR-/XDR-TB. *Eur. Respir. J.* **41,** 1386–1392 (2013).

142. Palmero, D. *et al.* First Series of Patients With XDR and Pre-XDR TB Treated With Regimens That Included Meropenem-clavulanate in Argentina. *Arch. Bronconeumol. English Ed.* **51,** e49–e52 (2015).

143. Tiberi, S. *et al.* Ertapenem in the treatment of multidrug-resistant tuberculosis: first clinical experience. *Eur. Respir. J.* **47,** 333–336 (2016).

144. Tiberi, S. *et al.* Effectiveness and safety of meropenem/ clavulanate-containing regimens in the treatment of MDR- and XDR-TB. *Eur. Respir. J.* **47,** 1235–1243 (2016).

145. van Rijn, S. P. *et al.* Pharmacokinetics of ertapenem in patients with multidrug-resistant tuberculosis. *Eur. Respir. J.* **47,** 1229–1234 (2016).

146. Tiberi, S. *et al.* Comparison of effectiveness and safety of imipenem/clavulanate-versus meropenem/clavulanate-containing regimens in the treatment of MDR- and XDR-TB. *Eur. Respir. J.* **47,** 1758–1766 (2016).

147. Royet, J. *et al*. Peptidoglycan recognition proteins: modulators of the microbiome and inflammation. *Nat. Rev. Immunol.* **11,** 837–851 (2011).

148. Dziarski, R. *et al*. Peptidoglycan Recognition Proteins and Lysozyme. in *Encyclopedia of Immunobiology* **2,** 389–403 (Elsevier, 2016).

149. Atilano, M. L. *et al.* Bacterial autolysins trim cell surface peptidoglycan to prevent detection by the *Drosophila* innate immune system. *Elife* **3,** 1–23 (2014).

150. Atilano, M. L. *et al*. Wall Teichoic Acids of *Staphylococcus aureus* Limit Recognition by the *Drosophila* Peptidoglycan Recognition Protein-SA to Promote Pathogenicity. *PLoS Pathog.* **7,** e1002421 (2011).

151. Vaz, F. *et al.* Accessibility to Peptidoglycan Is Important for the Recognition of Gram-Positive Bacteria in *Drosophila*. *Cell Rep.* **27,** 2480–2492.e6 (2019).

152. Kleinnijenhuis, J *et al*. Innate Immune Recognition of *Mycobacterium tuberculosis*. *Clin. Dev. Immunol.* **2011,** 1–12 (2011).

153. Hossain, M. M. & Norazmi, M.-N. Pattern Recognition Receptors and Cytokines in *Mycobacterium tuberculosis* Infection—The Double-Edged Sword? *Biomed Res. Int.* **2013,** 1–18 (2013).

154. Salvatore, P. P. & Zhang, Y. Tuberculosis: Molecular Basis of Pathogenesis. in *Reference Module in Biomedical Sciences* 1–15 (Elsevier, 2017).

155. Brooks, M. N. *et al.* NOD2 controls the nature of the inflammatory response and subsequent fate of *Mycobacterium tuberculosis* and *M. bovis* BCG in human macrophages. *Cell. Microbiol.* **13,** 402–418 (2011).

156. Hasegawa, M. *et al.* A critical role of RICK/RIP2 polyubiquitination in Nod-induced NF-κB activation. *EMBO J.* **27,** 373–383 (2008).

157. Tsolaki, A. G. *et al.* Functional and evolutionary genomics of *Mycobacterium tuberculosis*: Insights from genomic deletions in 100 strains. *Proc. Natl. Acad. Sci.* **101,** 4865–4870 (2004).

158. Meena, L. S. & Rajni, T. Survival mechanisms of pathogenic *Mycobacterium tuberculosis* H37Rv. *FEBS J.* **277,** 2416–2427 (2010).

159. Baena, A. & Porcelli, S. A. Evasion and subversion of antigen presentation by *Mycobacterium tuberculosis*. *Tissue Antigens* **74,** 189–204 (2009).

160. Pires, D. *et al.* Role of Cathepsins in *Mycobacterium tuberculosis* Survival in Human Macrophages. *Sci. Rep.* **6,** 1–13 (2016).

161. Pires, D. *et al. Mycobacterium tuberculosis* Modulates miR-106b-5p to Control Cathepsin S Expression Resulting in Higher Pathogen Survival and Poor T-Cell Activation. *Front. Immunol.* **8,** 1–13 (2017).

162. Schlesinger, L.S. *et al*. Differences in mannose receptor mediated uptake of lipoarabinomannan from virulent and attenuated strains of *Mycobacterium tuberculosis* by human macrophages. *J. Immunol*. **157,** 4558–4575 (1996).

163. Jansen, R. *et al*. Identification of genes that are associated with DNA repeats in prokaryotes. *Mol. Microbiol.* **43,** 1565–1575 (2002).

164. Makarova, K. S. *et al.* Evolution and classification of the CRISPR–Cas systems. *Nat. Rev. Microbiol.* **9,** 467–477 (2011).

165. Doudna, J. A. & Charpentier, E. The new frontier of genome engineering with CRISPR-Cas9. *Science* **346,** 1258096–1258096 (2014).

166. Jinek, M. *et al.* A Programmable Dual-RNA-Guided DNA Endonuclease in Adaptive Bacterial Immunity. *Science* **337,** 816–821 (2012).

167. Gasiunas, G. *et al*. Cas9-crRNA ribonucleoprotein complex mediates specific DNA cleavage for adaptive immunity in bacteria. *Proc. Natl. Acad. Sci.* **109,** E2579–E2586 (2012).

168. Marraffini, L. A. & Sontheimer, E. J. CRISPR interference: RNA-directed adaptive immunity in bacteria and archaea. *Nat. Rev. Genet.* **11,** 181–190 (2010).

169. Heler, R. *et al.* Cas9 specifies functional viral targets during CRISPR–Cas adaptation. *Nature* **519,** 199–202 (2015).

170. Choudhary, E. *et al*. Gene silencing by CRISPR interference in mycobacteria. *Nat. Commun.* **6,** 6267 (2015).

171. Singh, A. K. *et al.* Investigating essential gene function in *Mycobacterium tuberculosis* using an efficient CRISPR interference system. *Nucleic Acids Res.* **44,** e143–e143 (2016).

172. Rock, J. M. *et al.* Programmable transcriptional repression in mycobacteria using an orthogonal CRISPR interference platform. *Nat. Microbiol.* **2,** 16274 (2017).

173. Larson, M. H. *et al.* CRISPR interference (CRISPRi) for sequence-specific control of gene expression. *Nat. Protoc.* **8,** 2180–2196 (2013).

174. Qi, L. S. *et al*. Repurposing CRISPR as an RNA-Guided Platform for Sequence-Specific Control of Gene Expression. *Cell* **152,** 1173–1183 (2013).

175. Bikard, D. *et al*. Programmable repression and activation of bacterial gene expression using an engineered CRISPR-Cas system. *Nucleic Acids Res*. **41,** 7429–7437 (2013).

176. Peters, J. M. *et al.* Bacterial CRISPR: accomplishments and prospects. *Curr. Opin. Microbiol.* **27,** 121–126 (2015).

177. de la Fuente-Núñez, C. & Lu, T. K. CRISPR-Cas9 technology: applications in genome engineering, development of sequence-specific antimicrobials, and future prospects. *Integr. Biol.* **9,** 109–122 (2017).

178. Rock, J. Tuberculosis drug discovery in the CRISPR era. *PLOS Pathog.* **15,** e1007975 (2019).

179. Peters, J. M. *et al.* A Comprehensive, CRISPR-based Functional Analysis of Essential Genes in Bacteria. *Cell* **165,** 1493–1506 (2016).

180. Ehrt, S. *et al.* Controlling gene expression in mycobacteria with anhydrotetracycline and Tet repressor. *Nucleic Acids Res.* **33,** e21–e21 (2005).

181. McNeil, M. B. & Cook, G. M. Utilization of CRISPR Interference To Validate MmpL3 as a Drug Target in *Mycobacterium tuberculosis*. *Antimicrob. Agents Chemother.* **63,** 1–7 (2019).

182. Sambrook, J. & Russell, D.W. *Molecular Cloning, a laboratory manual.* (Cold Spring Harbor Laboratory Press, 2001).

183. Goude, R., Roberts, D. & Parish, T. Electroporation of mycobacteria. *Methods Mol Biol*. **465,** 203–215 (2009).

184. Cui, L. *et al.* A CRISPRi screen in *E. coli* reveals sequence-specific toxicity of dCas9. *Nat. Commun.* **9,** 1912 (2018).

185. Rousset, F. *et al.* Genome-wide CRISPR-dCas9 screens in *E. coli* identify essential genes and phage host factors. *PLOS Genet.* **14,** e1007749 (2018).

186. Nielsen, A. A. & Voigt, C. A. Multi-input CRISPR / C as genetic circuits that interface host regulatory networks. *Mol. Syst. Biol.* **10,** 763 (2014).

187. Wang, T. *et al.* Genome-wide screening identifies promiscuous phosphatases impairing terpenoid biosynthesis in *Escherichia coli*. *Appl. Microbiol. Biotechnol.* **102,** 9771–9780 (2018).

188. Gossen, M. & Bujard, H. Anhydrotetracycline, a novel effector for tetracycline controlled gene expression systems in eukaryotic cells. *Nucleic Acids Res.* **21,** 4411–4412 (1993).

189. Viswanathan, G. *et al*. Identification of Mycobacterial Genes Involved in Antibiotic Sensitivity: Implications for the Treatment of Tuberculosis with β-Lactam-Containing Regimens. *Antimicrob. Agents Chemother.* **61,** 1–6 (2017).

190. Wolff, K. A. *et al.* Protein Kinase G Is Required for Intrinsic Antibiotic Resistance in Mycobacteria. *Antimicrob. Agents Chemother.* **53,** 3515–3519 (2009).

191. Daiyasu, H. *et al*. Expansion of the zinc metallo-hydrolase family of the β-lactamase fold. *FEBS Lett.* **503,** 1–6 (2001).

192. Somboro, A. M. *et al*. Diversity and Proliferation of Metallo-β-Lactamases: a Clarion Call for Clinically Effective Metallo-β-Lactamase Inhibitors. *Appl. Environ. Microbiol.* **84,** 1–20 (2018).

193. Singh, G. *et al.* Characterization of a novel esterase Rv1497 of *Mycobacterium tuberculosis* H37Rv demonstrating β-lactamase activity. *Enzyme Microb. Technol.* **82,** 180–190 (2016).

194. Solapure, S. *et al.* In Vitro and In Vivo Efficacy of β-Lactams against Replicating and Slowly Growing/Nonreplicating *Mycobacterium tuberculosis*. *Antimicrob. Agents Chemother.* **57,** 2506–2510 (2013).

195. Pankey, G. A. & Sabath, L. D. Clinical Relevance of Bacteriostatic versus Bactericidal Mechanisms of Action in the Treatment of Gram-Positive Bacterial Infections. *Clin. Infect. Dis.* **38,** 864–870 (2004).

196. Yamori, S. *et al*. Bacteriostatic and Bactericidal Activity of Antituberculosis Drugs against *Mycobacterium tuberculosis*, *Mycobacterium avium-Mycobacterium intracellulare* Complex and *Mycobacterium kansasii* in Different Growth Phases. *Microbiol. Immunol.* **36,** 361–368 (1992).

197. Martínez, A., Torello, S. & Kolter, R. Sliding Motility in Mycobacteria. *J. Bacteriol.* **181,** 7331–7338 (1999).

198. Flanagan, J. N. & Steck, T. R. The Relationship Between Agar Thickness and Antimicrobial Susceptibility Testing. *Indian J. Microbiol.* **57,** 503–506 (2017).

199. Anes, E. *et al.* Dynamic life and death interactions between *Mycobacterium smegmatis* and J774 macrophages. *Cell. Microbiol.* **8,** 939–960 (2006).

Appendices

Appendix 1

OADC enrichment medium:

Weigh the following components to a Schott Flask:

- 25 g bovine albumin Fraction V (NZYTech).
- 10 g of Dextrose (Sigma Aldrich).
- 4.25 g of NaCl (Merck).
- Add 400 mL of MilliQ water and dissolve the mix by magnetic agitation for 1h.
- Add 0.02 g of catalase (Sigma-Aldrich) and 282 µL of Oleic acid (Sigma-Aldrich). Dissolve the mix by magnetic agitation for 30 min.
- Make up with MilliQ water to a final volume of 500 mL.
- Filter ON using a 0.2 µM PES filter flask (VWR) and store at 4°C.

Top Agar:

Add:

- 0.94 g of 7H9 (BD™ Biosciences).
- 1.4 g of agar (BD™ Biosciences).
- 200 mL of distilled water.
- 400 µL of glycerol (ThermoScientific).

Appendix 2

Annealed oligos – *M. smegmatis*

AO1

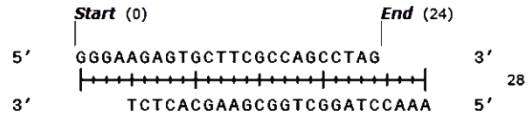

AO2

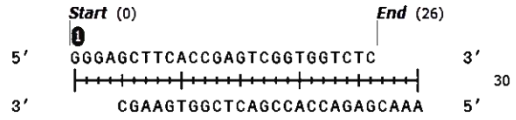

AO3

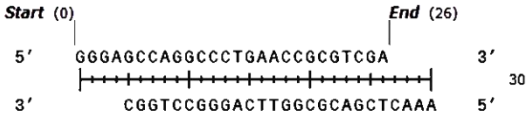

AO4

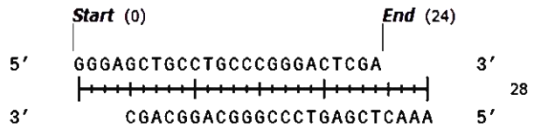

AO5

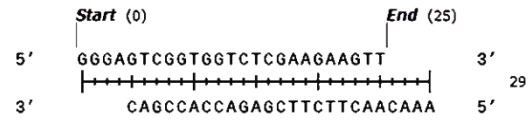

AO6

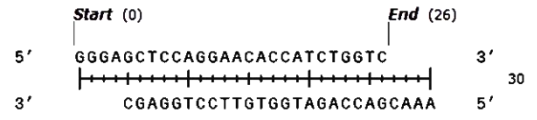

AO7

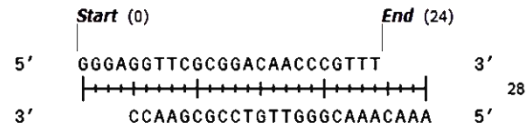

AO8

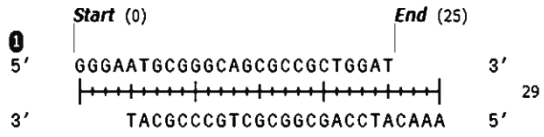

Annealed oligos – *Mtb* H37Ra

AO1

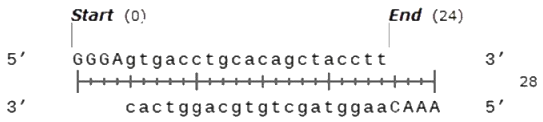

AO2

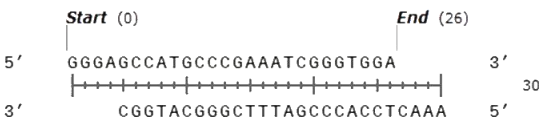

AO3

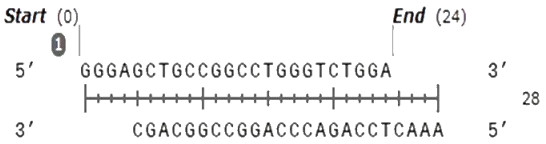

AO4

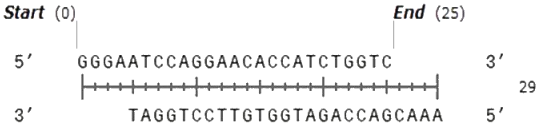

AO5

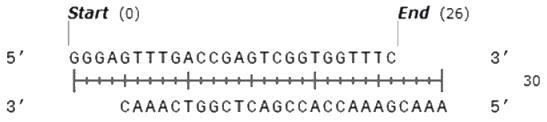

AO6

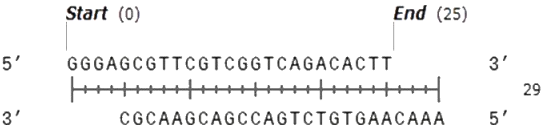

Appendix 3

M. smegmatis – Sequencing Results

-10 site

Insert

dCas9 handle

C1 - Sequencing output

5’ – TATCGCTTGTATGGGTATCGCTTGTATGGGAAGCCCCATGCGCCAGAGTTGTTTCT
GAAACATGGCAAAGGTAGCGTTGCCAATGATGTTACAGATGAGATGGTCAGACTAAACT
GGCTGACGGAATTTATGCCTCTTCCGACCATCAAGCATTTTATCCGTACTCCTGATGATG
CATGGTTACTCACCACTGCGATCCCCGGGAAAACAGCATTCCAGGTATTAGAAGAATAT
CCTGATTCAGGTGAAAATATTGTTGATGCGCTGGCAGTGTTCCTGCGCCGGTTGCATTC
GATTCCTGTTTGTAATTGTCCTTTTAACAGCGATCGCGTATTTCGCCTCGCTCAGGCGCA
ATCACGAATGAATAACGGTTTGGTTGATGCGAGTGATTTTGATGACGAGCGTAATGGCT
GGCCTGTTGAACAAGTCTGGAAAGAAATGCATAATCTTTTGCCATTCTCACCGGATTCAG
TCGTCACTCATGGTGATTTCTCACTTGATAACCTTATTTTTGACGAGGGGAAATTAATAG
GTTGTATTGATGTTGGACGAGTCGGAATCGCAGACCGATACCAGGATCTTGCCATCCTA
TGGAACTGCCTCGGTGAGTTTTCTCCTTCATTACAGAAACGGCTTTTTCAAAAATATGGT
ATTGATAATCCTGATATGAATAAATTGCAGTTTCATTTGATGCTCGATGAGTTTTTCTAAT
CAGAATTGGTTAATTGGTTGTAACACTGGCAGAGCATTACGCTGACTTGACGGGACGGC
GGCTTTGTTGAATAAATCGAACTTTTGCTGAGTTGAAGGATCAGATCACGCATCTTCCCG
ACAACGCAGACCGTTCCGTGGCAAAGCAAAAGTTCAAAATCACCAACTGGTCCACCTAC
AACAAAGCTCTCACCAACCGTGGCTCCCTCACGATATCAATAAACGAAAGGCTCAGTCG
AAAGACTGGGCCTTTCGTTTATCTGTTGTTTGAAAAAAAAAAGCGCCGCAACTGCGGCG
CTTTTTTTTTTGAATTCTCTGACCAGGGAAAATAGCCCTCTGACCTGGGGATTTGCGATC
CCTATCAGTGATAGATATAATCTGGGAAGAGTGCTTCGCCAGCCTAGGTTTTTGTACTC
GAAAGAAGCTACAAAGATAAGGCTTCATGCCGAAATCAACACCCTGTCATTTTATGGCA
GGGTGTTTTTTTTTTGTCGACTTGGGGACCCTAGAGGTCCCCTTTTTATTTTGAAGGCC -
3’

C2 - Sequencing output

5’ – GTGTGATAGATATAATTTGGGAGCTTCACCGAGTCGGTGGTCTCGTTTTTGTACTCG
AAAGAAGCTACAAAGATAAGGCTTCATGCCGAAATCAACACCCTGTCATTTTATGGCAG
GGTGTTTTTTTTTTGTCGACTTGGGGACCCTAGAGGTCCCCCTTTTTATTTTGAAGGCG -
3’

C3 - Sequencing output

5’ – GAGTTGTTTTGAAAGAGTTGTTTTGAAACAGGCAAAGGTAGCGTGCCAATGATGTA
CAGATGAGATGGTCAGACTAAACTGGCTGACGGAATTTATGCCTCTTCCGACCATCAAG

CATTTTATCCGTACTCCTGATGATGCATGGTTACTCACCACTGCGATCCCCGGGAAAAC
AGCATTCCAGGTATTAGAAGAATATCCTGATTCAGGTGAAAATATTGTTGATGCGCTGGC
AGTGTTCCTGCGCCGGTTGCATTCGATTCCTGTTTGTAATTGTCCTTTTAACAGCGATCG
CGTATTTCGCCTCGCTCAGGCGCAATCACGAATGAATAACGGTTTGGTTGATGCGAGTG
ATTTTGATGACGAGCGTAATGGCTGGCCTGTTGAACAAGTCTGGAAAGAAATGCATAAT
CTTTTGCCATTCTCACCGGATTCAGTCGTCACTCATGGTGATTTCTCACTTGATAACCTT
ATTTTTGACGAGGGGAAATTAATAGGTTGTATTGATGTTGGACGAGTCGGAATCGCAGA
CCGATACCAGGATCTTGCCATCCTATGGAACTGCCTCGGTGAGTTTTCTCCTTCATTACA
GAAACGGCTTTTTCAAAAATATGGTATTGATAATCCTGATATGAATAAATTGCAGTTTCAT
TTGATGCTCGATGAGTTTTTCTAATCAGAATTGGTTAATTGGTTGTAACACTGGCAGAGC
ATTACGCTGACTTGACGGGACGGCGGCTTTGTTGAATAAATCGAACTTTTGCTGAGTTG
AAGGATCAGATCACGCATCTTCCCGACAACGCAGACCGTTCCGTGGCAAAGCAAAAGTT
CAAAATCACCAACTGGTCCACCTACAACAAAGCTCTCACCAACCGTGGCTCCCTCACGA
TATCAATAAACGAAAGGCTCAGTCGAAAGACTGGGCCTTTCGTTTATCTGTTGTTTGAAA
AAAAAAAGCGCCGCAACTGCGGCGCTTTTTTTTTTGAATTCTCTGACCAGGGAAAATAG
CCCTCTGACCTGGGGATTTGCGATCCCTATCAGTGATAGATATAATCTGGGAGCCAGGC
CCTGAACCGCGTCGAGTTTTTGTACTCGAAAGAAGCTACAAAGATAAGGCTTCATGCCG
AAATCAACACCCTGTCATTTTATGGCAGGGTGTTTTTTTTTTGTCGACTTGGGGACCCTA
GAGGTCCCCTTTTTATTTTGAAGGCC - 3’

C4 – Sequencing output

5’ – CGCCAGAGTTGTTCGCCAGAGTTGTTTCTGAAACATGGCAAAGGTAGCGTTGCCAA
TGATGTTACAGATGAGATGGTCAGACTAAACTGGCTGACGGAATTTATGCCTCTTCCGA
CCATCAAGCATTTTATCCGTACTCCTGATGATGCATGGTTACTCACCACTGCGATCCCC
GGGAAAACAGCATTCCAGGTATTAGAAGAATATCCTGATTCAGGTGAAAATATTGTTGAT
GCGCTGGCAGTGTTCCTGCGCCGGTTGCATTCGATTCCTGTTTGTAATTGTCCTTTTAAC
AGCGATCGCGTATTTCGCCTCGCTCAGGCGCAATCACGAATGAATAACGGTTTGGTTGA
TGCGAGTGATTTTGATGACGAGCGTAATGGCTGGCCTGTTGAACAAGTCTGGAAAGAAA
TGCATAATCTTTTGCCATTCTCACCGGATTCAGTCGTCACTCATGGTGATTTCTCACTTG
ATAACCTTATTTTTGACGAGGGGAAATTAATAGGTTGTATTGATGTTGGACGAGTCGGAA
TCGCAGACCGATACCAGGATCTTGCCATCCTATGGAACTGCCTCGGTGAGTTTTCTCCT
TCATTACAGAAACGGCTTTTTCAAAAATATGGTATTGATAATCCTGATATGAATAAATTGC
AGTTTCATTTGATGCTCGATGAGTTTTTCTAATCAGAATTGGTTAATTGGTTGTAACACTG
GCAGAGCATTACGCTGACTTGACGGGACGGCGGCTTTGTTGAATAAATCGAACTTTTGC
TGAGTTGAAGGATCAGATCACGCATCTTCCCGACAACGCAGACCGTTCCGTGGCAAAG
CAAAAGTTCAAAATCACCAACTGGTCCACCTACAACAAAGCTCTCACCAACCGTGGCTC
CCTCACGATATCAATAAACGAAAGGCTCAGTCGAAAGACTGGGCCTTTCGTTTATCTGTT
GTTTGAAAAAAAAAAGCGCCGCAACTGCGGCGCTTTTTTTTTTGAATTCTCTGACCAGGG
AAAATAGCCCTCTGACCTGGGGATTTGCGATCCCTATCAGTGATAGATATAATCTGGGA
GCTGCCTGCCCGGGACTCGAGTTTTTGTACTCGAAAGAAGCTACAAAGATAAGGCTTCA
TGCCGAAATCAACACCCTGTCATTTTATGGCAGGGTGTTTTTTTTTTGTCGACTTGGGGA
CCCTAGAGGTCCCCTTTTTATTTTGAAGGGCC – 3’

C5 – Sequencing output

5’ – AGATGAGATGGTCAAGATGAGATGGTCAGACTAAACTGGCTGACGGAATTTATGCC
TCTTCCGACCATCAAGCATTTTATCCGTACTCCTGATGATGCATGGTTACTCACCACTGC
GATCCCCGGGAAAACAGCATTCCAGGTATTAGAAGAATATCCTGATTCAGGTGAAAATA
TTGTTGATGCGCTGGCAGTGTTCCTGCGCCGGTTGCATTCGATTCCTGTTTGTAATTGT
CCTTTTAACAGCGATCGCGTATTTCGCCTCGCTCAGGCGCAATCACGAATGAATAACGG
TTTGGTTGATGCGAGTGATTTTGATGACGAGCGTAATGGCTGGCCTGTTGAACAAGTCT
GGAAAGAAATGCATAATCTTTTGCCATTCTCACCGGATTCAGTCGTCACTCATGGTGATT
TCTCACTTGATAACCTTATTTTTGACGAGGGGAAATTAATAGGTTGTATTGATGTTGGAC
GAGTCGGAATCGCAGACCGATACCAGGATCTTGCCATCCTATGGAACTGCCTCGGTGA
GTTTTCTCCTTCATTACAGAAACGGCTTTTTCAAAAATATGGTATTGATAATCCTGATATG
AATAAATTGCAGTTTCATTTGATGCTCGATGAGTTTTTCTAATCAGAATTGGTTAATTGGT
TGTAACACTGGCAGAGCATTACGCTGACTTGACGGGACGGCGGCTTTGTTGAATAAATC
GAACTTTTGCTGAGTTGAAGGATCAGATCACGCATCTTCCCGACAACGCAGACCGTTCC
GTGGCAAAGCAAAAGTTCAAAATCACCAACTGGTCCACCTACAACAAAGCTCTCACCAA
CCGTGGCTCCCTCACGATATCAATAAACGAAAGGCTCAGTCGAAAGACTGGGCCTTTCG
TTTATCTGTTGTTTGAAAAAAAAAAGCGCCGCAACTGCGGCGCTTTTTTTTTTGAATTCTC
TGACCAGGGAAAATAGCCCTCTGACCTGGGGATTTGCGATCCCTATCAGTGATAGATAT
AATCTGGGAGTCGGTGGTCTCGAAGAAGTTGTTTTTGTACTCGAAAGAAGCTACAAAGA
TAAGGCTTCATGCCGAAATCAACACCCTGTCATTTTATGGCAGGGTGTTTTTTTTTTGTC
GACTTGGGGACCCTAGAGGTCCCCTTTTTATTTTGAAGGCG - 3’

C6 – Sequencing output

5’ – CCCCCCCCCTCCAACAAAGCTCTCCCCCAACCGTGGCTCCCTCCCGATATCAATAA
ACGAAAGGCTCAGTCGAAAGACTGGGCCTTTCGTTTATCTGTTGTTTGAAAAAAAAAAGC
GCCGCAACTGCGGCGCTTTTTTTTTTGAATTCTCTGACCAGGGAAAATAGCCCTCTGAC
CTGGGGATTTGCGATCCCTATCAGTGATAGATATAATCTGGGAGCTCCAGGAACACCAT
CTGGTCGTTTTTGTACTCGAAAGAAGCTACAAAGATAAGGCTTCATGCCGAAATCAACAC
CCTGTCATTTTATGGCAGGGTGTTTTTTTTTTGTCGACTTGGGGACCCTAGAGGTCCCCT
TTTATTTGAA - 3’

C7 – Sequencing output

5’ – GAGTTGTTTCTGAGAGTTGTTTCTGAAACATGGCAAAGGTAGCGTTGCCAATGATGT
TACAGATGAGATGGTCAGACTAAACTGGCTGACGGAATTTATGCCTTCTTCCGACCATC
AAGCATTTTATCCGTACTCCTGATGATGCATGGTTACTCACCACTGCGATCCCCGGGAA
AACAGCATTCCAGGTATTAGAAGAATATCCTGATTCAGGTGAAAATATTGTTGATGCGCT
GGCAGTGTTCCTGCGCCGGTTGCATTCGATTCCTGTTTGTAATTGTCCTTTTAACAGCGA
TCGCGTATTTCGCCTCGCTCAGGCGCAATCACGAATGAATAACGGTTTGGTTGATGCGA
GTGATTTTGATGACGAGCGTAATGGCTGGCCTGTTGAACAAGTCTGGAAAGAAATGCAT
AATCTTTTGCCATTCTCACCGGATTCAGTCGTCACTCATGGTGATTTCTCACTTGATAAC
CTTATTTTTGACGAGGGGAAATTAATAGGTTGTATTGATGTTGGACGAGTCGGAATCGCA
GACCGATACCAGGATCTTGCCATCCTATGGAACTGCCTCGGTGAGTTTTCTCCTTCATTA
CAGAAACGGCTTTTTCAAAAATATGGTATTGATAATCCTGATATGAATAAATTGCAGTTTC
ATTTGATGCTCGATGAGTTTTTCTAATCAGAATTGGTTAATTGGTTGTAACACTGGCAGA

GCATTACGCTGACTTGACGGGACGGCGGCTTTGTTGAATAAATCGAACTTTTGCTGAGT
TGAAGGATCAGATCACGCATCTTCCCGACAACGCAGACCGTTCCGTGGCAAAGCAAAA
GTTCAAAATCACCAACTGGTCCACCTACAACAAAGCTCTCACCAACCGTGGCTCCCTCA
CGATATCAATAAACGAAAGGCTCAGTCGAAAGACTGGGCCTTTCGTTTATCTGTTGTTTG
AAAAAAAAAAGCGCCGCAACTGCGGCGCTTTTTTTTTTGAATTCTCTGACCAGGGAAAAT
AGCCCTCTGACCTGGGGATTTGCGATCCCTATCAGTGATAGATATAATCTGGGAGGTTC
GCGGACAACCCGTTTGTTTTTGTACTCGAAAGAAGCTACAAAGATAAGGCTTCATGCCG
AAATCAACACCCTGTCATTTTATGGCAGGGTGTTTTTTTTTTGTCGACTTGGGGACCCTA
GAGGTCCCCTTTTTATTTTGAAGGGCC – 3’

C8 – Sequencing output

5’ – TTGTTCTGAAACATTTGTTCTGAAACATGGCAAAGGTAGCGTGCCAATGATGTTACA
GATGAGATGGTCAGACTAAACTGGCTGACGGAATTTATGCCTCTTCCGACCATCAAGCA
TTTTATCCGTACTCCTGATGATGCATGGTTACTCACCACTGCGATCCCCGGGAAAACAG
CATTCCAGGTATTAGAAGAATATCCTGATTCAGGTGAAAATATTGTTGATGCGCTGGCAG
TGTTCCTGCGCCGGTTGCATTCGATTCCTGTTTGTAATTGTCCTTTTAACAGCGATCGCG
TATTTCGCCTCGCTCAGGCGCAATCACGAATGAATAACGGTTTGGTTGATGCGAGTGAT
TTTGATGACGAGCGTAATGGCTGGCCTGTTGAACAAGTCTGGAAAGAAATGCATAATCT
TTTGCCATTCTCACCGGATTCAGTCGTCACTCATGGTGATTTCTCACTTGATAACCTTATT
TTTGACGAGGGGAAATTAATAGGTTGTATTGATGTTGGACGAGTCGGAATCGCAGACCG
ATACCAGGATCTTGCCATCCTATGGAACTGCCTCGGTGAGTTTTCTCCTTCATTACAGAA
ACGGCTTTTTCAAAAATATGGTATTGATAATCCTGATATGAATAAATTGCAGTTTCATTTG
ATGCTCGATGAGTTTTTCTAATCAGAATTGGTTAATTGGTTGTAACACTGGCAGAGCATT
ACGCTGACTTGACGGGACGGCGGCTTTGTTGAATAAATCGAACTTTTGCTGAGTTGAAG
GATCAGATCACGCATCTTCCCGACAACGCAGACCGTTCCGTGGCAAAGCAAAAGTTCAA
AATCACCAACTGGTCCACCTACAACAAAGCTCTCACCAACCGTGGCTCCCTCACGATAT
CAATAAACGAAAGGCTCAGTCGAAAGACTGGGCCTTTCGTTTATCTGTTGTTTGAAAAAA
AAAAGCGCCGCAACTGCGGCGCTTTTTTTTTTGAATTCTCTGACCAGGGAAAATAGCCC
TCTGACCTGGGGATTTGCGATCCCTATCAGTGATAGATATAATCTGGGAATGCGGGCAG
CGCCGCTGGATGTTTTTGTACTCGAAAGAAGCTACAAAGATAAGGCTTCATGCCGAAAT
CAACACCCTGTCATTTTATGGCAGGGTGTTTTTTTTTTGTCGACTTGGGGACCCTAGAGG
TCCCCTTTTTATTTTGAAGGCG – 3’

***Mtb* H37Ra – Sequencing Results**

-10 site

Insert

dCas9 handle

C1 – Sequencing output

5’ – CTCTGGACCTTTCGTTTATCTGTTGTTTGAAAAAAAAAAGCGCCGCAACTGCGGCG
CTTTTTTTTTTGAATTCTCTGACCAGGGAAAATAGCCCTCTGACCTGGGGATTTGCGATC
CCTATCAGTGATAGATATAATCTGGGAGTGACCTGCACAGCTACCTTGTTTTTGTACTCG
AAAGAAGCTACAAAGATAAGGCTTCATGCCGAAATCAACACCCTGT – 3’

C2 – Sequencing output

5’ – GCCAGAGTTGTTTGCCAGAGTTGTTTCTGAAACATGGCAAAGGTAGCGTTGCCAAT
GATGTTACAGATGAGATGGTCAGACTAAACTGGCTGACGGAATTTATGCCTCTTCCGAC
CATCAAGCATTTTATCCGTACTCCTGATGATGCATGGTTACTCACCACTGCGATCCCCG
GGAAAACAGCATTCCAGGTATTAGAAGAATATCCTGATTCAGGTGAAAATATTGTTGATG
CGCTGGCAGTGTTCCTGCGCCGGTTGCATTCGATTCCTGTTTGTAATTGTCCTTTTAACA
GCGATCGCGTATTTCGCCTCGCTCAGGCGCAATCACGAATGAATAACGGTTTGGTTGAT
GCGAGTGATTTTGATGACGAGCGTAATGGCTGGCCTGTTGAACAAGTCTGGAAAGAAAT
GCATAATCTTTTGCCATTCTCACCGGATTCAGTCGTCACTCATGGTGATTTCTCACTTGA
TAACCTTATTTTTGACGAGGGGAAATTAATAGGTTGTATTGATGTTGGACGAGTCGGAAT
CGCAGACCGATACCAGGATCTTGCCATCCTATGGAACTGCCTCGGTGAGTTTTCTCCTT
CATTACAGAAACGGCTTTTTCAAAAATATGGTATTGATAATCCTGATATGAATAAATTGCA
GTTTCATTTGATGCTCGATGAGTTTTTCTAATCAGAATTGGTTAATTGGTTGTAACACTGG
CAGAGCATTACGCTGACTTGACGGGACGGCGGCTTTGTTGAATAAATCGAACTTTTGCT
GAGTTGAAGGATCAGATCACGCATCTTCCCGACAACGCAGACCGTTCCGTGGCAAAGC
AAAAGTTCAAAATCACCAACTGGTCCACCTACAACAAAGCTCTCACCAACCGTGGCTCC
CTCACGATATCAATAAACGAAAGGCTCAGTCGAAAGACTGGGCCTTTCGTTTATCTGTTG
TTTGAAAAAAAAAAGCGCCGCAACTGCGGCGCTTTTTTTTTTGAATTCTCTGACCAGGGA
AAATAGCCCTCTGACCTGGGGATTTGCGATCCCTATCAGTGATAGATATAATCTGGGAG
CCATGCCCGAAATCGGGTGGAGTTTTTGTACTCGAAAGAAGCTACAAAGATAAGGCTTC
ATGCCGAAATCAACAGGGTGTCATTTTATGGCAGGGTGTTTTTTTTTGTCGACTTGGGGA
CCCTAGAGGTCCCCTTTTTATTTGAAGG – 3’

C3 – Sequencing output

5’ – ATTGGAAGCCCCATGATTGGAAGCCCCATGCGCCAGAGTTGTTTCTGAAACATGGC
AAAGGTAGCGTTGCCAATGATGTTACAGATGAGATGGTCAGACTAAACTGGCTGACGGA
ATTTATGCCTCTTCCGACCATCAAGCATTTTATCCGTACTCCTGATGATGCATGGTTACT
CACCACTGCGATCCCCGGGAAAACAGCATTCCAGGTATTAGAAGAATATCCTGATTCAG
GTGAAAATATTGTTGATGCGCTGGCAGTGTTCCTGCGCCGGTTGCATTCGATTCCTGTT
TGTAATTGTCCTTTTAACAGCGATCGCGTATTTCGCCTCGCTCAGGCGCAATCACGAAT

GAATAACGGTTTGGTTGATGCGAGTGATTTTGATGACGAGCGTAATGGCTGGCCTGTTG
AACAAGTCTGGAAAGAAATGCATAATCTTTTGCCATTCTCACCGGATTCAGTCGTCACTC
ATGGTGATTTCTCACTTGATAACCTTATTTTTGACGAGGGGAAATTAATAGGTTGTATTGA
TGTTGGACGAGTCGGAATCGCAGACCGATACCAGGATCTTGCCATCCTATGGAACTGC
CTCGGTGAGTTTTCTCCTTCATTACAGAAACGGCTTTTTCAAAAATATGGTATTGATAATC
CTGATATGAATAAATTGCAGTTTCATTTGATGCTCGATGAGTTTTTCTAATCAGAATTGGT
TAATTGGTTGTAACACTGGCAGAGCATTACGCTGACTTGACGGGACGGCGGCTTTGTTG
AATAAATCGAACTTTTGCTGAGTTGAAGGATCAGATCACGCATCTTCCCGACAACGCAG
ACCGTTCCGTGGCAAAGCAAAAGTTCAAAATCACCAACTGGTCCACCTACAACAAAGCT
CTCACCAACCGTGGCTCCCTCACGATATCAATAAACGAAAGGCTCAGTCGAAAGACTGG
GCCTTTCGTTTATCTGTTGTTTGAAAAAAAAAAGCGCCGCAACTGCGGCGCTTTTTTTTT
TGAATTCTCTGACCAGGGAAAATAGCCCTCTGACCTGGGGATTTGCGATCCCTATCAGT
GATAGATATAATCTGGGAGCTGCCGGCCTGGGTCTGGAGTTTTTGTACTCGAAAGAAGC
TACAAAGATAAGGCTTCATGCCGAAATCAACACCCTGTCATTTTATGGCAGGGTGTTTTT
TTTTGTCGACTTGGGGACCCTAGAGGTCCCCTTTTTATTTTGAAGGCC – 3’

C4 – Sequencing output

5’ – ATCAATCACCAAGTGGTCCACATACAACAAAGCTCTCACCAACCGTGGCTCCCTCA
CGATATCAATAAACGAAAGGCTCAGTCGAAAGACTGGGCCTTTCGTTTATCTGTTGTTTG
AAAAAAAAAAGCGCCGCAACTGCGGCGCTTTTTTTTTTGAATTCTCTGACCAGGGAAAAT
AGCCCTCTGACCTGGGGATTTGCGATCCCTATCAGTGATAGATATAATCTGGGAATCCA
GGAACACCATCTGGTCGTTTTTGTACTCGAAAGAAGCTACAAAGATAAGGCTTCATGCC
GAAATCAACACCCTGTCATTTTATGGCAGGGTGTTTTTTTTTTGTCGACTTGGGGACCCT
AGAGGTCCCCTTTTTATTTTGAAGGGGG – 3’

C5 – Sequencing output

5’ – AGAGTTGTTTTGAGAGTTGTTTTGAAACATGGCAAAGGTAGCTTGCCATGATGTACC
GATGAGATGGTCAGACTAAACTGGCTGACGGAATTTATGCCTCTTCCGACCATCAAGCA
TTTATCCGTACTCCTGATGATGCATGGTTACTCACCACTGCGATCCCCGGGAAAACAGC
ATTCCAGGTATTAGAAGAATATCCTGATTCAGGTGAAAATATTGTTGATGCGCTGGCAGT
GTTCCTGCGCCGGTTGCATTCGATTCCTGTTTGTAATTGTCCTTTTAACAGCGATCGCGT
ATTTCGCCTCGCTCAGGCGCAATCACGAATGAATAACGGTTTGGTTGATGCGAGTGATT
TTGATGACGAGCGTAATGGCTGGCCTGTTGAACAAGTCTGGAAAGAAATGCATAATCTT
TTGCCATTCTCACCGGATTCAGTCGTCACTCATGGTGATTTCTCACTTGATAACCTTATTT
TTGACGAGGGGAAATTAATAGGTTGTATTGATGTTGGACGAGTCGGAATCGCAGACCGA
TACCAGGATCTTGCCATCCTATGGAACTGCCTCGGTGAGTTTTCTCCTTCATTACAGAAA
CGGCTTTTTCAAAAATATGGTATTGATAATCCTGATATGAATAAATTGCAGTTTCATTTGA
TGCTCGATGAGTTTTTCTAATCAGAATTGGTTAATTGGTTGTAACACTGGCAGAGCATTA
CGCTGACTTGACGGGACGGCGGCTTTGTTGAATAAATCGAACTTTTGCTGAGTTGAAGG
ATCAGATCACGCATCTTCCCGACAACGCAGACCGTTCCGTGGCAAAGCAAAAGTTCAAA
ATCACCAACTGGTCCACCTACAACAAAGCTCTCACCAACCGTGGCTCCCTCACGATATC
AATAAACGAAAGGCTCAGTCGAAAGACTGGGCCTTTCGTTTATCTGTTGTTTGAAAAAAA
AAAGCGCCGCAACTGCGGCGCTTTTTTTTTTGAATTCTCTGACCAGGGAAAATAGCCCT
CTGACCTGGGGATTTGCGATCCCTATCAGTGATAGATATAATCTGGGAGTTTGACCGAG

TCGGTGGTTTCGTTTTTGTACTCGAAAGAAGCTACAAAGATAAGGCTTCATGCCGAAATC
AACCCCC – 3’

C6 – Sequencing output

5’ – GTATGGGAAGCCCCGTATGGGAAGCCCCATGCGCCAGAGTTTTTCTGAAACATGG
CAAAGGTAGCGTTGCCAATGATGTTACAGATGAGATGGTCAGACTAAACTGGCTGACGG
AATTTATGCCTCTTCCGACCATCAAGCATTTTATCCGTACTCCTGATGATGCATGGTTAC
TCACCACTGCGATCCCCGGGAAAACAGCATTCCAGGTATTAGAAGAATATCCTGATTCA
GGTGAAAATATTGTTGATGCGCTGGCAGTGTTCCTGCGCCGGTTGCATTCGATTCCTGT
TTGTAATTGTCCTTTTAACAGCGATCGCGTATTTCGCCTCGCTCAGGCGCAATCACGAAT
GAATAACGGTTTGGTTGATGCGAGTGATTTTGATGACGAGCGTAATGGCTGGCCTGTTG
AACAAGTCTGGAAAGAAATGCATAATCTTTTGCCATTCTCACCGGATTCAGTCGTCACTC
ATGGTGATTTCTCACTTGATAACCTTATTTTTGACGAGGGGAAATTAATAGGTTGTATTGA
TGTTGGACGAGTCGGAATCGCAGACCGATACCAGGATCTTGCCATCCTATGGAACTGC
CTCGGTGAGTTTTCTCCTTCATTACAGAAACGGCTTTTTCAAAAATATGGTATTGATAATC
CTGATATGAATAAATTGCAGTTTCATTTGATGCTCGATGAGTTTTTCTAATCAGAATTGGT
TAATTGGTTGTAACACTGGCAGAGCATTACGCTGACTTGACGGGACGGCGGCTTTGTTG
AATAAATCGAACTTTTGCTGAGTTGAAGGATCAGATCACGCATCTTCCCGACAACGCAG
ACCGTTCCGTGGCAAAGCAAAAGTTCAAAATCACCAACTGGTCCACCTACAACAAAGCT
CTCACCAACCGTGGCTCCCTCACGATATCAATAAACGAAAGGCTCAGTCGAAAGACTGG
GCCTTTCGTTTATCTGTTGTTTGAAAAAAAAAAGCGCCGCAACTGCGGCGCTTTTTTTTT
TGAATTCTCTGACCAGGGAAAATAGCCCTCTGACCTGGGGATTTGCGATCCCTATCAGT
GATAGATATAATCTGGGAGCGTTCGTCGGTCAGACACTTGTTTTTGTACTCGAAAGAAG
CTACAAAGATAAGGCTTCATGCCGAAATCAACACCC – 3’

Appendix 4

M. smegmatis – Recombinant plasmids (CRISPRi systems)

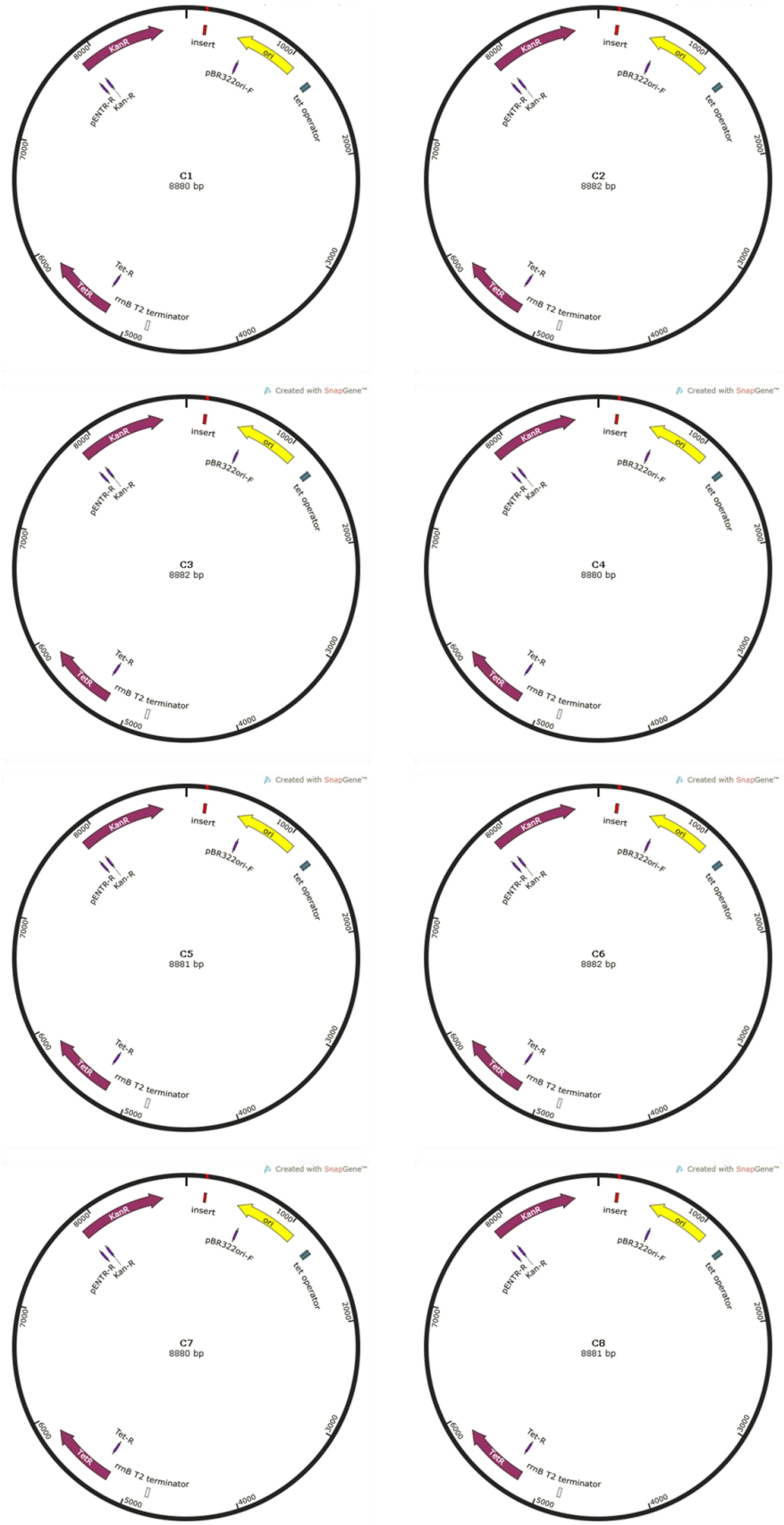

Mtb H37Ra – Recombinant plasmids (CRISPRi systems)